A STUDY ON THE EFFECTS OF LOSS OF IMPRINTING OF IGF-2 ON CELLULAR AND TISSUE LEVEL ORGANIZATION OF THE COLONIC CRYPT

by

Kiran Gireesan Vanaja

A dissertation submitted to Johns Hopkins University in conformity with the requirements for the degree of Doctor of Philosophy

Baltimore, Maryland

December, 2013

Abstract

Insulin like growth factor -2 (IGF-2), which is a secreted growth factor belonging to the Insulin signaling superfamily, plays an important role in embryonic growth but is epigenetically silenced on one parental allele in an imprinting mechanism in mammals post-birth. Loss of Imprinting (LOI) is the loss of this silencing mechanism, either spontaneous or inherited in nature, that results in a bi-allelic expression of IGF-2. LOI causes increased growth, seen in the colon as abnormally elongated crypts and a 5 fold increase in the chance of developing colorectal cancer. In an in-vitro system, IGF-2 LOI cells show rapid growth via increased proliferation, overexpression of the Insulin-like growth factor-1 receptor (IGF-1R) that IGF-2 signals through and an increased sensitivity to the inhibition of the IGF-1R signaling when compared to wild-type (WT) cells. It is shown here that IGF-2 LOI cells re-balance the two important kinases Akt and Erk that are activated downstream of the IGF-1R. While Erk signaling strength is increased, Akt signaling is attenuated in LOI cells in response to IGF-2 stimulation when compared to WT zcells. Since Erk activation is intricately linked to internalization of receptors, it is seen that LOI cells in conjunction with IGF-1R overexpression show increased internalization of activated IGF-1R. While these two mechanisms contribute to increased Erk signaling, Akt activation is shown to depend on total receptor levels and recycling of the internalized receptors to the cell surface. Erk is also seen to mediate ubiquitination of IGF-1R thereby presumably increasing the rate of internalization and also to mediate the increase in transcriptional levels of IGF-1R over longer periods of time. Using a computational model of the IGF-2 signaling pathway, we show that increased Erk activation can sustain the LOI phenotype via increased internalization and transcriptional regulation of IGF-1R. The computational model is trained using the Akt and Erk activation profiles measured over time and tested on the profiles measured in WT cells. Interestingly, it is shown that the re-balance in the signaling strength of Akt and Erk signaling in LOI cells propagates down to the level of the anti and pro-apoptotic determinants Bax and Bcl-2. It is shown that while Akt regulates Bcl-2 signaling strength, Erk mediates Bax signaling through an as yet undetermined mechanism. The re-balance in the Bax and Bcl-2 levels of LOI cells is shown to make the cells more vulnerable to Bcl-2 inhibition by the computational model that is developed further to include Bax, Bcl-2 signaling. The computational model further predicts, based on the spread in the values of Bax and Bcl-2 in individual cells, a window of values of Akt inhibition for which LOI cells apoptose while WT cells don't. This method of apoptosis is shown to involve activated Bax and the intrinsic apoptosis pathway of Caspase-9 and -3. Finally a stochastic model based on a random process called renewal process is developed to model the stem-cells of the colon crypt and is used to validate known parameters of crypt homeostasis.

Contents

Abstract ii
Introduction 1
Chapter 1 : Re-balance in the IGF-2 signaling network 7
Chapter 2 : Propagation of network re-balance and physiological implications 19
Chapter 3 : Increased sensitivity of LOI cells to IGF-1R kinase inhibition. 23
Chapter 4 : IGF-1 response 27
Chapter 5 : Stochastic model for the stem cell compartment 29
Discussion 35
Network Re-balance 35
Erk signaling determines and sustains the IGF-2 LOI phenotype 36
Propagation of network re-balance and apoptotic susceptibility 37
“Oncogene addiction” 37
Therapeutic Window 38
IGF-2 vs IGF-1 39
Development of colonic crypts 39
Stochastic Model 39
Materials and Methods 41
Computational model of IGF-2 signaling 43
Supplementary Figures 49
References 59

List of Tables

Table 1 : Parameters used in the rate equations (R.1 to R.12) - Values and method of estimation. 44
Table 2 : Initial values for system variables 46
Table 3 : Parameters / Variables changed in model to predict WT behavior. 47
Table 4 : Steady state values of Bax, Bcl2 and associated constants 48

List of Figures

Figure 1.1 : Loss of Imprinting of IGF-2 rewires the IGF-2 signaling pathway 8
Figure 1.2 : *Ligand induced short term receptor degradation* : 9
Figure 1.3 : *Rate of receptor internalization* 10
Figure 1.4 : *Ligand induced long term receptor transcription* 10
Figure 1.5 : *Internalization of receptors regulates Erk activation* : 11
Figure 1.6 : *Akt dynamics is driven by receptor degradation, recycling and cell surface phosphatases* 12
Figure 1.7 : *Erk signaling mediates long-term IGF1R transcription* 14
Figure 1.8 : *Erk signaling mediates IGF1R degradation* 14
Figure 1.9 : *Erk mediates IGF1R ubiquitination* 15
Figure 1.10 : *Systems model for IGF-2 signaling* 16
Figure 1.11 : Training, testing and prediction : 17
Figure 1.12 : *Positive feedback and thresholding effect* : 18

Figure 2.1 : *Bax and Bcl-2 show altered balance in LOI and WT cells* 19
Figure 2.2 : *Bax, Bcl-2 joint distribution:* 20
Figure 2.3 : *Anti/Pro- apoptotic panel* : 21
Figure 2.4 : *Erk regulates Bax not Bcl-2* 21
Figure 2.5 : *Computational model extension for Bax, Bcl-2 signaling* : 22

Figure 3.1 *NVPAEW541 abolishes Akt signaling selectively* 23
Figure 3.2 : : *Increased susceptibility to Bcl-2 inhibition* 24
Figure 3.3 : Enhanced sensitivity of LOI cells to Akt inhibition 25
Figure 3.4 : *Activated Caspase-9, Caspase-3 and Bax* 26

Figure 4.1 : LOI and WT response to IGF-1 28

Figure 5.1 : Model description of the Stem-Transit amplifying-Terminally differentiated cells renewal program of the colonic crypt homeostasis. 29
Figure 5.2 : The three forms of cell division in the stem cell pool 30
Figure 5.3 : The renewal process and renewal reward process : 32

List of Supplementary Figures

Figure S 1 : Receptor expression 49
Figure S 2 : Fold increase in pErk and pAkt 50
Figure S 3 : Total Akt and Erk 51
Figure S 4 : Multiple WT and LOI lines 52
Figure S 5 : Multiple cell lines quantification 53
Figure S 6 : Bulk Internalization 53
Figure S 7 : β-Arrestin and Mdm2 54
Figure S 8 : cMyc induction and expression 55
Figure S 9 : Bcl2 levels are affected by Akt signaling 56
Figure S 10: Bcl2 levels are not affected by Erk signaling 57
Figure S 11 : Activated Caspase-9 and -3 58
Figure S 12: Annexin V staining 58
Figure S 13: IGF-2 expression 59

Introduction

Fundamentals of epigenetics : Epigenetics refers to the set of changes, that doesn't involve a change in the underlying DNA sequence, inherited during both mitosis and meiosis, that drives different phenotypes and cellular outcomes. Epigenetic changes like DNA methylation and histone modification can cause a wide array of changes in gene expression profiles in cells and are known to regulate most biological processes. A change in an epigenetic state or an establishment of a new epigenetic state can often require an extracellular signal that when propagated into the nucleus can change the chromatin state of the cell recruiting modifiers and a slew of cellular machinery thus establishing a stable heritable state. Such stable changes can also drive deregulated growth thereby making epigenetic changes a recurrent theme in all states of progression of various tumors and cancers. Thus epigenetic changes are not only involved in the fundamental processes of growth, differentiation and organization but can also drive deregulated growth and malignancy (Feinberg, 2013).

Imprinting : Imprinted genes, which are found only in mammals and flowering plants, are genes that are epigenetically silenced depending on the parental nature of origin. For example, in humans, the maternal copy of IGF-2, a secreted hormone, is imprinted and epigenetically silenced while the paternal copy is expressed (Hu et al., 1997). In the case of IGF-2R, a mannose-6-phosphate receptor, the reverse is the case as the maternal copy is expressed and the paternal copy is silenced. The epigenetic imprinting is achieved by a series of methylation marks that silences the gene. In humans the IGF-2 locus is found in a region of Chromosome 15 that contains many imprinted genes. The silencing is achieved via the binding of CTCF to the imprinting control region (ICR) of the H19 gene and a differentially methylated region (DMR-1). The binding of CTCF prevents access to the enhancer elements that are used for IGF-2 expression. Thus imprinting is an epigenetic mechanism that tightly regulates the expression of genes (Ulaner et al., 2003a; Ulaner et al., 2003b; Yang et al., 2003).

IGF-2 significance and loss of imprinting : IGF-2 is a secreted growth hormone used predominantly in mammalian embryos to achieve exponential growth in tissue and size. IGF-2 along with IGF-1 (Insulin like growth factor-1), Insulin, their cognate receptors IGF-1R and Insulin receptor (IR) and six high-affinity binding proteins form a closely related signaling axis that regulate important cellular processes like survival, proliferation, metabolism and cellular differentiation amongst many other (Baserga et al., 1997). Although the IGF-2 expression is tightly regulated in tissues by epigenetic imprinting, the imprinting can be lost spontaneously in a tissue specific manner referred to as the Loss of Imprinting (LOI) of IGF-2. LOI of IGF-2 in the colon, leading to an approximately 2-fold increase in expression, results in abnormally elongated crypts in the colonic mucosa accompanied by a 5 fold increase in the probability of colorectal adenocarcinoma when compared with the general population (Sakatani et al., 2005). Similarly in the bones, LOI of IGF-2 can lead to Osteosarcoma (Ulaner et al., 2003a), one of the most

common forms of bone cancer. Also, LOI of IGF-2 in the kidney and peripheral blood leukocytes is accompanied by increased somatic overgrowth (gigantism) and increased predisposition to Wilms' tumor, a nephroblastoma seen in children (Ogawa et al., 1993). Thus the regulation and maintenance of imprinting of IGF-2 is an increasingly important factor for normal homeostasis in cells and tissue.

IGF-1R signaling : IGF-2 signals through the IGF-1R, a classic growth factor receptor tyrosine kinase, causing the phosphorylation and activation of the two downstream kinases Akt and Erk. IGF-1R and Insulin receptor (IR) share extensive (approx. 70%) sequence and structural homology and are remarkably similar in their size and exon organization (Ullrich et al., 1986). Both IGF-1R and IR are synthesized as single pro-receptor with a 30 aminoacid signal peptide that is removed during translocation. The modified and glycosylated pro-receptor is cleaved at a Arg-Lys-Arg-Arg site to generate an alpha and a beta sub-unit. These alpha and beta sub-units are linked via di-sulphide bonds to assemble the functional IGF-1R which is a hetero-tertramer composed of two alpha and two beta sub-units respectively. The alpha sub-units are fully extracellular while the beta units span the membrane and contain the cytoplasmic tyrosine kinase signaling domain (Ward and Garrett, 2004). IGF-1R can also form hetero-tetramers with IR isoforms. IR has two isoform, IR-B and IR-A. IR-B is predominantly expressed in the muscle, adipose tissue and the liver and is used in the regulation of glucose uptake while IR-A which is usually expressed in embryonic tissue and in certain tumors has great affinity for binding IGF-2 (Sciacca et al., 2002). The IGF-2R on the other hand is a generic Mannose-6-phosphate receptor and lacks the intrinsic cytoplasmic kinase activity of the IGF-1R. The IGF-2R acts to bind, sequester and degrade IGF-2 (Nolan et al., 1990).

On binding its ligand, IGF-1R undergoes a conformational change and autophosphorylates the tyrosines Y1131, Y1135 and Y1136 on its cytoplasmic tail. The tyrosine residues Y1131, Y1135 and Y1136 form the important activation loop, the tyrosine Y950 serves as a docking site for important signaling molecules and the lysine K1003 binds ATP (Baserga, 2005). The phosphorylated tyrosines recruit adaptor molecules like IRS-1 and activate Akt via the PI3k pathway (Baserga et al., 1997; Pollak, 2012). The phosphorylated IGF-1R also recruits factors like Shc, Grb2 and Sos and activates Erk via Ras and the MAPK pathway (Baserga et al., 1997; Peruzzi et al., 1999; Pollak, 2012). Akt, a ser/thr kinase, plays a central role in glucose metabolism, transcription, translation, apoptosis and survival signaling, cellular proliferation, differentiation and migration. Erk, which is also a ser/thr kinase, plays an important role in proliferation, cell cycling and differentiation. Activated Erk translocates into the nucleus and activates a host of transcription factors that regulate many cellular processes. Although both Akt and Erk are downstream effectors of the IGF-1R, their relative strengths can be affected by many of the adaptor complexes and processes that can independently regulate the kinases. In smooth muscle cell culture, a shift in the balance of signaling from PI3k to Erk signaling induced by different growth factor receptors can cause the cells to de-differentiate (Hayashi et al., 1999). Recently it was shown that in PC-12 cells, a two-dimension Erk-Akt signaling scheme determined

cell-fate decision in response to NGF (Chen et al., 2012). Thus IGF-2, acting through the IGF-1R can cause differential fates in cells depending on the Akt, Erk signaling strength.

Receptor trafficking : The signaling activity of IGF-1R and other growth factor receptors in general are regulated by endocytosis and intracellular trafficking (Burke et al., 2001). Activated receptors are clustered into pits (small invaginations in the cell membrane) and internalized rapidly into these clathrin coated pits (Ramanan et al., 2011). These pits then pinch off from the membrane and form vesicles that the receptors continue signaling from. These vesicles can then either fuse with vesicles coming out of the transgolgi and recycle back to the membrane or be targeted to the lysosomes for degradation(Sorkin and Goh, 2009). Receptors that are targeted to the lysosomes for degradation have been known to not bind the ligand anymore and not be in an active state of signaling (Burke et al., 2001). Thus an emerging theme in vesicular trafficking is the modulation of receptor signaling via compartmentalization into vesicles and their trafficking.

In addition to the elements of the endocytic and vesicular trafficking machinery, other known adaptor molecules have known to play a role in modulating activated receptor signaling in the context of Erk and Akt signaling. β-Arrestin 1 and 2 are proteins that play a major role in the desensitization of GPCR / 7 transmembrane receptors signaling. They have been shown to not only play an important role as an endocytic adaptor but to behave as scaffolding structures for the activation of MAP kinases like Erk1/2 and other pathways (Girnita et al., 2007). In fact the β-Arrestin 1 mediated Erk activation was shown to be independent of the second messenger when the classical receptor tyrosine kinase activity is impaired. Another class of molecules that are known to play an important role in receptor signaling are E3 ubiquitin ligases like Mdm2, Nedd4 and c-Cbl. Mdm2 is the regulator of the tumor suppressor protein p53. Mdm2 ubiquitinates p53 and is also known to actively shuttle between the nucleus and cytoplasm controlling the levels of p53. Mdm2 was shown to be involved in ubiquitinating IGF-1R and thus behaving as a E3 ligase (Girnita et al., 2003). Similarly another ubiquitin ligase Nedd4 was shown to associate with IGF-1R and in a dose dependent manner increase the ubiquitination of IGF-1R when stimulated with IGF-1 in mouse embryonic fibroblasts (Vecchione et al., 2003). Recently it was shown that another E3 ubiquitin ligase associated with EGFR signaling, c-Cbl, on ligand stimulation with IGF-1, associated with IGF-1R and polyubiquitinated it. Interestingly it was shown there that Mdm2 associated with IGF-1R at lower doses of IGF-1 while c-Cbl associated with IGF-1R for higher doses of IGF-1. It was also shown that while Mdm2 mediated ubiquitination resulted in a clathrin coated endocytic route for IGF-1R, the c-Cbl mediated ubiquitination resulted in a caveolin mediated endocytic route (Sehat et al., 2008). Thus both adaptor molecules like β-Arrestins and E3 ubiquitin ligases can play an important role in receptor signaling and Erk activation.

Computational models of Erk and Akt signaling : Given the importance of Erk and Akt signaling in cellular homeostasis, the dynamic nature of the Akt, Erk response to different ligands in different growth factor systems, the diverse nature of cellular fates dictated by transient vs sustained response of these kinases and the multiple adaptor proteins and cascades involved in

their activation, these two pathways have been modeled computationally in many different systems. Although there aren't many examples of computational models of IGF-1R signaling in literature, models of Akt and Erk signaling activated via growth factor receptors should prove instructive. A computational model of Heregulin induced Erb receptor (EGFR) activation leading to Akt and Erk signaling suggested substantial cross-talk between the Akt and Erk pathway via PI3k and its phosphorylation of the Ser-259 residue on Raf-1. The model also strongly suggested the modulation of the activity of members of the Akt and Erk pathway by the phosphatase PP2A. In the model, activated receptor-complexes activated PI3k which then activated Akt. The receptor complexes also phosphorylated Shc which then recruited adaptors Grb2, Sos thereby activated Ras. Ras activation initiates the MAPK cascade by activating Raf-1 which also cross-talks with the MAPK pathway (Hatakeyama et al., 2003). Other models of the Akt and Erk pathway include a study that focused on the cross-regulation of EGF and Insulin signaling in HEK293 cells. The model was used to study the effect of Insulin on Erk signaling which is minimal on its own but gets amplified in the presence of very low doses of EGF. The model revealed certain cross-talk mechanisms upstream of Ras and the importance of the critical nodes like Gab1, Shc, IRS-1, Src Kinase, Shp2 phosphatase in amplifying the PIP3 signals that are converted to enhanced Erk activity (Borisov et al., 2009)

Oncogene / IGF-2 addiction : In an in-vivo colon tumor model for IGF-2 LOI, it was seen that the mice displayed an enhanced responsiveness to a drug targeting the IGF-1R kinase function. The mouse model carried a deletion in the H19 gene and an additional 10 kb of the upstream region including the differentially methylated region (DMR) thus regulating the silencing of IGF-2. When treated with Azoxymethane (AOM), the animals formed an increased number of aberrant crypt foci (ACF) in the colon when compared to matched WT (LOI negative) mice. Subsequent treatment with NVPAEW541 a potent inhibitor of the IGF-1R kinase triggered a significant decrease in the number of ACF in LOI mice, while the WT mice showed no change in the number of ACF. Oncogene addiction is a term used in cancer literature to describe the increased dependence of a particular cancer on the oncogene driving it. Such cancer cells are also shown to be increasingly sensitive to inhibition of the oncogene (Sharma and Settleman, 2007). Some of the common driver genes seen in oncogene addiction include Myc, Ras proteins, Epidermal growth factor receptor (EGFR), Platelet derived growth factor receptor (PDGFR), Phosphatase and tensin homologue (PTEN) etc. (Weinstein and Joe, 2008). Thus, the IGF-2 LOI animal model shows an increased dependence on IGF-2 signaling reminiscent of oncogene addiction in cancers.

Colon crypt modeling : Tissue renewal is one of the most important aspects of systemic homeostasis. Organs like the intestine, blood, skin etc undergo various stages of massive renewal throughout the day in a living multicellular organism, such that the cycle of losing cells that perform the function of the organ to various environmental challenges is intricately balanced by the renewal of the organ such that the organ maintains its size and functional organization throughout its life (Frank, 2007). . A considerable majority of the organs employ the classic stem – transit amplifying – differentiated cells renewal program wherein a small pool of

relatively slowly proliferating stem cells (Bach et al., 2000; Ghazizadeh and Taichman, 2001; Potten and Booth, 2002) ensure genomic integrity and form an indefatigable, replenishable source of more functional differentiated cells. As dictated by the architecture of the organ and the needs of the organ, dividing stem cells can, with defined probabilities, either self-renew or differentiate into transit amplifying cells, which no longer have the stem cell property. These transit amplifying cells then rapidly proliferate, make up the core of the structure of the organ and after a certain number of cycles, fully differentiate into the functional cells of the organ. Needless to say, the stem cells, by virtue of their unlimited capacity for cell division, dictate the dynamics of the cell numbers in the crypt. In summary, given the need to maintain genomic integrity and geometrically defined structure of self-renewing organs, stem cells divide infrequently and also employ both symmetric and asymmetric cell divisions to perform the dual nature of maintenance of the stem cell pool and the required number of progeny to differentiate and perform the functional roles of the organ (Morrison and Kimble, 2006; Watt and Hogan, 2000)

The crypts in the colon are perhaps the most well characterized and studied examples of epithelial tissue renewal system. Colonic crypts are minute finger like invaginations in the colonic epithelium that are composed of a single layer of cells and are shaped in the form of a test tube (Simons and Clevers, 2011). The crypts provide a continuous stream of cells mainly enterocytes and goblet cells to the colonic epithelium and are responsible for replenishing the same as they slough off into the lumen of the colon. The crypt is organized into a small pool of stem cells at the bottom (Barker et al., 2007; Bjerknes and Cheng, 2002), a large pool of rapidly proliferating cells along the length of the crypt which constitute the transit-amplifying pool and a pool of fully differentiated non-proliferating cells along the upper third of the length of the crypt. As the self-renewing stem cells divide, the newly formed daughter cells advance up along the length of the crypt and partially differentiate into the cells of the transit amplifying compartment. These partially differentiated cells in the transit amplifying compartment proliferate rapidly and are responsible for supplying differentiated cells to the colonic epithelium at the rate at which they are lost into the lumen of the colon. As the cells in the transit amplifying compartment rise up the length of the colon they stop proliferating, acquire very differentiated phenotypes and become the functional cells of the colonic epithelium (Simons and Clevers, 2011). IGF-2 LOI in the colon alters the balance between undifferentiated and differentiated cells along the length of the crypt. This is also accompanied by an increase in the average length of the crypts.

Noise is inherent in all biological systems, most often manifesting itself as stochasticity in measured responses and observed values of system variables. The stochasticity can be a function of many known and unknown processes and serves to impart useful properties to the system like robustness, variability, ability to recover from crippling errors and such (Wang and Zhang, 2011). In terms of the colonic crypt, there is inbuilt stochasticity in almost every aspect of the dynamics and organization of the crypt i.e., in the density of the number of crypts per unit area of the colonic epithelium, in the number of levels of the cylindrical organization of the

crypt, in the total number of cells in each crypt, in the number of stem cells, number of transit amplifying cells, in the cell cycle time of cells in the different compartments, effectively from the tissue level organization to the cellular details of cell cycling and proliferation (Boman et al., 2008).

Many attempts have been made to develop mathematical models to understand the homeostasis and aberrant behavior, in the case of cancer, of the colonic crypts(Gerike et al., 1998) (Buske et al., 2011; Johnston et al., 2007). Most of the models that have been recently developed are deterministic in nature in that cell cycle analysis, number of stem cells etc are defined by ordinary differential equations (Boman et al., 2008). Although they have been used in other population based systems truly stochastic models have not really been used to describe the behavior of tissue renewal or in this case crypt organization and homeostasis. Stochastic models have the advantage of being able to model the colonic crypt in its true form and account for the noise, randomness and inherent variability that are evident when repeated measurements are made of the crypt parameters. They also have the added advantage that the average behavior of system parameters predicted by the stochastic models will correspond to the values predicted by the deterministic models.

Renewal process is a stochastic random process that is a generalization of the Poisson process (Cox, 1970). It is a counting process on the space of integers and is defined by the time intervals between the occurrence of events and the probabilities of the counting at each such event occurrence. A renewal reward process can be defined on the same renewal process with the incremental changes in the renewal process constituting the counting process (Cox, 1970). As the main events that occur in the stem cell pool are the spontaneous mitosis of the cells into two daughter cells and the probabilistic event of those cells choosing to either stay as stem cells or differentiate (Boman et al., 2007), it is quite easy to note the similarity between the events in the stem cell pool and the renewal process. Furthermore, the main function of the process, formation of appropriate numbers of differentiated functional cells, can be seen as a reward. We can then attempt to model the number of cells in the stem cell pool as a renewal process and the process of differentiation whereby these cells lose their stem cell properties and become the transit amplifying cells as a renewal reward process.

In addition to the simplicity of representation and the inherent stochasticity associated it, both features being very useful when dealing with stem cell differentiation process, the use of renewal theory enables us to take advantage of the vast number of results and theorems developed independently of description of biological processes. As shown below, by using the fundamental theorem of renewal-reward process, for example, we can quite easily derive an equation for the average rate of cells differentiating and exiting the stem cell pool in terms of other parameters that define the stem cell pool. We then use this result to test the validity of a prediction on the cell division time of the stem cells which to date remains not conclusively proven.

Chapter 1 : Re-balance in the IGF-2 signaling network

A previous analysis from our lab and our collaborator's (Kaneda et al., 2007) suggested that there might be important differences in the kinetics of activation of canonical signaling pathways stimulated by IGF-2. Re-examination of the kinetic activation profiles of the two dominant pathways activating the kinases Akt and Erk1/2, surprisingly suggested that, although both these pathways are activated by the same ligand, their maximal activities change in divergent directions in LOI cells vs. WT cells (Fig. 1.1A, 1.1B). More specifically, when stimulated with 100ng/ml of IGF-2, the activity of Akt was significantly attenuated and the activity of Erk -- enhanced in LOI cells vs. WT cells. This result was seen for both the peak values of the temporal activity profiles (Fig 1.1A inset) and for the signaling activities integrated over 3 hr. time period (Supplementary Fig S1). The results of this immunoblot analysis were supported by immunocytochemistry experiments performed on population of single cells (Supplementary Fig S2). The results raised several questions: 1) what is the mechanism of the differential regulation of two pathways, both of which are activated by the same receptor-ligand complex? ; 2) is this mechanism related to the differential expression of the IGF-2 receptor IGF-1R displayed by LOI cells (Kaneda et al., 2007); 3) is the differential change in the pathway activities in LOI vs. WT cells connected to the increased proliferation and elevated sensitivity to IGF-1R kinase inhibition displayed by LOI cells? The following analysis set out to answer these questions.

Although activation of growth factor receptors can lead to enhanced activities of both Erk and Akt pathways (Lemmon and Schlessinger, 2010; Siddle, 2011), the intracellular signaling compartments supporting these pathways are distinct (Jullien et al., 2002) (Vieira et al., 1996). Indeed, prior studies suggested that the Akt pathway is preferentially activated at the plasma membrane, whereas the Erk pathway -- in the internalized vesicles (Biedi et al., 2003) (Chow et al., 1998) (Vasilcanu et al., 2008). Therefore receptor internalization or recycling can increase the propensity for activation of one of the branches of the signaling network at the expense of the other (Holbrook et al., 1999) (Sorkin and von Zastrow, 2009) (Tan et al., 2013) thus rebalancing the pathway activities within the signaling network (Chen et al., 2012) (Lu et al., 2011; Ren et al., 2010; Worster et al., 2012) The increased accumulation of IGF-2 in the vicinity of LOI cells associated with doubling of the copy of the active IGF-2 can increase signal mediated receptor internalization, creating potential for network rebalancing (Clemmons, 2007). We indeed observed significant ligand-induced internalization and concomitant degradation of IGF-1R over 3 hrs. in LOI but not WT cells (Fig. 1.2A, B and Fig 1.3). Receptor degradation was completely abrogated by inhibitors of lysosomal (Chloroquine) and proteasomal (MG132) degradation (Fig. 1.2A). Surprisingly, longer term stimulation of LOI but not WT cells also revealed an increase in transcriptional regulation of IGF-1R (Fig. 1.4). These results suggested that both the amount and the localization of the IGF-1R can be controlled by IGF-2 mediated signaling in LOI cells.

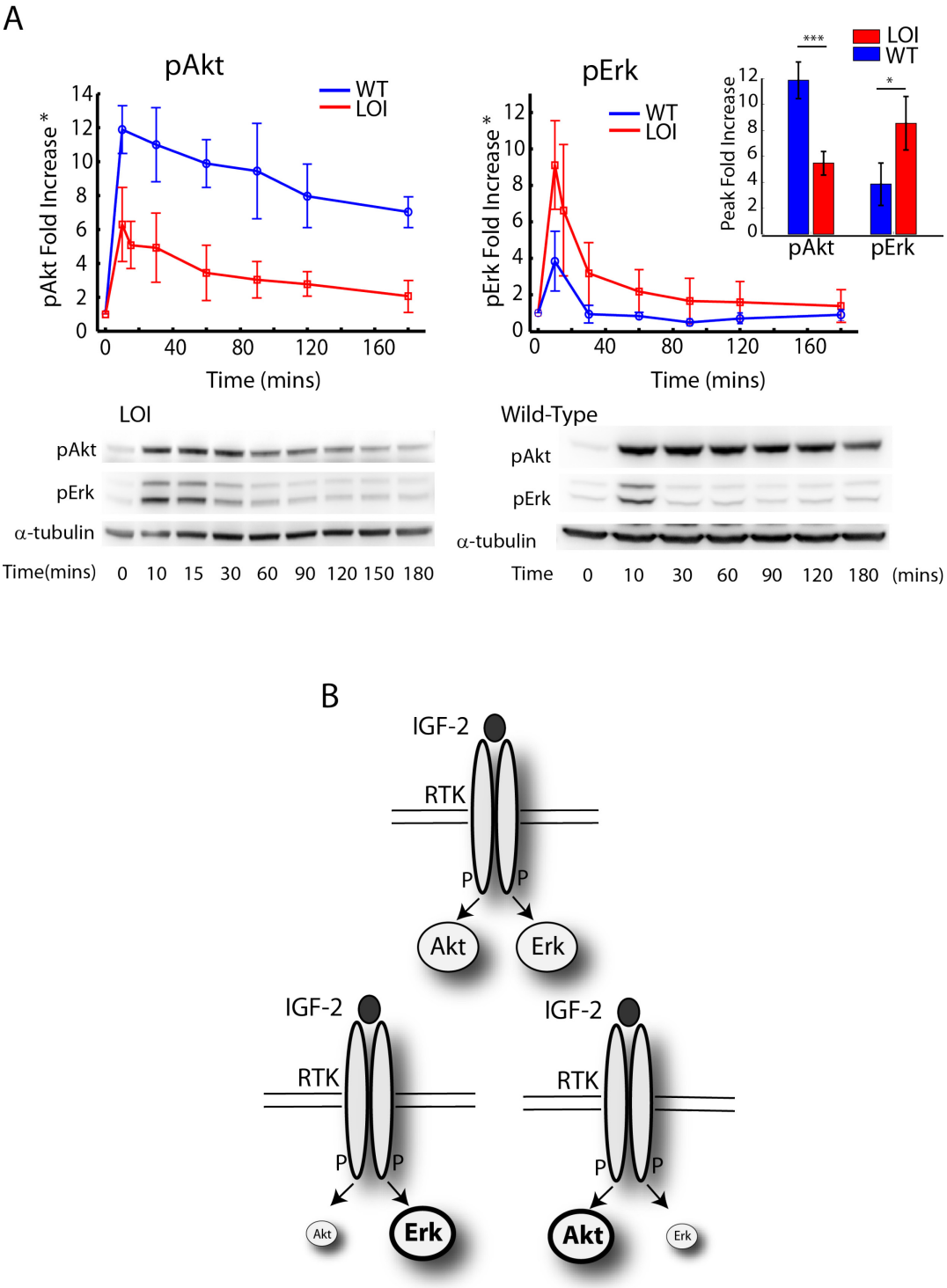

Figure 1.1 : Loss of Imprinting of IGF-2 rewires the IGF-2 signaling pathway

Exponentially growing LOI and WT cells were serum starved overnight and stimulated with IGF-2 100ng/ml for the indicated time points, harvested and analyzed by Western blotting. A) The pAkt profiles for both LOI and WT cells peak at 10 minutes and adapts to a steady state value while the pErk profiles for both WT and LOI cells peak at 10 minutes and then returns to basal levels by 30 min. LOI cells show a much stronger pErk stimulation as opposed to a much weaker pAkt stimulation when compared to WT cells (Inset: Peak values at t=10 min, Student's t test with N=3) B) Re-balancing of the IGF-2 signaling network.

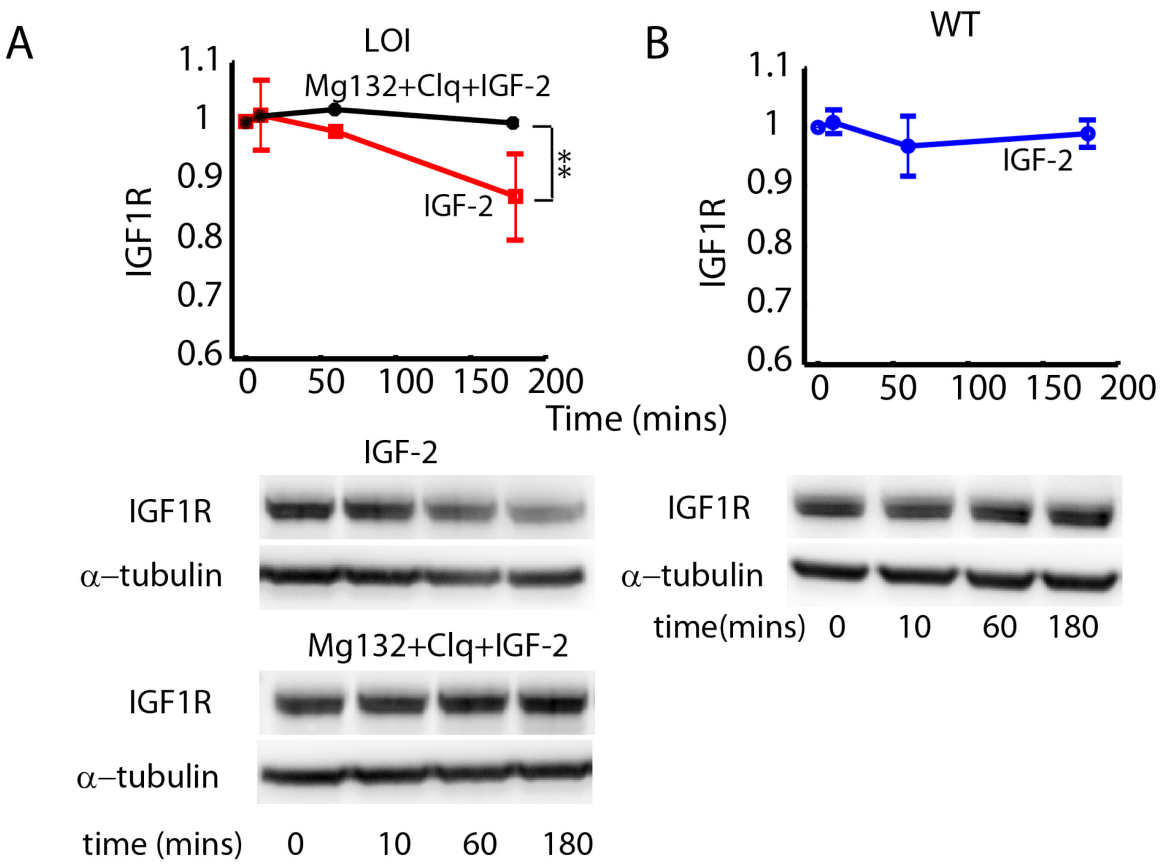

Figure 1.2 : ***Ligand induced short term receptor degradation*** **:**

A,B) LOI and WT cells were serum starved overnight, stimulated with IGF-2 (100ng/ml) for the indicated time points, harvested at the end of it and analysed by Western blotting after normalizing every band by value t=0. The same experiment was repeated with inhibitors of lysosomal (Clq) and proteasomal (Mg132) degradation and plotted in black. Statistics used – student's t test with N=3.

Does the receptor internalization affect Erk and Akt signaling (alt. does it lead to 'rebalancing of the network'?) A small molecule inhibitor of receptor endocytosis Monodansylcadaverine (MDC) (McMahon and Boucrot, 2011; Schutze et al., 1999) completely abolished Erk signaling in LOI cells (Fig. 1.5A). On the other hand, the Akt signaling, although mildly attenuated, occurred with similar dynamics in the absence of the receptor internalization (Fig. 1.5B). This result supported the importance of receptor trafficking in differential stimulation of the branches of the signaling network, but also raised the question of what might account for adaptation of Akt activity in the absence of receptor internalization? Potential mechanisms include reduction of the amount of

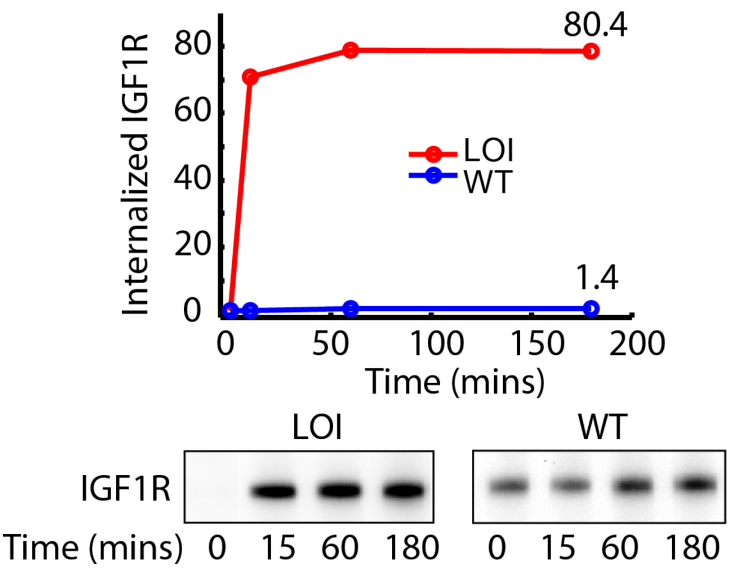

Figure 1.3 : ***Rate of receptor internalization***

Cell surface receptors of LOI and WT cells were biotinylated with NHS-biotin on ice, treated with IGF-2(100ng/ml) and allowed to internalize at 37degC for the indicated times and then harvested after the remaining surface biotin was cleaved. The internalized Biotin was pulled down with Streptavidin beads and analyzed by Western blotting.

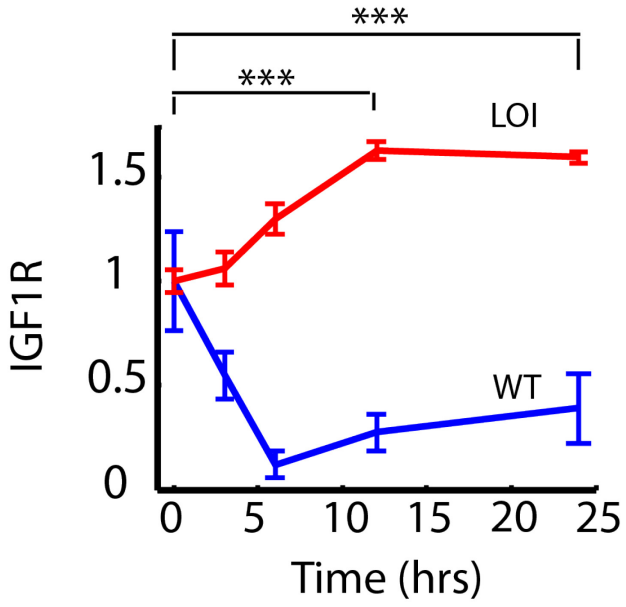

Figure 1.4 : ***Ligand induced long term receptor transcription***

LOI and WT cells were serum starved overnight, stimulated with IGF-2(100ng/ml) for the indicated time points, harvested and analysed by qRT-PCR. IGF1R expression was normalized against β-Actin in each well and further normalized to respective values at t=0 and plotted as a function of time. Statistics used student's t test with N=3.

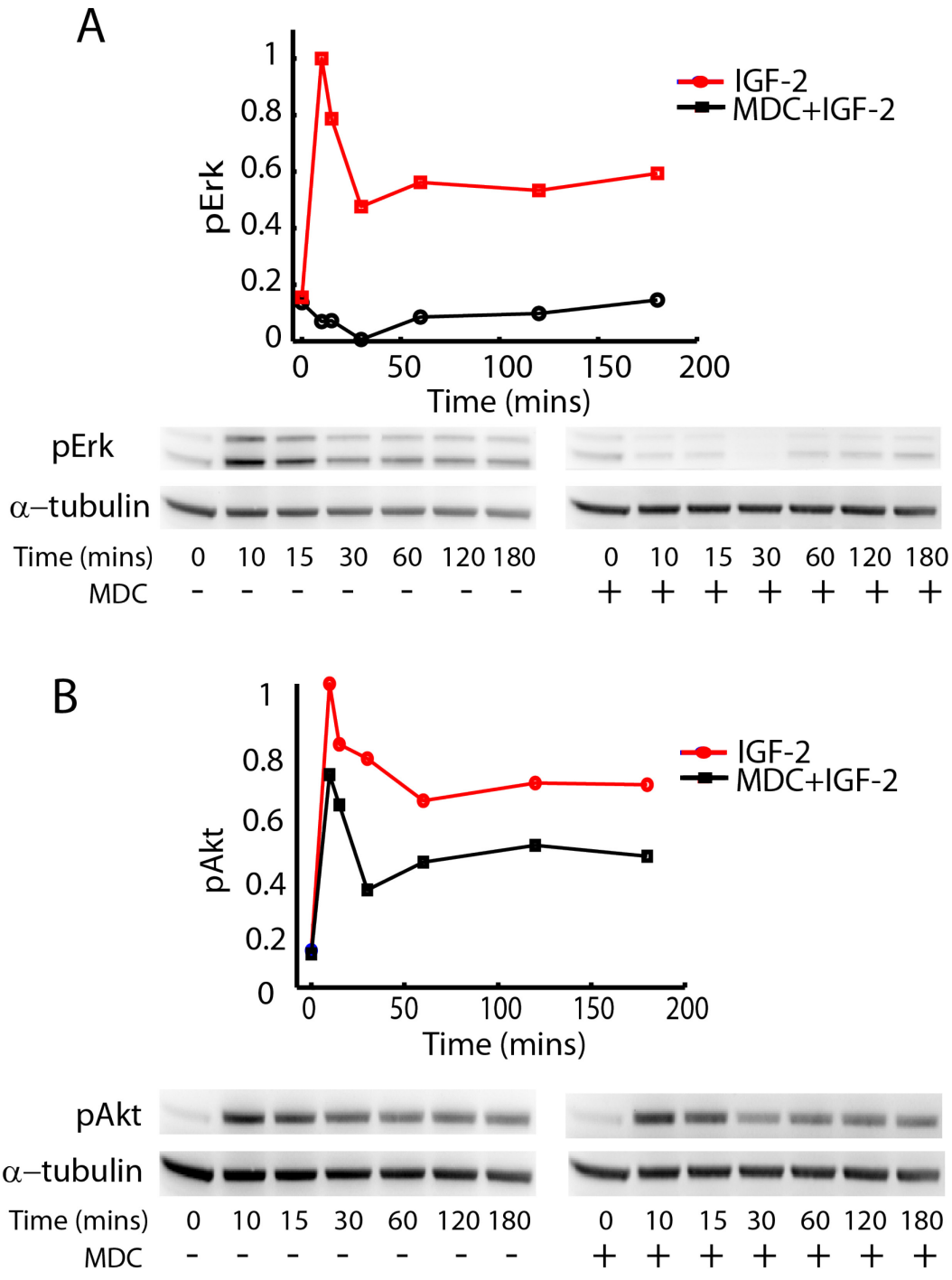

Figure 1.5 : ***Internalization of receptors regulates Erk activation*** **:**

LOI cells were serum starved overnight and treated with either 100µM MDC (Monodansylcadaverine) for 1 hour followed by IGF-2 or just IGF-2 for the indicated timepoints, harvested and analysed by Western blotting. A) Internalization inhibition abrogates Erk signaling while B) retaining all the elements of Akt signaling.

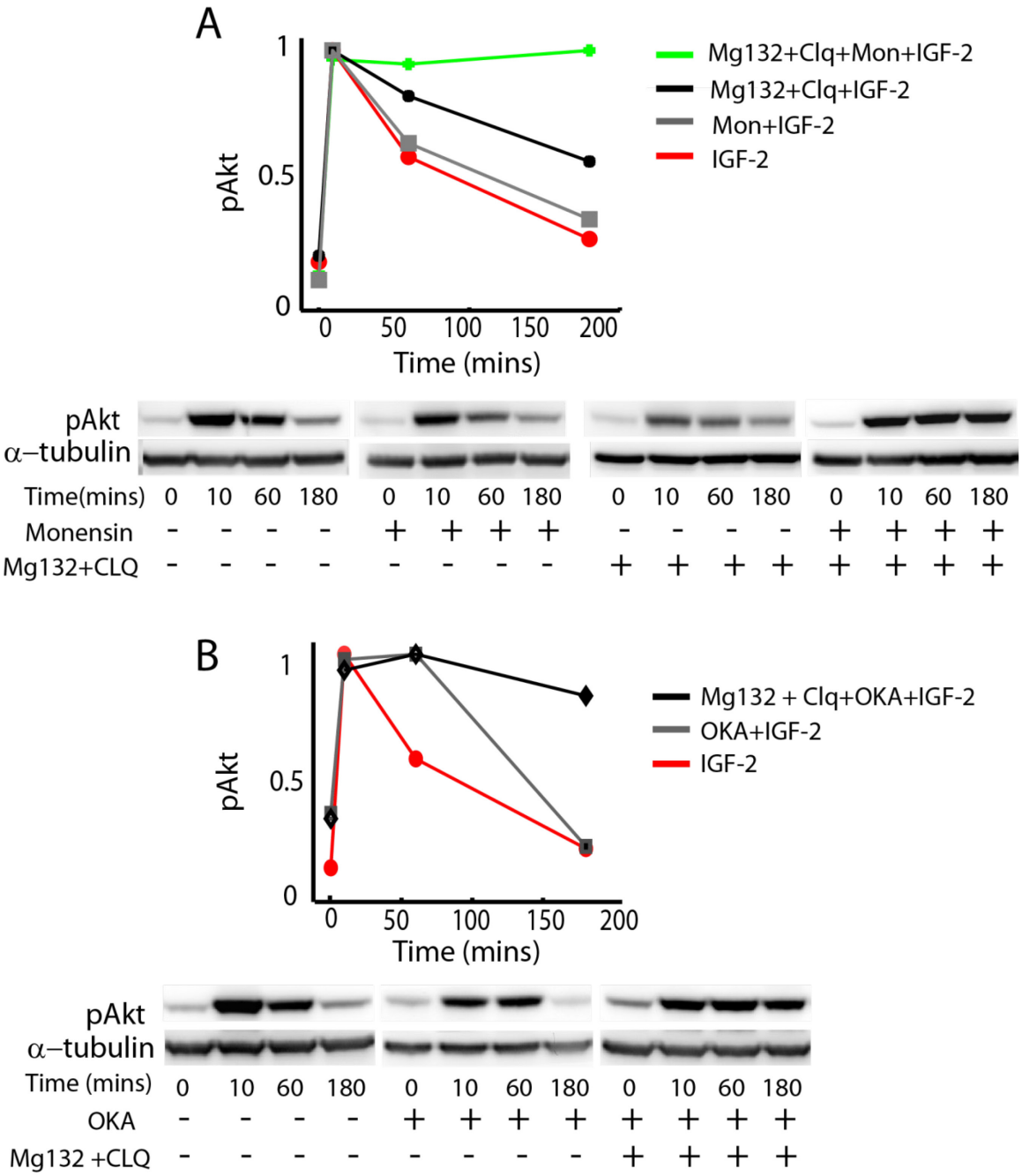

Figure 1.6 : ***Akt dynamics is driven by receptor degradation, recycling and cell surface phosphatases***

Exponentially growing LOI cells were serum starved overnight and treated with either Monensin Sodium (recycling inhibitor) or a combination of Mg132(proteasomal inhibitor) + Chloroquine(lysosomal inhibitor) or a combination of all the three for 60 minutes followed by IGF-2 stimulation for 10 minutes, harvested and analyzed by Western blotting. C) Receptor recycling to the surface and receptor degradation cause the adaptation of pAkt levels from their peak values to a steady state value. As in the previous experiment cells were treated with Okadoic Acid (OKA - inhibitor of the cell surface pAkt phospatase -PP2A) instead of Monensin and analyzed via Western blotting. D) It can be seen that by inhibiting the cell surface Akt phosphatases and receptor degradation the same result can be obtained as before.

active receptors due to receptor degradation (Fig. 1.2A) (Girnita et al., 2003), other aspects of receptor trafficking and phosphatase activity at the plasma membrane. To explore these possibilities, we first used the cocktail of inhibitors of receptor degradation (MG132 + Chloroquine) and vesicle recycling (Monensin) (Marnell et al., 1982). This cocktail completely abolished the adaptation in Akt response (Fig. 1.5 A), whereas either the inhibitor of degradation or inhibitor of recycling alone failed to do so (Fig. 1.5A). The effect of the cocktail was replicated when Okadaic acid -- an inhibitor of cell surface phosphatase PP2A (Liu et al., 2003) was used instead of Monensin (Fig. 1.6A). Okadaic Acid or the receptor degradation inhibitors used separately failed to abrogate the Akt adaptation (Fig. 1.6B). These results, in combination, suggested that an increased receptor internalization in LOI cells can indeed lead to preferential activation of Erk, with the activity of Akt regulated at the plasma membrane by both the availability of the receptors and the action of the plasma membrane localized PP2A.

The observation of a long term increase in IGF-1R transcription and preferential activation of the Erk pathway in IGF-2 stimulated LOI cells suggested that Erk might influence IGF-1R expression in a feedback fashion. Indeed, we found that a Mek inhibitor U0126, which abolishes Erk signaling, abrogated the increase in the IGF-1R mRNA levels, after LOI cell stimulation with IGF-2 over a period of 24 hours (Fig. 1.7). Interestingly, when analyzed over a shorter term (15 min.), LOI cells pre-treated with U0126 and stimulated with IGF-2 showed a significant increase in IGF-1R protein levels (Fig. 1.8). This result suggested that the Erk pathway might also control the short term receptor degradation following IGF-2 mediated cell stimulation. Indeed, we observed that, in the presence of a proteasomal inhibitor MG-132 used to prevent the degradation of ubiquitinated proteins and to enhance their detection, the Mek inhibitor U0126 decreased ubiquitination of IGF-1R (Fig. 1.9). Since it was shown previously that ubiquitination of IGF1R is a necessary step for its internalization (Sehat et al., 2007), these results suggest that enhanced activity of the Erk signaling pathway in LOI cells can regulate both the short term

receptor internalization and degradation, and a longer term receptor synthesis.

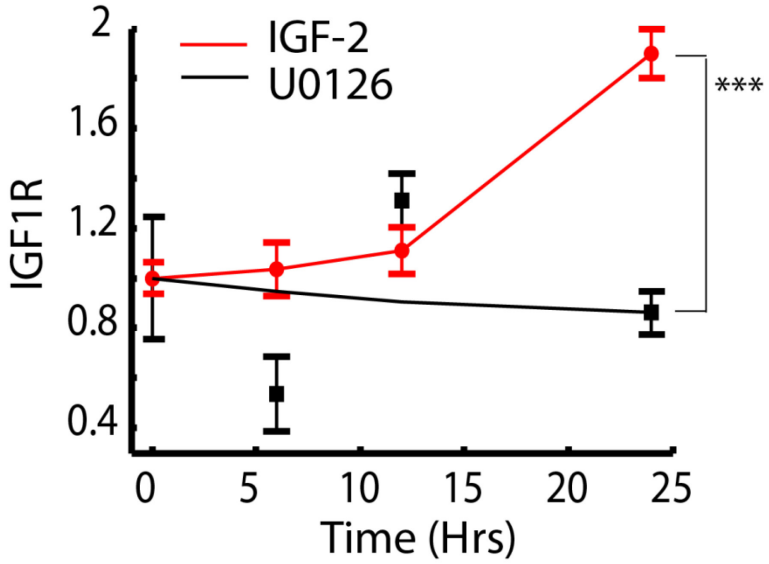

Figure 1.7 : ***Erk signaling mediates long-term IGF1R transcription***

LOI cells were serum starved overnight and treated with the Mek inhibitor U0126 (or no inhibitor in the case of positive control) for 60 minutes, stimulated with IGF-2 for the timepoints indicated and analysed by qRT-PCR for IGF1R expression. The IGF1R expression in each well was normalized to the β-Actin and plotted as fold expression over value at t=0. Use of the Mek inhibitor abolishes the Erk mediated IGF1R long-term transcription seen in LOI cells. Statistics used, student's t test with N=3

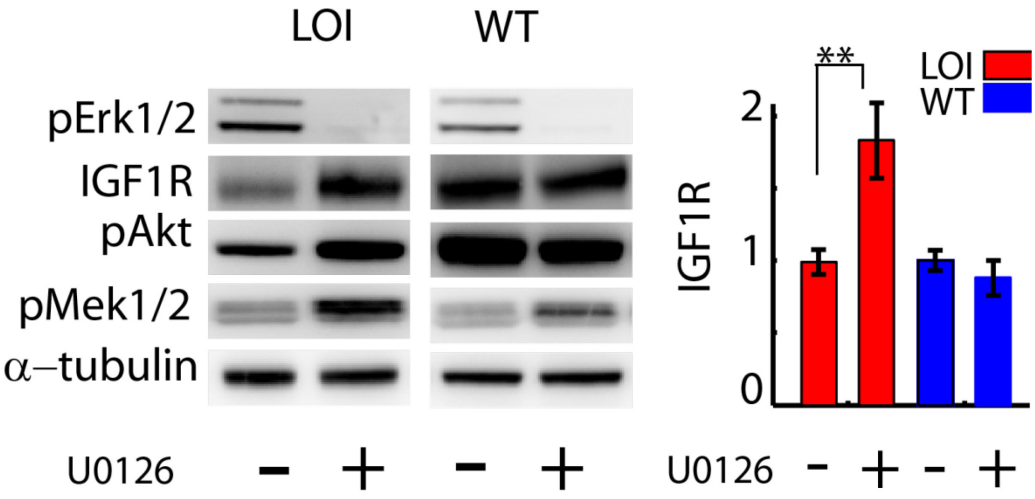

Figure 1.8 : ***Erk signaling mediates IGF1R degradation***

LOI and WT cells were serum starved overnight and treated with the Mek inhibitor U0126 (or no inhibitor in the case of positive control) for 60 minutes, stimulated with IGF-2 for 10 minutes, harvested in lysates and analysed by Western blotting. Increased IGF1R levels in LOI cells show an Erk mediated short-term degradation while the IGF1R levels stay the same in WT cells. The pAkt levels mirror the IGF1R levels.

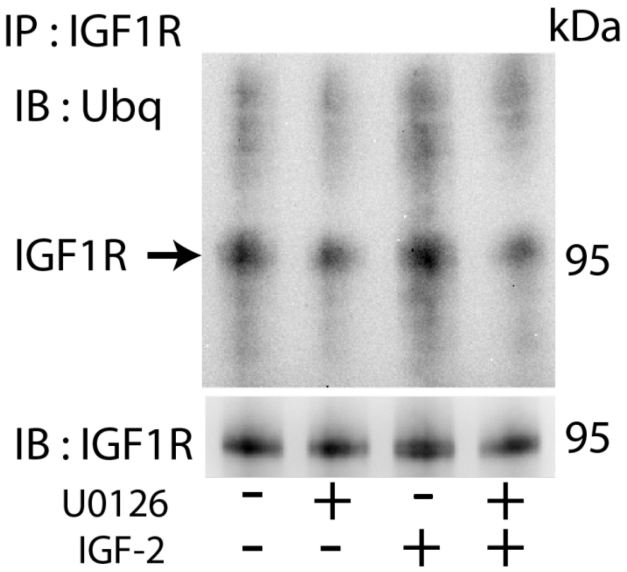

Figure 1.9 : ***Erk mediates IGF1R ubiquitination***

LOI cells were serum starved overnight and treated with MG132 (proteasomal inhibitor), U0126 (Mek inhibitor) or no U0126 for control, IGF-2 for 10 minutes, harvested in lysates and immunoprecipitated with anti-IGF1R antibodies. The samples were then analyzed by immunoblotting with anti-Ubiquitin and anti-IGF1R antibodies. Mek inhibitor decreases / abolishes the Erk mediated IGF1R ubiquitination driven by IGF-2 stimulation.

The results above thus suggested that a feedback loop may exist in LOI cells, in which the Erk pathway can enhance its own signaling activity by increasing internalization and synthesis of IGF-1R. This positive feedback might help explain elevated levels of expression of this receptor found in LOI cells and enhanced Erk-dependent proliferation of these cells. To explore this possibility further, we developed a computational model of the IGF-2-IGF-1R-Akt-Erk signaling network (Fig. 1.10), which we trained on the experimental datasets shown in symbols in the left hand panels of Figs 1.11 (also in Fig. 1.1A). The model prediction for the dynamics of the WT cell responses, simulated under the assumption that these cells were only different from LOI cells in terms of the receptor expression and rate of its internalization, qualitatively matched the experimental data (in blue, top and bottom right panels Fig. 1.12). The computational model further predicted that the Erk mediated positive feedback impinging on receptor regulation could lead to a sustained increase in both receptor expression and Erk signaling, usually associated with the LOI phenotype. This result suggested that the enhanced expression of the IGF-2 ligand can ultimately trigger a new state of the cell, characterized by an enhanced Erk signaling, decreased Akt signaling, and elevated IGF1R expression.

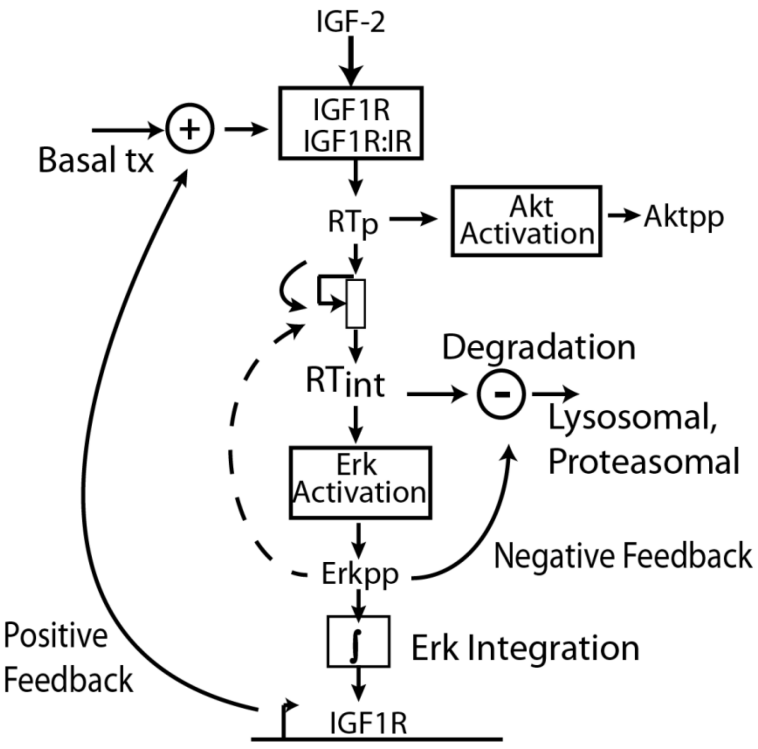

Figure 1.10 : ***Systems model for IGF-2 signaling***

Model incorporating all the elements of LOI signaling driven by IGF-2 stimulation

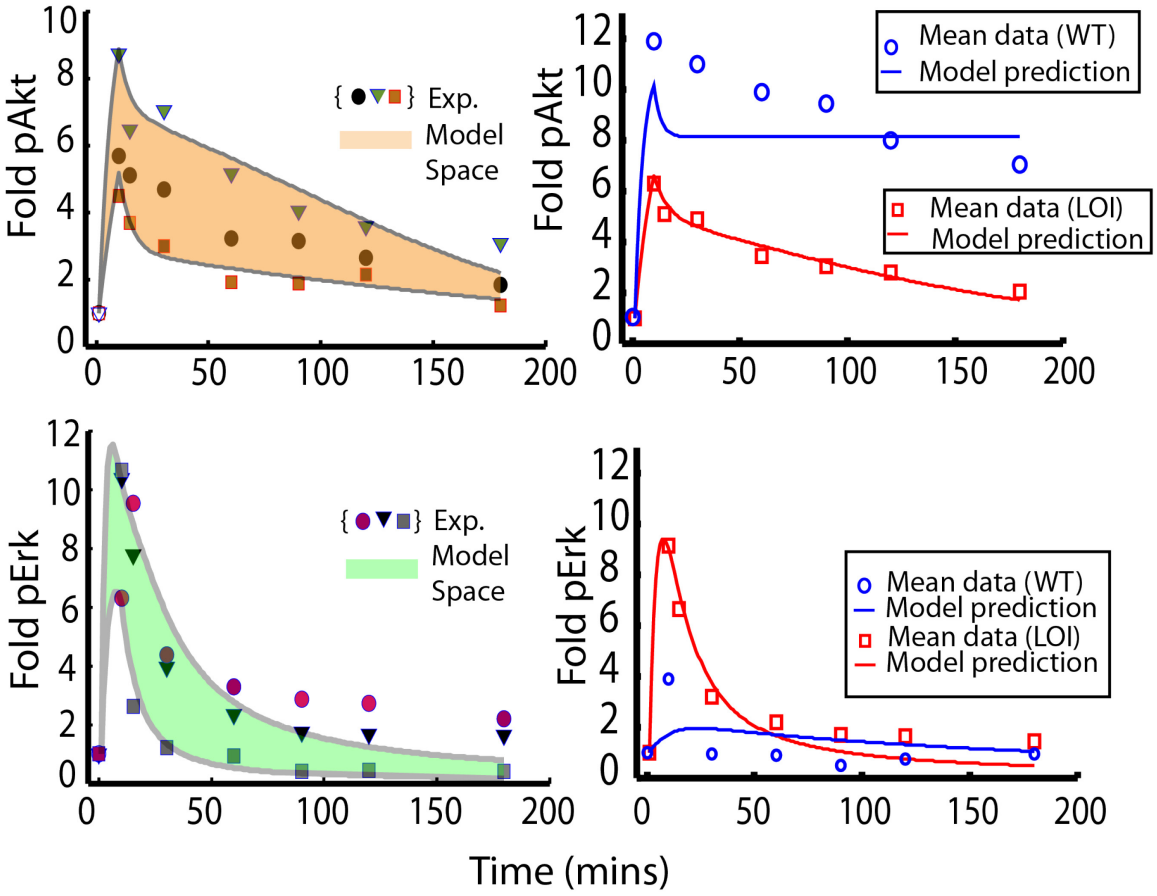

Figure 1.11 : Training, testing and prediction :

The model was trained on 3 sets of experimental data used before to obtain the pAkt and pErk profiles of LOI cells stimulated with IGF-2 cells. 3 sets of parameters of the model were estimated based on the 3 sets of data and the corresponding model fits are shown in the left panels. The 3 sets of parameters estimated from the data were then averaged to obtain the trained mean set of parameters. This model was then used to predict the average pAkt and pErk response of the LOI cells to IGF-2 as shown in red in the panels on the right. The number of IGF1R, IGF1R:IR and the internalization rate of the model were changed to stimulate WT behavior and the model prediction for pAkt and pErk of WT cells to IGF-2 is shown in blue

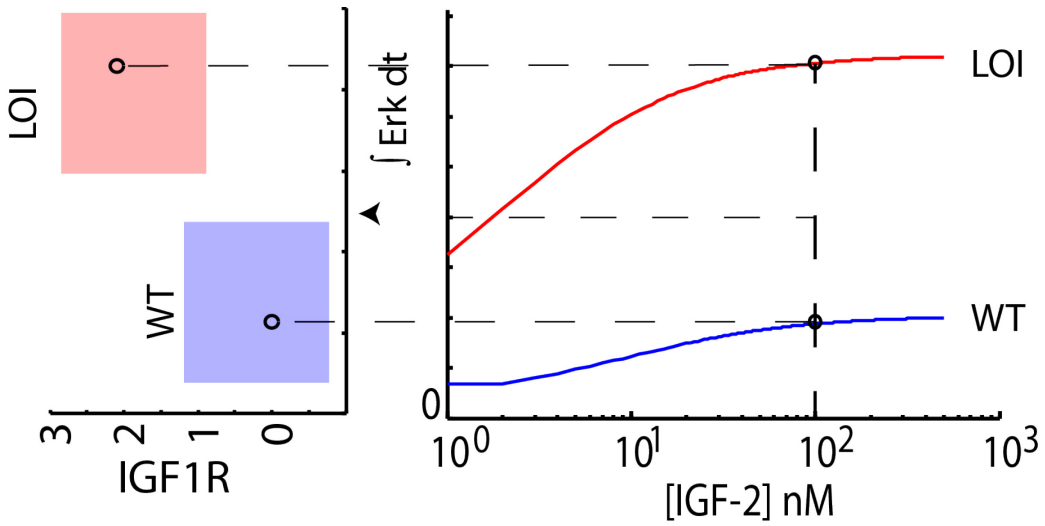

Figure 1.12 : ***Positive feedback and thresholding effect*** **:**

The Erk mediated positive feedback on IGF1R can be used to explain the difference in LOI and WT cells and postulate the presence of a threshold. The Erk integration is plotted for values of IGF-2 and the IGF1R transcriptional feedback as a function of the Erk integration.

Chapter 2 : Propagation of network re-balance and physiological implications

What are the consequences of altered balancing of the Erk and Akt signaling pathway activities in LOI vs. WT cells, particularly in regulation of cell survival when challenged with the IGF-1R kinase inhibitors? Both of these signaling pathways have the potential to control cell proliferation and survival, in part through regulation of the balance of abundance of pro- and anti-apoptotic Bcl family proteins (Kennedy et al., 1997) (Scheid et al., 1999). We indeed found that Bax, a pro-apoptotic member of the Bcl family, was overexpressed in LOI cells vs. WT cells following IGF-2 stimulation (Fig. 2.1A). Conversely, Bcl-2, an anti-apoptotic member of the Bcl family was expressed at lower levels in LOI cells under the same conditions (Fig. 2.1B).

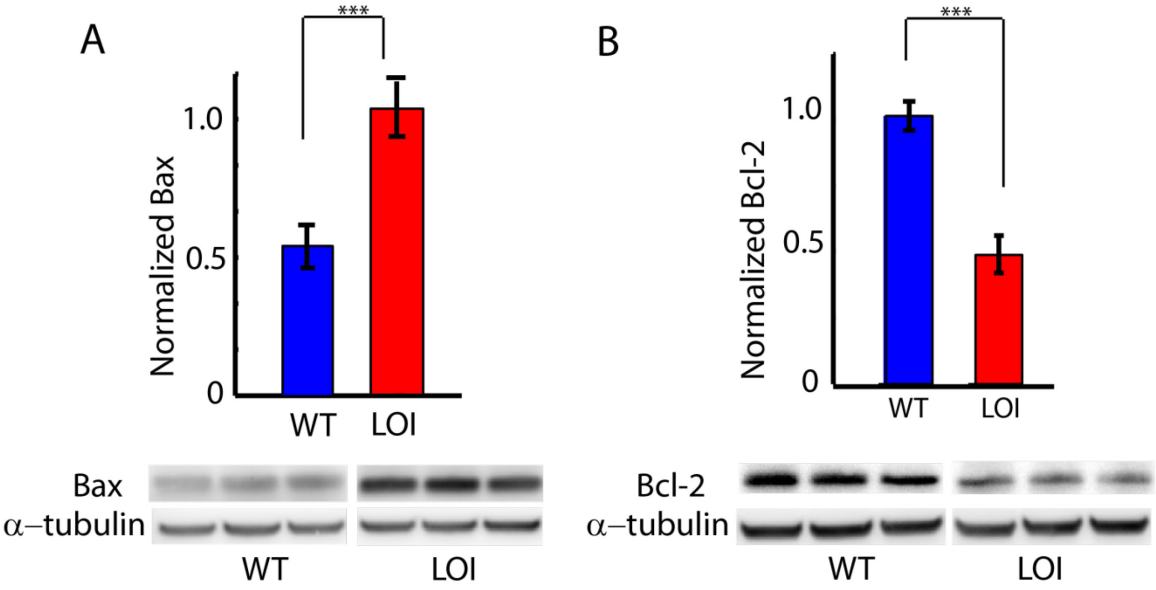

Figure 2.1 : ***Bax and Bcl-2 show altered balance in LOI and WT cells .***

Exponentially growing WT and LOI cells were serum starved overnight and stimulated with 10%FBS for 24 hours, harvested in lysates and analyzed by Western blotting for A)pro-apoptotic Bax and B)anti-apoptotic Bcl-2. Student's t test was used with N=3

The change in the balancing between Bax and Bcl-2 in WT vs. LOI cells was confirmed in individual cells double-stained using antibodies against these proteins (Fig. 2.2). Examination of expression of other members of the Bcl-2 protein family suggested the roles of other pro and anti – apoptotic proteins like Bak-1 and Bcl-Xl, although their levels were not significantly different between WT and LOI cells (Fig. 2.3). To explore a possible relationship with differential signaling activity in LOI cells, we determined whether Bax or Bcl-2 expression levels would be

affected by the perturbation of the IGF-2 stimulated signaling activities. We found that LOI cells pre-treated with the Mek inhibitor U0126 at various doses followed by IGF-2 stimulation for 24

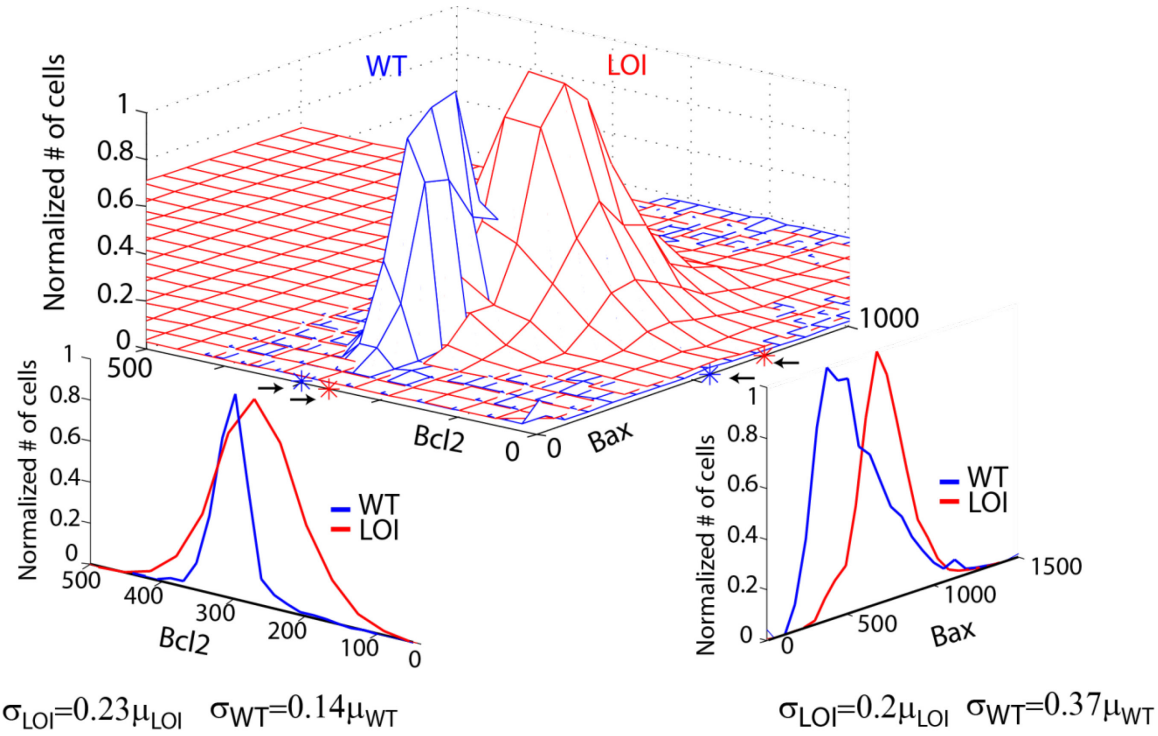

Figure 2.2 : ***Bax, Bcl-2 joint distribution:***

WT and LOI cells were co-stained for Bax and Bcl-2 and analyzed by immunofluorescence. The mean intensity in each cell was computed and plotted as a 2d-histogram. The Bax, Bcl-2 marginal distributions are also computed and plotted. The sample mean and the sample variance for the Bcl2 and Bax distributions for both WT and LOI cells are also shown.

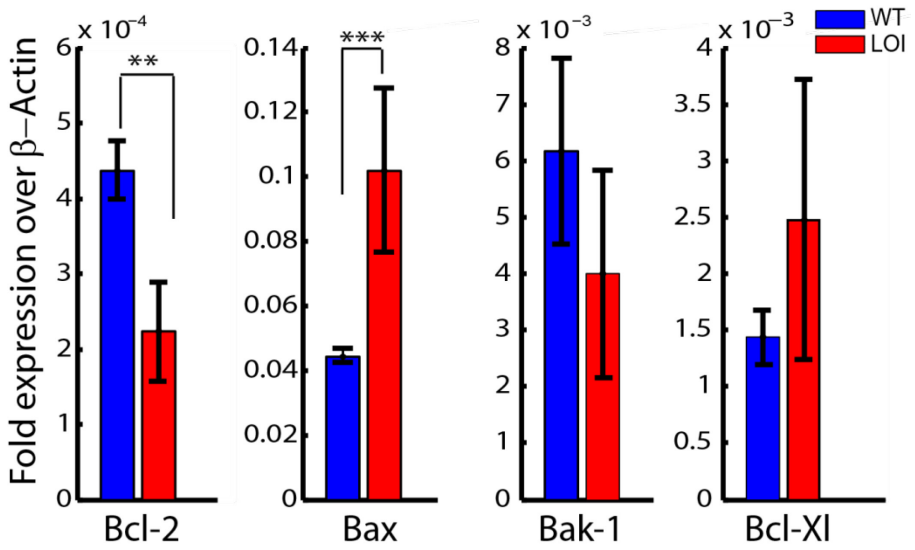

Figure 2.3 : ***Anti/Pro- apoptotic panel*** **:**

Exponentially growing LOI and WT cells were analyzed by qRT-PCR for 4 anti/pro-apoptotic proteins of the Bcl family. The expression of mRNA transcripts was plotted after normalizing to β-Actin values in the same well.

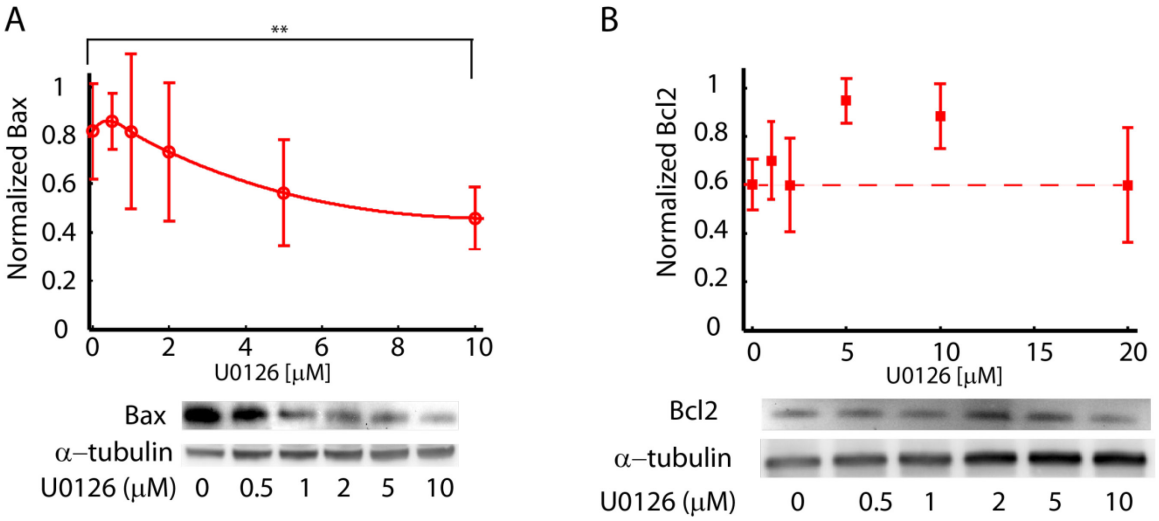

Figure 2.4 : ***Erk regulates Bax not Bcl-2***

LOI cells were serum starved overnight and then treated with varying concentrations of U0126 (Mek inhibitor) for 60 min followed by IGF-2 for 24 hours. The cells were harvested and analyzed via Western blotting for A) Bax and B) Bcl-2**.** Student's t test with N=3 was used.

hours showed a dose dependent response of Bax protein levels (Fig 2.4A), but also interestingly in those of c-Myc (Supplementary Fig. S). On the other hand Bcl-2 levels were not affected by Erk signaling levels as the Mek inhibitor U0126 showed no effect in a dose response experiments

on Bcl-2 (Fig 2.4B). Similarly, the expression of Bcl-2 showed dose-dependent sensitivity to a PI3K inhibitor LY294002 following similar IGF-2 stimulation (Supplementary Fig.S9). These results suggested that both canonical IGF-2 activated signaling pathways can indeed impinge on regulation of pro- and anti-apoptotic processes, through regulation of the Bcl family proteins.

To provide quantitative support for this hypothesis, we expanded the computational model using a simple assumption, postulating that the abundance of Bax and Bcl-2 is a function of Erk and Akt activities respectively integrated over time (Fig. 2.5). Using this assumption (see Supp. Materials for other details on the model expansion) we could predict the relative abundances of Bax and Bcl-2 proteins in LOI and WT (Lindner et al., 2013; Raychaudhuri and Das, 2013) (Fig. 2.5). In combination, these results provided support for the hypothesis that re-balancing of signaling pathways in the IGF-2 stimulated signaling network can lead to further re-balancing of Bcl family proteins leading to differential propensity of LOI and WT cells to undergo apoptosis. We provide further evidence for this hypothesis.

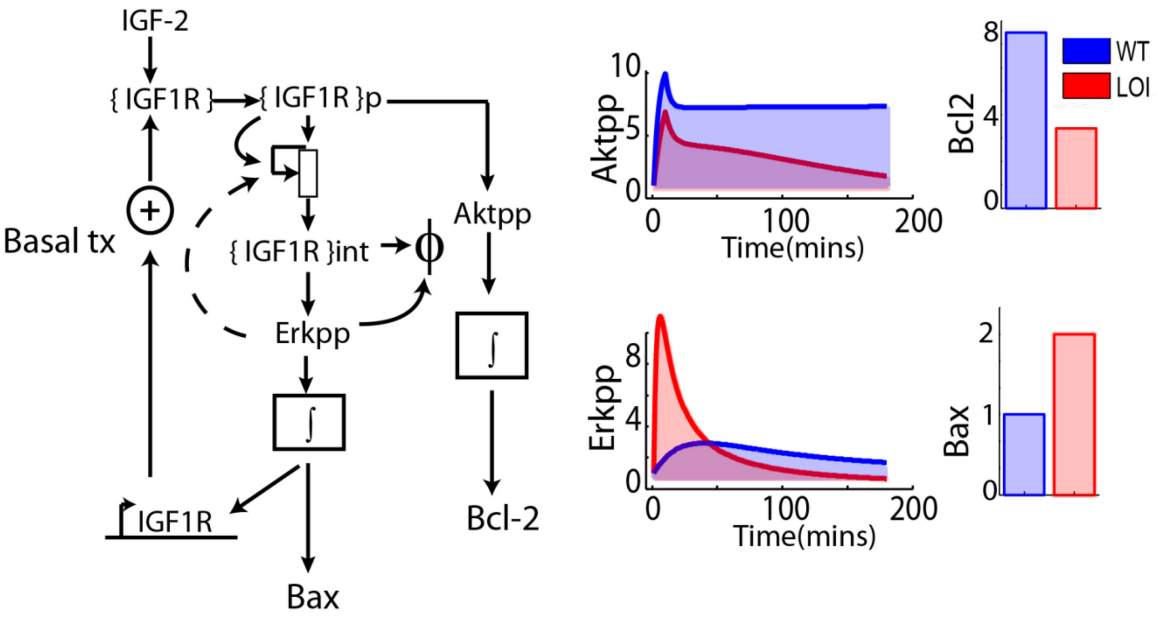

Figure 2.5 : ***Computational model extension for Bax, Bcl-2 signaling*** **:**

The IGF-2 computational signaling model was extended to include Bax, Bcl-2 signaling downstream of Akt-Erk signaling. The Akt and Erk signals are integrated to obtain Bax and Bcl-2 signals.

Chapter 3 : Increased sensitivity of LOI cells to IGF-1R kinase inhibition.

The re-balance of Bcl-2 and Bax can lead to differential sensitivity of LOI vs. WT cells to agents affecting the components of the signaling network (Oltvai et al., 1993; Perlman et al., 1999). Indeed, our prior observations suggested that LOI but not WT cells are highly sensitive to inhibition of the IGF-1R kinase activity by NVPAEW-541 (Kaneda et al., 2007). NVPAEW-541 was preferentially found to de-activate Akt while having a much milder effect on Erk (Fig. 3.1).

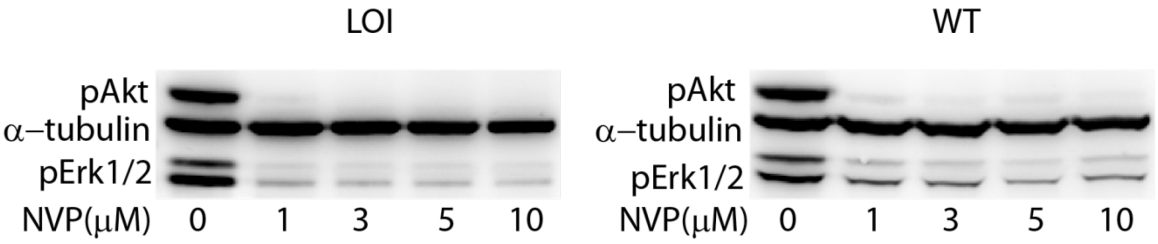

Figure 3.1 ***NVPAEW541 abolishes Akt signaling selectively***

WT and LOI cells were serum starved overnight and treated with indicated doses of NVPAEW541 for 60 minutes followed by IGF-2 for 10min. The cells were harvested in a lysate and analyzed by Western blotting. Both LOI and WT cells show an attenuated Erk signaling while the Akt signaling is completely abolished.

We therefore explored computationally whether the expanded model of the signaling network would predict higher sensitivity of LOI cells vs. WT cells to the inhibition of the IGF-1R kinase. Indeed, the model predicted that a given level of IGF1R inhibition can lead to distinct levels of Akt activity in these cells and, as a consequence, allow for greater 'domain' of tolerance to the perturbation under which Bcl-2 levels would still exceed the levels of Bax (Fig. 3.2). Since the relative excess of Bax vs. Bcl-2 (or vice versa) is thought to lead to the pro-apoptotic (vs. anti-apoptotic response) response, this result suggested that a much greater dose of the kinase inhibitor was required to induce the death response in WT vs. LOI cells.

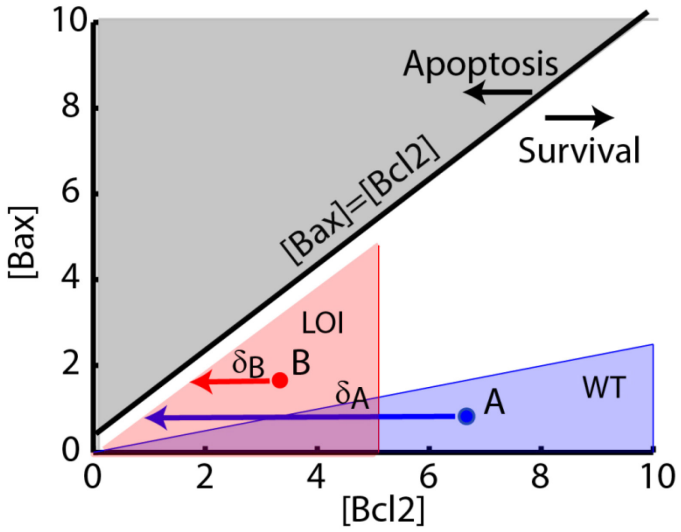

Figure 3.2 : : *Increased susceptibility to Bcl-2 inhibition*

Simulated Bax, Bcl-2 distributions for LOI and WT cells were plotted based on [Bcl-2] > [Bax] for survival. [Bcl-2]=[Bax] line separates the survival region from the apoptosis region. The centroids for the Bax, Bcl-2 distributions of WT and LOI cells are marked and the distances of the centroids from the [Bcl-2]=[Bax] line is also shown.

We first quantified this prediction by taking into account variability in the levels of Bax and Bcl-2 expression in the LOI and WT cell populations (Fig. 3.3B). Given this variability we could predict the % survival of the cellular population following exposure to various doses of NVPAEW-541 using the Bcl-Akt derived relationship from the computational model (Fig. Fig. 3.3A). The results yielded good match with the experimental analysis, providing additional support for model assumptions and for the proposed mechanism for the differential sensitivity by LOI and WT cells to IGF1R kinase inhibitor (Fig. 3.3C and Fig 3.3D)

The stoichiometric imbalance of Bax and Bcl-2 can trigger apoptosis through the instrinsic mitochondrial apoptotic pathway. This results in activation of the Caspases pathway, particularly the initiator Caspase-9 and the effector Caspase-3 (Kluck et al., 1997). The activities of both Caspases-9 and -3 were dramatically upregulated in LOI vs. WT cells within a few hours following exposure to NVPAEW-541 (Fig. 3.4A and 3.4B), consistent with many instances of increased upregulated (activated) Bax expression levels in these cells at these earlier time points of 5 hrs. following the stimulation with the drug (Fig. 3.4C). Annexin-V staining provided further support for regulated cell death in LOI cells (Supplementary Fig S). Overall, these results were consistent with the apoptotic regulation of cell death in LOI cells treated with the IGF-IR kinase inhibitor, expected as a result of differential Bax/Bcl-2 expression in LOI vs. WT cells

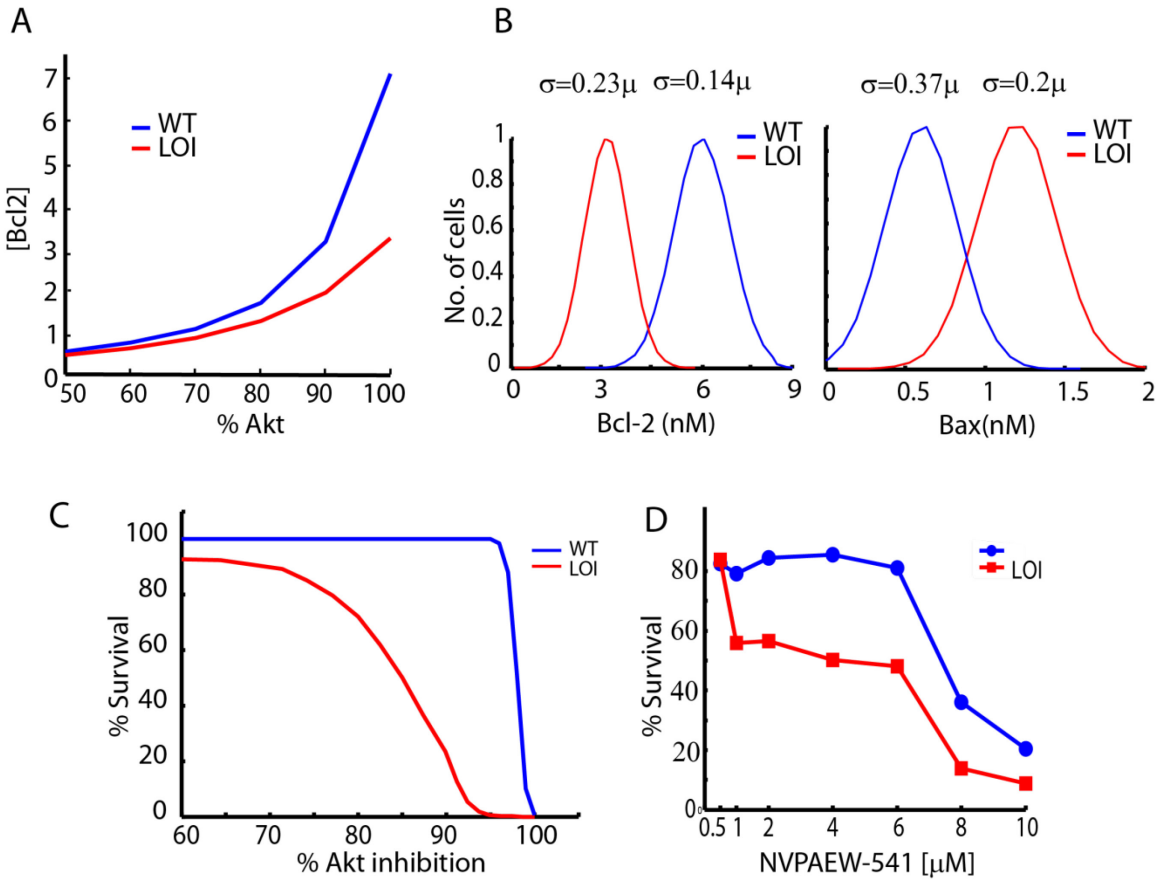

Figure 3.3 : Enhanced sensitivity of LOI cells to Akt inhibition

Using the IGF-2 signaling model a mapping from Akt inhibition to Bcl-2 inhibition was computed and plotted. Akt signaling was inhibited according to the percentages shown on the x-axis and the corresponding Bcl-2 levels were plotted on the y-axis. C) Bax, Bcl-2 distributions were generated with means corresponding to the centroids of the Bax, Bcl-2 distributions as shown in panel A) and using the standard deviations computed from the doubly-stained joint distributions measured and shown in Fig 4F. D) Based on the number of cells alive as dictated by [Bcl-2]>=[Bax], the percentage of Bcl-2 inhibition was plotted against the percentage of cell survival for WT and LOI cells. *Survival curves* E) WT and LOI cells were serum starved overnight and treated with indicated doses of IGF1R kinase inhibitor NVPAEW541 for 24 hours, analyzed for cell survival by Alamar blue dye. The survival is plotted as a percentage of the cells surviving as a function of the dose. No drug treatment was used as a control.

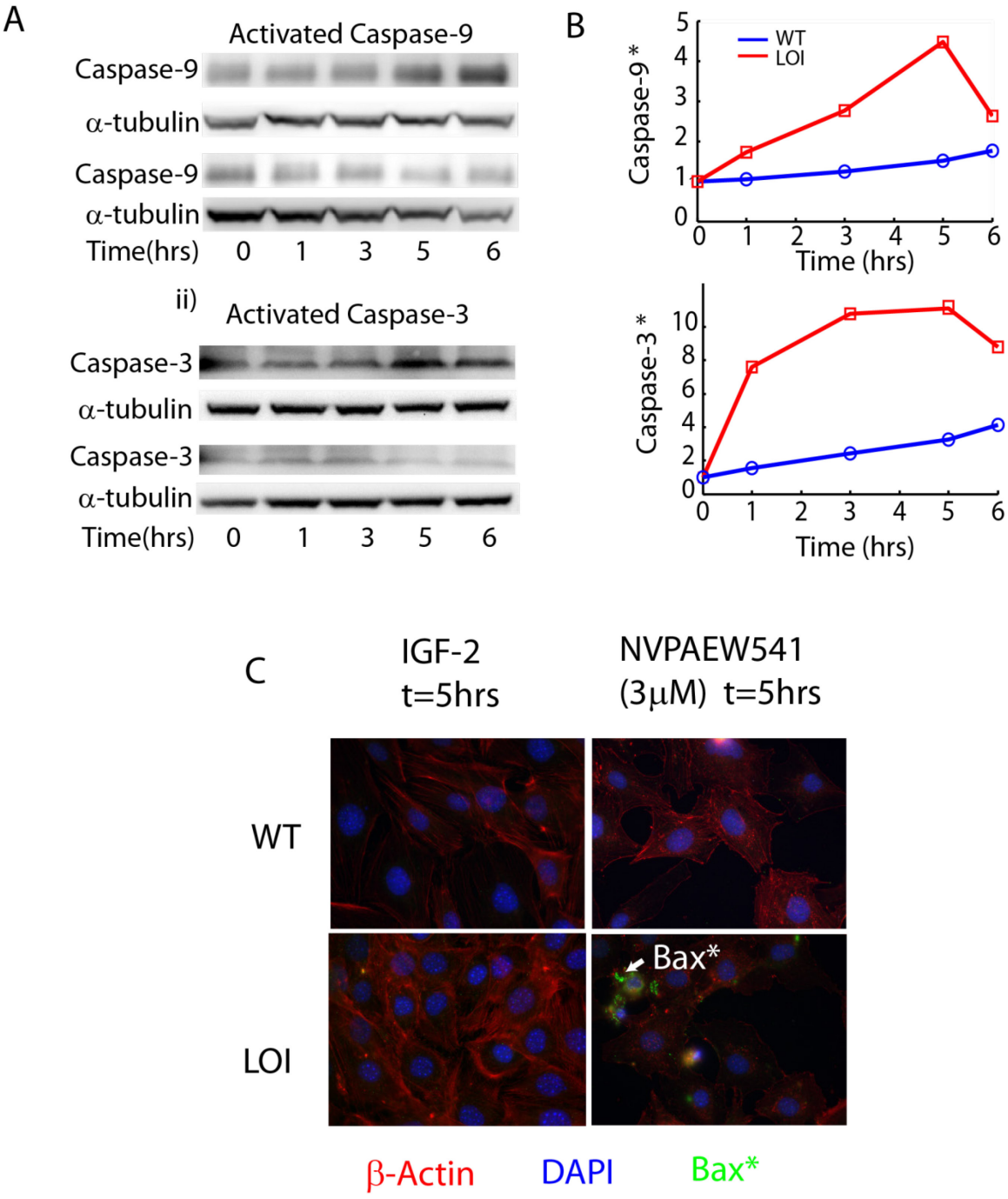

Figure 3.4 : ***Activated Caspase-9, Caspase-3 and Bax***

A) WT and LOI cells were serum starved and treated with 5μM NVPAEW541 for the indicated time points, harvested in lysates and analyzed by Western Blotting for activated Caspase-9 and Caspase-3. Both the early Caspase-9 and the effector Caspase-3 are seen to activated by t=5 hours in LOI cells while no activation is seen in WT cells. B) The Caspase-9 and Caspase-3 activation was measured by using substrates with Caspase cleavage site conjugated to fluorophores in both LOI and WT cells. Caspase activation produced a fluorescent signal proportional to the Caspase activity**.** C) LOI cells were serum starved overnight and treated with either IGF-2 or 5uM NVPAEW541 for 5 hours, fixed on coverslips and analyzed by immunofluorescence for antibodies specific to activated Bax. Bax activation as seen in the green channel begins to appear at t=5 hours.

Chapter 4 : IGF-1 response

The results presented so far provide evidence for the hypothesis that LOI cells, by virtue of increased expression of IGF-2, can enter a new state characterized by both an enhanced proliferation and higher propensity to undergo apoptosis, with the latter effect particularly pronounced if IGF-1R and Akt activities are suppressed. However, it is not clear, if re-balancing of the signaling network is specific to IGF-2, or can potentially be mimicked by an increase of other ligands capable of binding to IGF-1R, including IGF-1. This question can also be expanded to include the notion that IGF-I and IGF-II bind to IGF1R homo-dimers or IGF1R-Insulin Receptor (IR) heterodimers with different affinities. We found that the propensities to form the receptor homo- and hetero-dimers varied between LOI and WT cells, with LOI cells displaying both higher levels of receptors and higher relative occurrence of IGF1R homodimers (Fig. 4.1A). Since IGF-1 preferentially binds to IGF-1R homodimers, the assumptions of the IGF-2 triggered network activity used in our prior analysis were unchanged. However, since IGF-I has altered specificity of binding to both homo- and hetero-dimers of IGF-1R, we examined computationally and experimentally, how the activities of the signaling pathways within LOI and WT cells would respond to this ligand. We found good agreement between model predictions and experimental data, both of which suggested that IGF-I triggered activities of Akt and ERK are both strongly upregulated in the LOI vs. WT cells (Fig. 4.1B). Therefore, this ligand, unlike IGF-2, does not trigger re-balancing of the network activity. This differential effect of IGF-1 vs. IGF-2 in LOI cells, was not due to its inability to upregulate IGF1R in these cells (Fig. 4.1C). This upregulation was expected based on enhancement of Erk signaling, and it indeed occurred. Rather, the model strongly suggested that the differential affinity of IGF-1 to the receptor complexes can result and into less pronounced internalization of activated receptors thus permitting enhancement of Akt activity in LOI cells. his result suggests thatTherefore network rebalancing can occur due to enhanced expression of a growth factor ligand, but this effect is not universal and depends on the ligand identity.

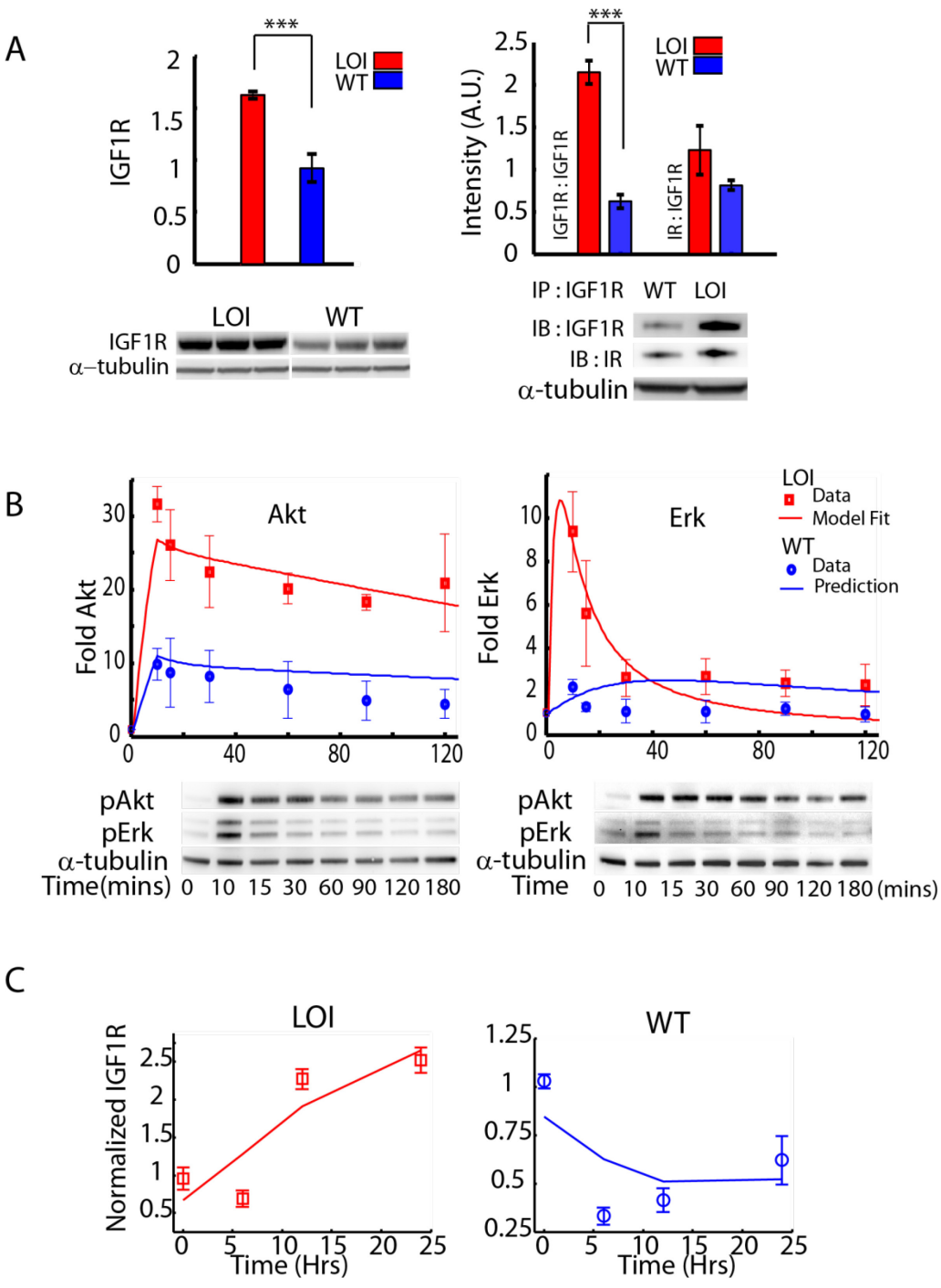

Figure 4.1 : LOI and WT response to IGF-1

A) LOI and WT cells were immunoprecipitated with IGF-1R abs and probed with IGF-1R and IR. B)LOI and WT cells were stimulated with IGF-1 for the indicated time points and analysed by Western blotting. The fold increase in pAkt and pErk over control (t=0) are plotted as a function of time (error bars). The IGF-2 signaling model was trained on pAkt and pErk response to IGF-1 stimulation. The model parameters were re-estimated to fit the average pAkt and pErk profiles as explained in the text. The model prediction for WT responses was obtained and plotted (blue solid lines) and compared with experimentally observed values (blue error bars). C)LOI and WT cells were stimulated with IGF-1(100ng/ml) for the indicated time points and analysed by qRT-PCR for IGF-1R mRNA expression.

Chapter 5 : Stochastic model for the stem cell compartment

The model follows the stem-transit amplifying-terminally differentiated program of the crypt as shown in Fig 1. The stem cell pool has no input and is self-contained. Stem cells can divide into two daughter cells and hence generate an event, the dividing cells can either remain as stem cells or differentiate and become transit amplifying cells. The transit amplifying cells proliferate rapidly and stay as transit amplifying cells for integral number of cell cycles and then differentiate into the terminally differentiated cells.

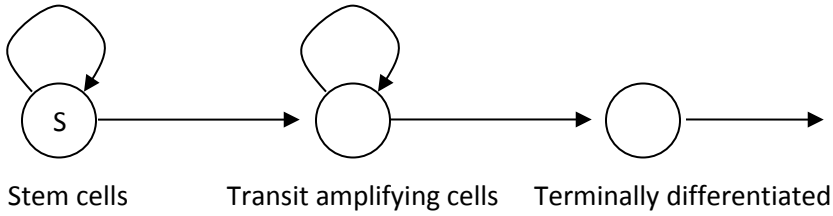

Figure 5.1 : Model description of the Stem-Transit amplifying-Terminally differentiated cells renewal program of the colonic crypt homeostasis.

Stem Cell Compartment: The stem cell pool is composed of cells that proliferate slowly, renew indefinitely and are responsible for the maintenance of the crypt. The stem cells reside at the bottom of the crypt and are relatively few in number. Owing to the inherent stochasticity and the probabilistic nature of cell division and differentiation, the number of stem cells in a crypt at any given time instant of is a random variable with a mean value and variance. Consequently, as a function of time the number of stem cells in a crypt can be described as a random process. Let $N_S(t)$ be that random process. Events in this compartment are generated when a stem cell undergoes mitosis, say at $t = t_a$, and at each cell division one of 3 things can happen,

a) $N_S(t_a)$ decreases by 1 to $N_S(t_a) = N_S(t) - 1$, where $t < t_a$, a case of symmetric division and when both the daughter cells differentiate and leave the compartment,

b) $N_S(t_a)$ remains the same, $N_S(t_a) = N_S(t)$, where $t < t_a$, a case of asymmetric division and when one of the daughter cell stays in the compartment while the other daughter cell differentiates and leaves the compartment and ,

c) $N_S(t_a)$ increases by 1 to $N_S(t_a) = N_S(t) + 1$, where $t < t_a$, a case of symmetric division where both the daughter cells remain as stem cells and stay in the compartment.

If the time sampling is sufficiently fine, we can avoid the situation of two cells dividing at the same time and thus simplify the system specification.

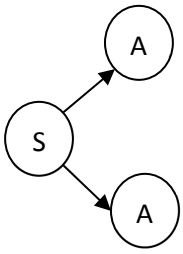

1. Symmetric division with both daughter cells differentiating.

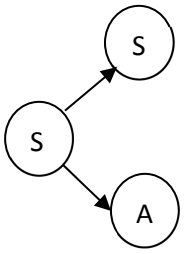

2. Asymmetric division and differentiation

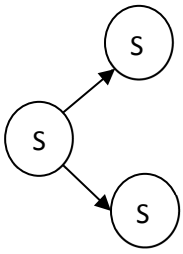

3. Symmetric division with two daughter stem cells

Figure 5.2 : The three forms of cell division in the stem cell pool

Let $\{ t_0, t_1, t_2, \ldots\ldots t_n, t_{n+1}, \ldots\ldots \}$ be the time instants at which events occur in the stem cell compartment and let { S_1, S_2, S_3 …, S_n, S_{n+1}, … } be the corresponding time intervals between successive cell divisions such that $S_1 = t_1 - t_0$ is the time to the first division and S_2 is the time interval between the second and the first cell division and so on. We can safely assume that S_1, S_2,.. etc are a sequence of independent, identically distributed random variables such that $0 < E[S_i] < \infty$ be true $\forall\ i$, where $E[.]$ is the expectation operator.

Let $I(t)$ be the indicator function that gives the jump in $N_S(t)$ at each time instant, such that $N_S\ (t_i + \Delta) - N_S(t_i - \Delta) = I\ (t_i)$ be the height of the jump at $t = t_i$ for any arbitrarily small Δ. $I(t)$ is the amount by which N_S changes i.e. by 0, +1 or -1 corresponding to the 3 outcomes of cell division. Also, let J_I be such that $J_I = \sum_{n=0}^{I} S_n$, the sum of all time intervals between cell divisions (also called the holding times in random processes parlance). $N_S\ (t)$ defined as $N_S\ (t) = \sum_{n=1}^{\infty} I\ (J_n \leq t\ )$ is a renewal process. Assuming wide-sense stationarity / time invariance $\bar{N}_S\ (t) = E[N_S(t)] = \bar{N}_S$ is the average number of stem cells expected to be found in a crypt.

Let us define $\{W_1, W_2, W_3, \ldots\ldots W_n, W_{n+1}, \ldots\}$ as the events that lead to stem cells differentiating and leaving the compartment. This happens when i) when both the daughter stem cells after division differentiate and leave the compartment corresponding to a jump of -1

in $N_S(t)$ and ii) when one daughter stem cell differentiates and leaves the compartment corresponding to a jump of 0 in $N_S(t)$. Since its reasonable to assume that the probabilities of symmetric and asymmetric differentiation in crypt stem cells don't change with time, $\{W_1, W_2, W_3, \ldots..W_n, W_{n+1}, \ldots\}$ is a set of independent and identically distributed random variables. So W_1 and its sample space can defined as

$$W_1 = \begin{Bmatrix} +2 & both\ daughter\ stem\ cells\ leave\ compartment \\ +1 & one\ daughter\ stem\ cell\ leaves\ the\ comparment \\ 0 & none\ of\ the\ daugter\ cells\ leave\ the\ compartment \end{Bmatrix}$$

And the associated probabilities can be written as,

$$p_{W_1} = \begin{Bmatrix} p\ \ for\ W_1 = +2 \\ q\ \ for\ W_1 = +1 \\ r\ \ for\ W_1 = 0 \end{Bmatrix};\ \ where\ p + q + r = 1$$

Also let $E[W_1] = \sum_W W_1\ p_{W_1}$ be such that $0 < E[W_1] < \infty$, then the random variable $Y_t = \sum_{i=1}^{t} W_i$ defined over $\{W_1, W_2, W_3, \ldots..W_n, W_{n+1}, \ldots\}$ and $\{S_1, S_2, S_3, \ldots..S_n, S_{n+1}, \ldots\}$ is a **renewal reward process**. The convenience of formulating the cells differentiating and exiting the stem cells compartment as a renewal reward process is in being able to relate fundamental biological quantities of the crypt dynamics using fundamental renewal reward theorems.

The important parameters that define the stem cell compartment are the number of stem cells at any point in time, the average cycling time of stem cells and the probabilities of symmetric and symmetric division. Directly from the model definition the number of stem cells in the compartment is given directly by $N_{SC}(t)$, the probabilities of division are given by p, q and r and as shown below the average cycling time can be expressed in terms of these parameters.

From the fundamental theorem of elementary renewal reward processes we have,

$$\lim_{t\to\infty} \frac{E[Y(t)]}{t} = \frac{E[W_1]}{E[S_1]}$$

The equation basically relates the time average or rate of exit of stem cells (the left hand side) from the stem cell compartment to the probabilities of the various mitosis outcomes and the average cell cycle time (right hand side of the equation) in the stem cell compartment. $E[W_1]$ can be enumerated as,

$$E[W_1] = p \times 2 + q \times 1 + r \times 0$$

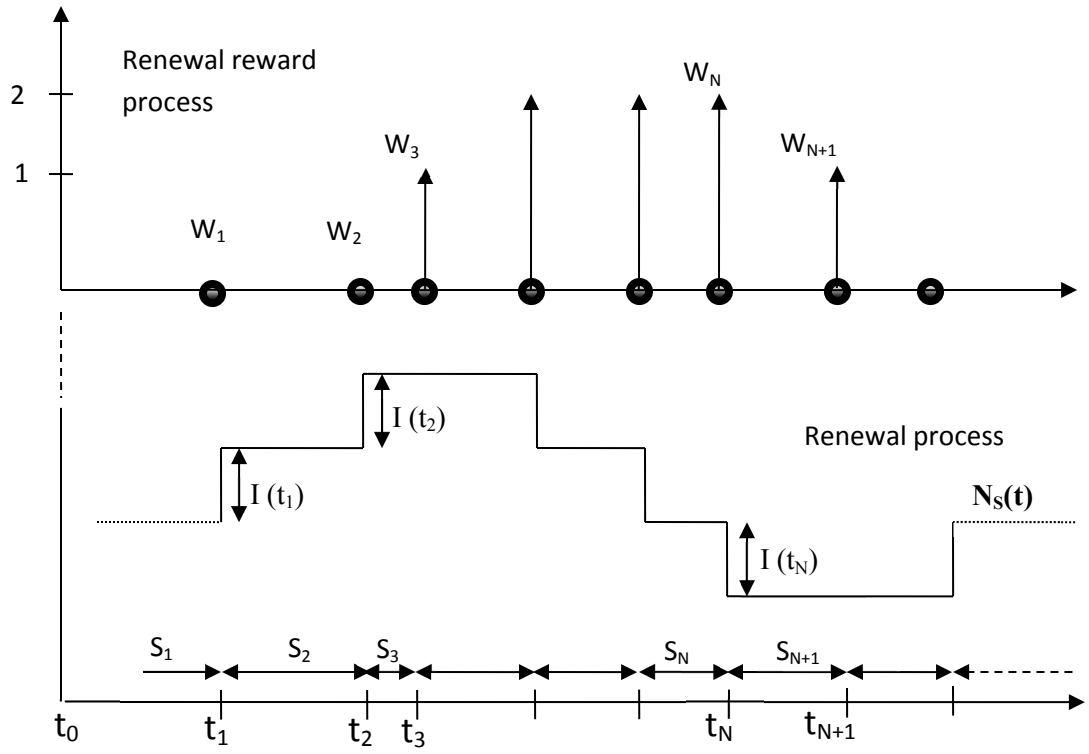

Figure 5.3 : The renewal process and renewal reward process :

Every time a stem cell divides, based on either of the 3 cell division outcomes highlighted in the text $\boldsymbol{N_S(t)}$ changes by the corresponding $\boldsymbol{I(t)}$ which then forms the basis of the renewal reward process.

Assuming that all stem cells in the crypt have an equal chance of dividing, we can approximate $E[S_1]$ as,

$$E[S_1] = \frac{C}{\bar{N}_{SC}} ;$$

where C is the cell cycle time and $\bar{N}_{SC}$ *is the average number of stem cells.*

Use if the above equation makes intuitive sense because if there were N stem cells with a cell cycle time of C hours, we would expect a cell to divide every C / N hours on an average. Thus, we have

$$R_{SC}^{out} = \frac{\bar{N}_{SC} \times (2p + q)}{C}$$

as the equation for the rate of exit of stem cells from the compartment.

The Transit Amplifying Compartment : The cells that comprise the transit amplifying compartment proliferate prodigiously to make up for the high rate of loss of cells from the terminally differentiated compartment and the very low proliferation rate of the cells in the

stem cells compartment. The stem cells exiting from the stem cell compartment enter the transit amplifying compartment, go through cycles of mitosis and then leave the compartment. Given the enter, proliferate and exit nature of this compartment, it can be analyzed purely as a rate amplifier. Assume an epoch of time C_{TA} equal to the average cell cycle time of the transit amplifying cells. The number of cells that enter during C_{TA} is determined by the rate of exit of stem cells R_{SC}^{out} such that $K = R_{SC}^{out} \times C_{TA}$ is the number of cells that enter the transit amplifying compartment during a time C_{TA}. Every C_{TA} that elapses the K cells double and another K cells enter the compartment. If the first set of K cells that enter stay for $L = l \times C_{TA}$ hours where l is any integer, then rate of exit of cells from the compartment can be easily given as

$$R_{TA}^{out} = 2^{l} \times R_{SC}^{out}$$

The number of cells found in the TA compartment can also be easily expressed as,

$$N_{TA} = K \times \left(2^{0} + 2^{1} + 2^{2} + \ldots\ldots + 2^{l} \right) = K \times \left(2^{l+1} - 1\right) cells$$

Prediction of stem cell division time in homeostasis:

A typical human colonic crypt contains on an average about 82 levels of cells from the bottom to the top of the crypt. The bottom most level contains 1 cell and levels 2 to 7 contain 6, 12, 18, 24, 30 and 36 cells respectively. The straight portion of the crypt from levels 8 to 82 contain 42 cells per each level adding to about 3193 cells per crypt (Boman et al., 2008). From stem cell markers staining data, Musashi-1 and Lgr5, it is evident that the stem cells predominantly populate the bottom 3 to 4 levels of the crypt. There are about 19 cells in the bottom 3 levels while there are 37 cells in the bottom 4 levels. For the purposes of an illustrative example we can take the average of these two numbers, 30 as the number of stem cells in a crypt. Data from S-phase labeling and Ki-56 labeling indicate that levels 4 to 45 which have more than or about the average level of S-phase staining can be considered to be the transit amplifying compartment comprising of rapidly proliferating cells. From the distribution of the number of cells / level, levels 4 to 45 contain 1686 cells. The remainder 3193 – (1686+30) = 1477 is the number of cells in the terminally differentiated compartment / crypt. $N_{SC} = 30, N_{TA} = 1686 \; and \; N_{TD} = 1477$ respectively.

The crypt turnover rate is about 5 days and it's expected that 95% of the cells in a crypt are turned over in a 5 day period, thus the rate of loss of cells from the crypt or the terminally differentiated compartment is $R_{Out} = \frac{0.95 \times 3193}{120} = 25.27$ cells / hour. Since there is almost no proliferation in the terminally differentiated compartment, the average rate of cells exiting out of the Transit Amplifying compartment is the same, $R_{TA}^{out} = R_{Out}$. From the previous section we have,

$$R_{TA}^{out} = 2^{l} \times R_{SC}^{out}$$

And so we have $R_{SC}^{out} = 2^{-l} \times R_{TA}^{out} = 2^{-l} \times 25.27$ cells / hour.

Previous work in estimating critical parameters of the crypt dynamics have resulted in many estimates of parameters. Here we use some of the parameters available in literature and test the predictions of the model and hence its validity. The number of stem cells in a crypt is put at about 30 / crypt, so $\bar{N}_{SC} = 30$ cells / crypt. Given the very unlikely chance of symmetric division and the more common occurrence of an asymmetric division with the stem cells, we can use $p = 0.05, q = 0.9$ and $r = 0.05$. Since the stem cells proliferate a lot slower than the cells of the transit amplifying compartment, we test a prediction for the stem cell cycling time $C = 90\ hours$. With these values

$R_{SC}^{out} = \frac{\bar{N}_{SC} \times (2p+q)}{C} = \frac{30 \times (0.1+0.9)}{90} = 0.333$ cells / hour

$$R_{TA}^{out} = 2^{l} \times R_{SC}^{out}$$

$$l = \log_2\left(\frac{25.27}{0.33}\right) = 6.26$$

Thus a value of $l = 6.26$ indicates that cells in the transit amplifying compartment cycle about 6.26 times or undergo about 6.26 successive divisions before they become terminally differentiated. Also from literature we have the cell cycle times in the transit amplifying compartment as $C_{TA} = 29.9\ to\ 39.9\ hours$. Thus N_{TA} is bound by,

$$N_{TA} = \frac{K \times \left(1 - 2^{l+1}\right)}{(1-2)} = \frac{(35 \pm 4.9) \times 0.33 \times (1 - 2^{7.29})}{-1} = 1800 \pm 266\ cells$$

Where $C_{TA} = 35\ hours$ is the mean value. This average value of $N_{TA} = 1800$ cells approximately matches 1686, the of number of cells in the transit amplifying compartment obtained by s-phase labeling of the crypt

Discussion

Network Re-balance – IGF-2 LOI signaling network is an example of a re-balanced network. Re-balancing refers to the altering in the signal strength of one downstream pathway at the expense of the other parallel pathway. Although Akt and Erk are activated beginning at the IGF-1R, their relative strengths can be varied by affecting any of the receptor trafficking processes or the adapter molecules that connect to Akt and Erk signaling. In the IGF-2 LOI cells Akt signaling is attenuated while Erk signaling is concomitantly enhanced. This re-balancing in signaling strengths can consequently affect in proportional ways the downstream targets and processes mediated by both Akt and Erk. Since Erk mediates amongst other things the growth and proliferation of cells, network re-balance puts the cells in the "fast-lane" as a rapidly proliferating group of cells.

Growth factors and growth factor receptor signaling can have significant consequences in the face of network re-balancing as Akt and Erk activation are a common theme amongst all growth factor signaling systems (Oda et al., 2005). A flavor for the effect of re-balancing can be obtained by looking at the effect of different growth factors on cells that express receptors for them. By virtue of their differential coupling to the mechanisms that regulate and activate Akt and Erk different growth factor receptors can activate Akt and Erk to different degrees (Haugh and Meyer, 2002) (Park et al., 2003). This activation of Akt and Erk to different degrees can also determine opposing cell fates in systems where Akt and Erk signaling strengths determine cell fates. EGF (Epidermal growth factor) and PDGF (Platelet derived growth factor) are two growth factors that can elicit different Akt and Erk signaling signatures in cells. While EGF is known to produce strong Erk signaling, PDGF signals more via the PI3K pathway to preferentially activate Akt (Normanno et al., 2006) (Tallquist and Kazlauskas, 2004). In human Mesenchymal stem cells it was shown that EGF signaling caused the cells to differentiate and form bone-forming cells while PDGF did not induce the differentiation although the two growth factors appeared to recruit 90% of similar phospho-tryosine proteins (Kratchmarova et al., 2005). PI3K was shown to be the control point as PDGF strongly activated Akt signaling and inhibition of Akt signaling induced differentiation of cells (Kratchmarova et al., 2005).

In PC-12 cells, which are a neural progenitor cell line that differentiates into neurons when treated with NGF (Neural growth factor), it was shown that there existed a two-dimensional phospho-Akt and phospho-Erk landscape that determined differentiation versus proliferation in cells treated with NGF (Chen et al., 2012). This boundary was shown to be a curved surface and invariant in position to various perturbations of upstream elements of the Akt and Erk pathway (Chen et al., 2012). Network re-balancing thus is a methodology whereby cells can alter their downstream Akt and Erk signaling strengths and potentially alter proliferation, growth rates, differentiation and other fates connected to Akt, Erk signaling.

Erk signaling determines and sustains the IGF-2 LOI phenotype –

Erk signaling solely mediates and sustains the IGF-2 LOI phenotype. Erk is shown to mediate the long-term transcriptional increase in IGF-1R and also mediate the ubiquitin driven degradation of IGF-1R. As far as we know, there hasn't been any evidence so far in the literature about Erk mediated positive transcriptional regulation of IGF-1R although a few pieces of connecting evidence can be suggested. The IGF-1R regulatory region, surprisingly, lacks the canonical TATA box or the CAAT motifs that are used in eukaryotes as transcription start sites and instead is highly GC rich. The transcription is initiated from a special initiator motif that is adjacent to upstream Sp1 sites. Sp1 is a ubiquitous zinc-finger based nuclear transcription factor that stimulates transcription from RNA-pol II based promoters (Werner, 2012).

Amongst the many known factors that bind to IGF-1R, p53 in its wild-type state is a tumor suppressor gene product that stops progression through the cell cycle stages when in its phosphorylated state. p53 in its nuclear localized state binds to specific sequences in the promoter of many genes thereby regulating it. p53 binds to the IGF-1R promoter region thereby suppressing its expression while mutations in p53 that occur in the central DNA binding region of the protein relieve the suppression and increase IGF-1R expression (Werner et al., 1996). Another protein that closely associates with the status of p53 in the cells is the nuclear transcription factor Wilms tumor suppressor gene product (WT1) which structural studies have shown to possess multiple binding sites upstream and downstream of the transcription initiation site of the IGF-1R promoter. It has been shown that depending on the mutant status of the p53 protein in the cell, WT1 exerts its suppressive or oncogenic properties on IGF-1R transcription i.e. in a p53 mutant system WT1 cannot suppress the increased expression of IGF-1R. Mutations in WT1 are implicated in Wilms tumor which is a pediatric form of renal malignancy. BRCA1 is a tumor suppresser which functions as a regulator in cell-cycle progression, DNA damage, repair and maintaining genomic integrity. Mutations in BRCA1 drastically enhance the risk of breast cancer and ovarian cancer. Although BRCA1 hasn't been shown to bind to the IGF-1R promoter region directly, it can interact and modulate the activity of other proteins that bind. In prostate cancer, it has been shown that BRCA1 interacts with Androgen Receptor (AR) and exerts a repressive effect on IGF1R (Schayek et al., 2009)

Evidence for pCREB regulation of IGF-1R comes from prostate cancer where the cancer is usually androgen responsive in the beginning and then progresses to an androgen independent, aggressive and resistant to therapies state. It has been shown that sex hormones binding to both AR and ER markedly upregulate IGF-1R in prostate cancer cells. This upregulation does not involve the binding of the receptors to the DNA responsive elements instead it has been shown that it involves the c-Src / Extracellular signal regulated kinase (Erk1/2) and the PI3k pathways (Genua et al., 2009). CREB (cAmp response element binding protein) is a cellular transcription factor that binds to regions called the cAmp response elements in the regulatory regions of many target genes and increase their transcription. ER and AR both cause phosphorylation of CREB at Ser133 enabling the binding of CREB to CBP/P300 (CREB binding protein) and causing increased transcription. It was also shown by bioinformatics analysis that the human IGF-1R

promoter contains 3 CREB sites in the 5' UTR region. It was also shown that phospho-CREB binding to IGF1R promoter in response to sex steroids was necessary for IGF-1R transcriptional increase (Genua et al., 2009) Given the ubiquitous nature of Erk signaling, activation of Erk signaling also causes a Calcium flux, a cAmp response and hence phosphorylation of CREB and the activation of downstream targets(Wu et al., 2001). Similarly the PI3k/Akt pathway is also known to phosphorylate CREB at Ser133 and activate downstream target genes (Du and Montminy, 1998). Thus both Erk1/2 and the PI3k/Akt pathways can activate CREB and induce the recruitment of CBP to CREB

Ubiquitination is a post-translational modification, which apart from marking a protein for degradation via the proteasomal machinery, is been known to play an increasingly important role in receptor mediated endocytosis and Erk regulation (Acconcia et al., 2009; Nguyen et al., 2013). Ubiquitination of the receptor (EGFR, IGF-1R) and associated adaptor proteins has been found to be a critical step in receptor mediated endocytosis and Erk activation (Nguyen et al., 2013). Many E3 ligases are known to be associated with growth factor receptor signaling and internalization. c-Cbl, Nedd4 and Mdm2 are 3 known E3 ligases that have been associated with ubiquitination of receptors (Nguyen et al., 2013) . Although there is considerable evidence of a number of players in the MAPK pathway doubling up as ubiquitin agents, a role for Erk in mediating receptor ubiquitination has so far not been reported in our understanding.

Propagation of network re-balance and apoptotic susceptibility - Given that Akt mediates a strong pro-survival signal via inhibition of Caspase-9, phosphorylation of Bad and Bcl-2, it was expected that Akt signaling changes be reflected in the balance of anti-apoptotic proteins. Erk signaling on the other hand, as far as we know, has not been connected to pro-apoptotic signaling although there is evidence for anti-apoptotic phosphorylation of Bad (Jin et al., 2002). The suggestion that Erk signaling can increase pro-apoptotic Bax implies a penalty for fast cycling cells in terms of the loss of the stoichiometric excess of anti-apoptotic Bcl-2 over pro-apoptotic Bax in IGF-2 LOI cells. This mechanism of Bax regulation by Erk signaling is unknown and might involve other players like cMyc. cMyc which is a central regulator in many homeostatic processes has been shown to influence Bax levels (Juin et al., 2002) and is dependent on both Akt and Erk signaling for its accumulation and stabilization (Sears et al., 2000). Thus by virtue of the propagation downstream of the re-balance in Erk – Akt signaling, LOI cells re-balance their pro and anti- apoptosis signaling by decreasing Bcl-2 levels and increasing Bax levels.

"Oncogene addiction" – It is a known fact that cancers of all forms, malignancies and tissue types are borne out as a result of the accumulation of multiple genetic abnormalities and epigenetic changes harbored over long periods of time (Greenman et al., 2007). Although the genetic aberrations and epigenetic changes can be found in a wide variety of regulators from growth factors, tumor suppressors to phosphatases, some cancers are reliant exclusively on a single driver mutation to fuel growth and metastasis (Goustin et al., 1986; Ostman et al., 2006;

Thompson, 2009). Such cancers stop growing and in some cases restore normal health in patients when the single driver mutation is reversed or inhibited thus exhibiting "oncogene addiction" or the possession of an "Achilles' heel" in the mutation (Weinstein, 2002; Weinstein and Joe, 2008). A few mechanisms have been proposed in literature to explain this dependence, since cancer cells are known to have dysregulated many genes and their regulators, the signaling network is expected to be quite different from normal wild-type cells. These altered signaling networks might be rewired to the extent that different genes might end up performing different cellular roles to different extents as compared to WT cells and thus interruption of a key driver in these networks might adversely affect the cellular outcomes as opposed to Wild-type normal cells (Weinstein and Joe, 2008). Other studies have proposed a mechanism called "Oncogene Shock" where activation of critical oncogenes can attenuate the rates of pro-survival and pro-apoptotic signals (Sharma et al., 2006). In this situation, because of the greater decrease in the rates of pro-survival signals as compared to pro-apoptotic signals, in the face of inhibition of the oncogene there is greater cell death and decreased growth.

IGF-2 LOI cells both in-vivo and in in-vitro culture show an addiction to IGF-2 although these cells are not cancerous in nature. An increase in IGF-1R expression, coupled with an increased internalization rate drives an increased Erk signaling which sustains the increased IGF-1R expression and the LOI phenotype. The re-balance in Erk and Akt signaling is shown to alter the anti and pro- apoptotic balance by altering the levels of Bcl-2 and Bax. Thus the LOI cells by virtue of their increased Bax and decreased Bcl-2 are more susceptible to loss of IGF-2 signaling via the inhibition of the IGF-1R kinase. Although the re-balance of Bax and Bcl-2 levels as shown here is conceptually similar to the "Oncogene Shock" mechanism described above, important differences remain – The re-balance is not directly due to an oncogene as it is in the former case, the IGF-2 LOI cells have a plausible mechanism for generating the re-balance and the IGF-2 LOI system's addiction is due to change in the levels of pro and anti-apoptotic proteins and not by the change in their rates of attenuation.

Although a mechanism for IGF-2 addiction has been proposed here this is by no means a general solution for a mechanistic understanding of oncogene addiction. It could very well be that the oncogene that drives the addiction along with the other genetic and epigenetic changes could have re-wired the underlying signaling network or it could be a combination of driver mutation induced change in the network coupled with re-balancing of pro- and anti– apoptotic factors. More so, since not all cancers show the addiction to an oncogene this could very well be limited to a particular form and have different mechanistic underpinnings in different cancers. More research would be needed to identify differences and similarities.

Therapeutic Window – One of the requirements of effective treatment of a drug is an existence of a "therapeutic window" wherein the dosage of the drug is deemed to be effective without necessarily causing a system wide reaction or adverse side-effect. In terms of cancer treatment it can be seen as the ability to exclusive target and eliminate cancer cells while not much affecting normal cells and homeostasis. As seen here, the Bax/Bcl-2 re-balancing and the spread in the distribution of values, creates a corollary of a therapeutic window in addition to

IGF-2 addiction. A dose of IGF-1R kinase inhibitor in this window has twice the effect on LOI cells as it has on WT cells. Although LOI of IGF-2 is not a cancer or a tumor, the in-vitro survival curves indicate that, the cells can be safely targeted by taking advantage of the therapeutic window thus diminishing the chance of the development of LOI of IGF-2 into colorectal cancer.

IGF-2 vs IGF-1 - Although IGF-2 and IGF-1 are a part of the Insulin signaling superfamily, signaling through the same set of receptors and receptor complexes albeit with different affinities, only IGF-2 is imprinted evolutionarily and not IGF-1. More evidence and proof for the selective silencing / imprinting of IGF-2 comes from the signaling responses of IGF-1. Although IGF-1 triggers an increased expression of IGF-1R via an increased Erk signaling it doesn't create the re-balance in Akt and Erk signaling as seen in LOI cells when stimulated with IGF-2. Presumably, this lack of re-balance in Akt and Erk could preserve the balance of the pro- and anti- apoptotic proteins Bax and Bcl-2 as seen in WT cells. This further illustrates the special nature of IGF-2 signaling because any transient increase in IGF-2 levels (similar to a temporary loss of imprinting scenario) which can cause increased growth and size can be quickly ameliorated when the IGF-2 increase disappears because the IGF-2 addiction mechanism and the therapeutic window ensures that loss of IGF-2 results in cell death, reduction in growth and a return to normal homeostasis. Such a mechanism would be exclusive to IGF-2 and not IGF-1 and underscores the importance of IGF-2 as an imprinted gene.

Development of colonic crypts - Intestinal and colonic crypts develop from the embryonic primitive gut post birth by invagination of the epithelium into the mesenchyme. A recent theory that was proposed to explain the attainment of the final steady state crypt length in terms the optimal control theory and time to full length crypt called the "bang-bang" theory proposed a two-step strategy of an initial pool of stem cells that expand to the required final number of stem cells followed by a second step of asymmetric division of stem cells into differentiated cells to produce the requisite number of differentiated cells (Itzkovitz et al., 2012). Since growth factor signaling is required to switch from an all stem cell population to a mixed population, IGF-2 LOI should result in maybe a greater set/pool of stem cells followed by a greater number of differentiated cells. More light could be shed on the development scheme of crypts in the intestine and colon by studying the development of intestinal tissue of the IGF-2 LOI system.

Stochastic Model - We have presented here a stochastic random process based model for the homeostasis and organization of the colonic crypt. The pool of stem cells is modeled as a renewal process with every cell division creating the event and the subsequent decision to either remain a stem cell or differentiate creating the counting process. The differentiation and exit of cells from the stem cell pool is modeled as a renewal reward process and by using the fundamental theorem of the reward process we have been able to quantify the rate of exit of cells from the stem cell pool.

The stem cells have been the most elusive and secretive of all the cells in the colonic epithelium and it is only in the last few years that a definitive marker, Lgr5, has been found that can reliably

mark the stem cell pool. Much less is known either about the nature of the symmetric or asymmetric division in the stem cell pool and the probabilities with which they occur. The very infrequent if not dormant cell cycling times of the stem cells have also been a question that hasn't been resolved adequately due to the extreme difficulty in marking these cells for proliferation markers. Using the equation for the rate of differentiation of the stem cells and numbers obtained from the general knowledge of the crypt dynamics we tested a value for the cell cycling time of the stem cells. Using this value we were able to verify, within bounds, the approximate number of cells expected to be found in the transit amplifying compartment and thus validating the value for the stem cells cycling time.

The advantage of using the renewal and the renewal reward process is that some of the simple yet powerful theorems and results derived for these stochastic processes can be used to describe the processes and dynamics of the crypt evolution and organization. The stem cell pool and the rate of differentiation of the stem cells determine the existence of the crypt and its size respectively. Apart from the mean rate, the variance of the rate of differentiation of stem cells, which can also be analytically expressed, gives a wealth of information regarding the stochasticity in crypt length and numbers observed. Renewal reward theory enables us to analytically express the variance as well and this in turn can lead to the development of other aspects of crypt dynamics, namely feedback regulation, that is not explicitly discussed here.

It can also be easily seen that this model can, in principle, be used to analyze the effects of mutations in the stem cell compartment that can lead to colon associated cancers. For example the APC mutation leads to an increase in the probability of symmetric cell division where both the daughter cells remain stem cells thereby increasing the number of stem cells. This can then easily lead to a decrease in the differentiation rate and thus to a reduced pool of transit amplifying cells. Thus the corresponding stochastic models not only enable a more faithful representation of the inherent randomness in crypt biology but allows derivation of expected or average results that are observed in experiments and provide a handle to discuss dynamical variability that might lead to cancer and other abnormalities.

Materials and Methods

Materials : Anti - pAkt, pErk1/2, IGF1R, IR, Ubiquitin, pMek1/2, cMyc, Bax, Caspase-9, Caspase-3 antibodies, LY294002, U0126 were purchased from Cell Signaling Technology, MA. Anti α-tubulin mouse antibody was from Sigma-Aldrich. Anti Bcl-2, Bak-1, Bcl-Xl were from SantaCruz Biotechnologies, CA. Goat Anti-mouse, anti-rabbit, Alexafluor 480,594,633 conjugated secondary antibodies, CellMask deep-red whole cell stain, Hoechst, FM143-fx dye, Streptavidin conjugated and Protein A/G dynabeads, iBlot dry blotting apparatus were from Invitrogen technologies, CA. Alamar blue was from AbD Serotech, CO. MDC, Monensin Sodium, MG-132, Okadoic Acid were purchased from EMD Millipore, USA.

Western Blotting : Cells were grown to 95% confluency, serum starved overnight, treated to experimental conditions and harvested in denaturing SDS based lysis buffers, suspended in 4x loading buffer and heated to 95 degC for 5 minutes and stored for archival at -20degC. Lysates (about 20µg) are reduced with DTT and subjected to gel-electrophoresis in precast Bis-Tris gels under reduced conditions and transferred to 0.2µ Nitrocellulose membrane in a dry-transfer iBlot apparatus. Membranes were blocked with 5%BSA in PBS and then incubated with the relevant primary antibody followed by the secondary with 5 to 6 washes in washing buffer in between. The membranes were developed using PicoWest chemiluminescence substrate and imaged using BioRad imaging station. The images of the blots were then quantified using the gel band intensity analysis macro in ImageJ.

Immunofluorescence : Cells were seeded on 35 mm Mattek dishes and allowed to attach for 10 to 12 hours. Cells were then serum starved overnight in DMEM media with 0%FBS and stimulated with IGF-2 of indicated concentration for the indicated period of time. The cells are then washed in ice-cold PBS and fixed in 4% Fomaldehyde. The cells are then permeabilized with 0.1% TritonX-100 in PBS and then blocked with 10% goat serum for 1 hour. The cells are incubated with primary antibody at the specified concentration in blocking buffer and incubated overnight at 4degC. After washing thoroughly the cells are incubated with the appropriate secondary antibody, Hoechst dye and CellMask Deep Red at the specified concentrations for 1hr at room temperature. The cells are then washed thoroughly in PBS and imaged on a Zeiss AxioObserver Z1 inverted microscope with DAPI, GFP/FITC, Cy3/Rhodamine and Cy5 excitation and emission filter sets. The fluorescence signal from the target protein is quantified using custom Matlab code based on the Watershed algorithm. Using the Hoechst stain for the nucleus and the CellMask stain for the cytoplasm, the cell boundary is marked and the fluorescence signal quantified as mean signal / cell.

Cell survival assay : Cells were seeded at a density of 2000 cells/well in a dark walled, transparent bottom 96 well assay plate overnight and then serum starved for 24 hours followed by 24 hours of NVPAEW541 treatment. 10% Alamar blue was added to each well and fluorescence measured at 590nm in a plate reader. No drug control was used to express the percentage of cell survival.

Annexin V : Cells were grown to 95% confluency, serum starved overnight, treated with NVP drug, trypsinized to make single cell suspension, washed in wash buffer and incubated with AnnexinV:PE as indicated by the BD protocol. The cells were also counterstained with 7-AAD to exclude dead cells. The cells were analyzed by flow cytometry, gated and plotted with AnnexinV against sidescatter.

Cell surface biotinylation and receptor internalization rate : Cells are grown in flasks to 95% confluency and serum starved overnight. Cells are washed in ice-cold PBS and incubated with Supho-NHS-SS-Biotin to label all cell surface receptors. The cells are washed and stimulated with IGF-2 at 37degC to aid internalization of the receptors. After stimulation the remaining biotin on the receptors on the surface are cleaved with glutathione reducing agent and the cells are lysed in IP buffer. The lysate is then incubated with streptavidin coated dynabeads to pull down biotin labeled receptors and analyzed by Western blotting. The blots are then probed with Anti-IGF1R antibodies to quantify internalized IGF1R.

Internalization rate with FM143FX : Cells were seeded on Mattek dishes and left overnight for attachment. They were then serum starved overnight and incubated with 100uM FM143FX dye for 15 minutes at 4degC for the dye to stain the cell surface. The dye is then removed, cells washed to remove excess of the dye and the DMEM medium (without phenol red) replaced back. The cells were incubated with IGF-2 at 37degC for various times. After the set time points the cells were washed, fixed and imaged for the internalized dye. Cells were also counterstained with Hoechst 33342 and HCS CellMask^{TM} Deep Red (Life Technologies, CA) to stain the nucleus and the cytoplasm. The internalized dye was then quantified by using the nuclear and cytoplasmic stain as a mask to delineate the cell using custom Matlab code based on the Watershed algorithm.

qRT-PCR assays : Cells were grown to confluence and collected as pellets in RNAprotect cell reagent (Qiagen, CA). According to instructions of the RNEasy kit (Qiagen, CA) total RNA was extracted from the cells. The RNA was then converted to cDNA according to the instructions of the QuantiTec Rev. Transcription kit (Qiagen,CA). Using custom Taqman assays (AppliedBiosystems, CA) for the various gene targets, the cDNA was added to the Taqman probes in triplicates in a pcr mix in 384 well plates. Using multiple dyes for the gene of interest and β-actin in the same well, the fold expression of the gene of interest normalized to β-actin is determined from the respective Ct.

Computational model of IGF-2 signaling

IGF-2 binds cell surface receptors (IGF1R and IGF1R:Insulin Receptor (IR) heterotetramers) and autophosphorylates them on their cytoplasmic tails (R.2 and R.5 below). The phosphorylated receptors are aggregated into clathrin coated pits and internalized into vesicles (R.6). The plasma membrane localized receptors activate Akt (through the PI3K pathway) (R.9). The internalized receptors in the vesicles activate Erk (R.10) through a sequence of adaptors and signaling cascades. A fraction of the internalized receptors are degraded via proteasomal and lysosomal pathways (R.7) and another fraction is recycled back to the surface of the cell (R.3). We have shown that activated Erk can negatively regulate IGF1R by ubiquitylating cell surface IGF1R (R.4) while it can positively regulate IGF1R by its increased transcription over 24hours (R.12). Phosphorylated Akt is acted upon by the phosphatase PP2A to return Akt to its de-phosphorylated state (R.8) while Erk is known to exert a negative feedback onto itself and causes the return in its phosphorylated state to baseline (R.11). While the net concentrations of all protein species (phosphorylated + unphosphorylated) are taken to be a constant, the IGF1R levels are driven by the basal transcription rate (R.1)

The descriptive pathway detailed above was converted to rate equations as below,

$v_0 = btr$; Basal transcription of IGF1R R.1

$v_1 = \frac{k_1[IGF1R][Lig]}{K_1+[Lig]}$; IGF-2 binding of IGF1R and activation R.2

$v_2 = 0.5k_2[RT_{int}]$; Internalized receptor complexes recycling back to the cell surface. R.3

$v_3 = k_3[Erk_{pp}]$; Erk mediated ubiquitination of IGF-1R complexes R.4

$v_4 = \frac{k_4[IGF1R:IR][Lig]}{K_4+[Lig]}$; IGF2 binding and phosphorylation of the IGF1R: IR complex R.5

$v_5 = k_5[RT_P]$; Fraction of phosphorylated receptors that get internalized R.6

$v_6 = k_6[RT_{int}]$; Fraction of internalized receptors degraded via lysosomal and proteasomal pathways. R.7

$v_7 = \frac{k_7[PP2A][Akt_{pp}]}{K_7+[Akt_{pp}]}$; Akt dephophorylation by PP2A phosphatase R.8

$v_8 = \frac{k_8[Akt]\left[RT_P^{N_1}\right]}{K_8^{N_1}+[RT_P^{N_1}]}$; Akt activation by the receptor complexes on the cell surface R.9

$v_9 = \frac{k_9[Erk][RT_{int}^{N_2}]}{K_9^{N_2}+[RT_{int}^{N_2}]}$; Erk activation by the internalized receptor complexes R.10

$v_{10} = \frac{k_{10}[Erk_{pp}][Erk_{pp}]}{K_{10}+[Erk_{pp}]}$; Erk driven negative feedback onto itself R.11

$v_{11} = Btr * (Erk\_fb\_delay)$; A delayed Erk driven positive transcriptional feedback on IGF1R R.12

Where $[IGF1R]$ and $[IGF1R{:}IR]$ are the total cell surface receptors, $[RT_P]$ and $[RT_{int}]$ are the activated cell surface and internalized receptors respectively, [Akt] and [Erk] are non-phosphorylated Akt and Erk while $\left[Akt_{pp}\right]$ and $[Erk_{pp}]$ are the phosphorylated Akt and Erk. Btr is the basal transcription rate, while [Lig] is IGF-2. The parameters used in the equations are listed below in Table. 1 along with the method used to estimate them.

Table 1 : Parameters used in the rate equations (R.1 to R.12) - Values and method of estimation.

Parameters	Value (Mean ± SD)	Method
Btr	3000 / sec	Estimate from data fitting
k_1	1 / sec	Conversion factor
K_1	50 nM	(Surinya et al., 2008),(Forbes et al., 2002),(Danielsen et al., 1990)
k_2	0.01 / sec	Estimate from data fitting
k_3	0.0005 /sec	Estimate from data fitting
k_4	1 /sec	Conversion factor
K_4	50 nM	(Surinya et al., 2008),(Forbes et al., 2002),(Danielsen et al., 1990)
k_5	0.9 /sec	Estimated from data fitting and bound experimentally
k_6	0.01 /sec	Estimate from data fitting
k_7	13.2± 3.9 /sec	Estimate from data fitting
K_7	75.3 ± 24.9 nM	Estimate from data fitting
k_8	0.7 ± 0.2 /sec	Estimate from data fitting
K_8	(8.1 ± 2.3) x 10^4 nM	Estimate from data fitting

k_9	0.4 ± 0.1 /sec	Estimate from data fitting
k_{10}	(1.5 ± 0.8) x 10^3 /sec	Estimate from data fitting
K_{10}	0.14 ± 0.03 nM	Estimate from data fitting
N_1	3.5	Estimate from data fitting
N_2	3.5	Estimate from data fitting

ODE equations for implementation of model : The model described above was implemented by a system of ordinary differential equations (ODE) listed below. The behavior of the model was studied by numerically solving the system of ODEs.

$$\frac{d[IGF1R]}{dt} = v_0 - v_1 + v_2 - v_3 + v_{11} \quad \text{O.1}$$

$$\frac{d[IGF1R{:}IR]}{dt} = v_0 - v_4 + v_2 \quad \text{O.2}$$

$$\frac{d[RT_p]}{dt} = v_1 + v_4 - v_5 \quad \text{O.3}$$

$$\frac{d[RT_{int}]}{dt} = -2v_2 + v_5 - v_6 \quad \text{O.4}$$

$$\frac{d[Akt_{pp}]}{dt} = v_8 - v_7 \quad \text{O.5}$$

$$\frac{d[Akt]}{dt} = v_7 - v_8 \quad \text{O.6}$$

$$\frac{d[Erk_{pp}]}{dt} = v_9 - v_{10} \quad \text{O.7}$$

$$\frac{d[Erk]}{dt} = v_{10} - v_9 \quad \text{O.8}$$

The system of ODE equations was written and implemented in Matlab Ver R2011b. The equations were solved using custom written code. The model was allowed to attain a steady

state from the initial conditions listed in Table 2 by running the simulation with no ligand input ([IGF-2]=0) until all variables attained a constant concentration.

Table 2 : Initial values for system variables

Molecular Species	Value	Reference
$IGF1R$	75 x 10^3	(Wiley et al., 2003)
$IGF1R{:}\,IR$	50 x 10^3	Measured relative to IGF1R
RT_p	0	
RT_{int}	0	
Akt	100 nM	(Barnett et al., 2005), (Hatakeyama et al., 2003)
Akt_{pp}	0 nM	
Erk	2000 nM	From (Hatakeyama et al., 2003)
Erk_{pp}	0 nM	
$PP2A$	10 nM	From (Hatakeyama et al., 2003)

The model equations were written in Matlab ver R2011b and the system of ODE equations solved using custom written code. To define an initial steady state for the system analogous to serum starving of cells, the model was simulated starting from the values listed in Table 2 and allowed to run until all variables settled to a constant value. These values were used as the initial steady state of the system prior to stimulation by IGF-2.

Model Training : To train the model and to estimate the parameters listed in Table 1, the fold increase in pAkt and pErk activation in response to IGF-2 stimulation (Fig 1.1A), were used. For a given set of model parameters the model output (pAKt and pErk) was computed as a function of time. The model parameter estimation was set up as a minimization of the sum of the mean square error of the model output and the experimental values of both pAkt and pErk (T.1)

$$\min_{\forall\, Model\ Parameters} \sum \{Model(pAkt) - Exp(pAkt)\}^2 + \{Model(pErk) - Exp(pErk)\}^2 \qquad \text{T.1}$$

The Direct (Divided Rectangles) algorithm (D. R. Jones, 1993) based on a modified Lipschitzian optimization was the algorithm used to minimize the above cost function. The estimation was done for all the three sets of data used in Fig 1.1A. The mean and standard deviation (SD) of each of the parameters are listed in Table 1. The model output of pAkt and pErk profiles trained on the 3 data sets from Fig 1.1A are shown together in Fig 1.11. To test the training of the

model, the model output using the mean of the estimated parameters was compared against the mean of the 3 sets of data used in training. The comparison is plotted in red for Akt and Erk on the right side of Fig 3E. To test the predictive ability of the model we simulated WT behavior by using WT values of receptors (both IGF1R and IGF1R:IR heterotetramers) and internalization rate only as shown in Table 3. The rest of the parameters were kept the same as before. The model output simulating WT fold increase in pAkt and pErk compared with experimental pAkt and pErk data for WT cells from Fig 1.1A is shown in blue in the right panel of Fig 1.11

Table 3 : Parameters / Variables changed in model to predict WT behavior.

Parameters/Variables	Relevance	Value	Reference
IGF1R	Initial Value	$30x10^3$	Measured experimentally
IGF1R:IR	Initial Value	$15x10^3$	Measured experimentally
k_5	Internalization rate	0.01 /sec	Measured experimentally

The positive transcriptional feedback of Erk onto IGF-1R (Fig 3A) is implemented as below.

$$Erk\_fb\_delay = \begin{cases} 0 & for\ t \leq 12hrs \\ \dfrac{(t-12)}{24}\Big|_{t=12hr}^{t=24hrs} & for\ 12 < t \leq 24hrs \end{cases}$$

Anti and Pro-apoptotic extension of IGF-2 signaling model : As shown in Fig. 4A and Fig. 4B, Bax and Bcl2 levels in LOI cells share a reciprocal relationship with the Bax and Bcl2 levels in WT cells. The computational model for IGF-2 signaling was extended to simulate steady levels of Bax and Bcl2. As shown in Fig 4D, Bax steady state levels depend on the strength of Erk signaling while it has been shown before and in Supp Fig XX that Bcl2 levels depend on the strength of Akt signaling.

$$[Bax] = k_{Bax} * max(pErk)$$

$$[Bcl2] = k_{Bcl2} * max(pAkt)$$

To estimate values of kbax and kbcl2 the steady state values of Bax and Bcl2 had to be established. Various estimates of Bax and Bcl2 values in mammalian cells put the concentration in between 1 and 10nM[refx][refy][refz]. The following is also known,

$$[Bcl2_{WT}] = 2 * [Bcl2_{LOI}]$$

$$[Bax_{WT}] = 0.5 * [Bax_{LOI}]$$

Using the condition for survival of a cell in terms of pro and anti apoptotic proteins,

For every $[0 \leq Bcl2_{LOI} \leq 10nM, 0 \leq Bax_{LOI} \leq 10nM] that\ satisfies, [Bcl2_{LOI}] \geq [Bax_{LOI}]$

We have $[0 \leq Bcl2_{WT} \leq 10nM, 0 \leq Bax_{WT} \leq 10nM]\ that\ satifies\ 0.5 * [Bcl2_{WT}] \geq 2 * [Bax_{WT}]$

The Bcl2,Bax values of WT and LOI cells that satisfy the above equations form a triangular region as shown in Fig 5A. The centroids of these regions are taken as the steady state values of Bax and Bcl2 for WT and LOI cells respectively.

Table 4 : Steady state values of Bax, Bcl2 and associated constants

WT		LOI	
Bcl2	6.6nM	Bcl2	3.3nM
Bax	1.3nM	Bax	2.6nM
K_{Bcl2}	0.55nM	K_{Bcl2}	0.55nM
K_{Bax}	0.33nM	K_{Bax}	0.3nM

Model learning and prediction of IGF-1 signaling : To simulate IGF-1 modeling, as with IGF-2, the model was trained on the fold increase in pAkt and pErk of LOI cells in response to IGF-1 Fig 6A. The model learning is also shown in Fig 6A. The Kd of binding of IGF-1 to the cell surface receptor complexes of IGF1R and IGF1R:IR was kept as $1/10^{th}$ that of IGF-2 binding during the training (Surinya et al., 2008). To predict WT Akt and Erk responses, the internalization rate of the receptors in WT model was varied until the model prediction matched the experimental data Fig 6B. The IGF-1 binding values to the cell surface receptor complexes and the Internalization rate used to predict WT responses are shown in Table 5.

Table 5 : Parameter comparison between IGF-1 and IGF-2 signaling models.

IGF-1				**IGF-2**			
WT		**LOI**		**WT**		**LOI**	
Internalization rate				**Internalization rate**			
k5	0.5	k5	0.9	k5	0.01	k5	0.9
Kd of Binding	**IGF1R**	**IGF1R:IR**		**Kd of Binding**	**IGF1R**	**IGF1R:IR**	
K_1	5nM	5nM		K_1	50nM	50nM	
K_4	5nM	5nM		K_4	50nM	50nM	

Supplementary Figures

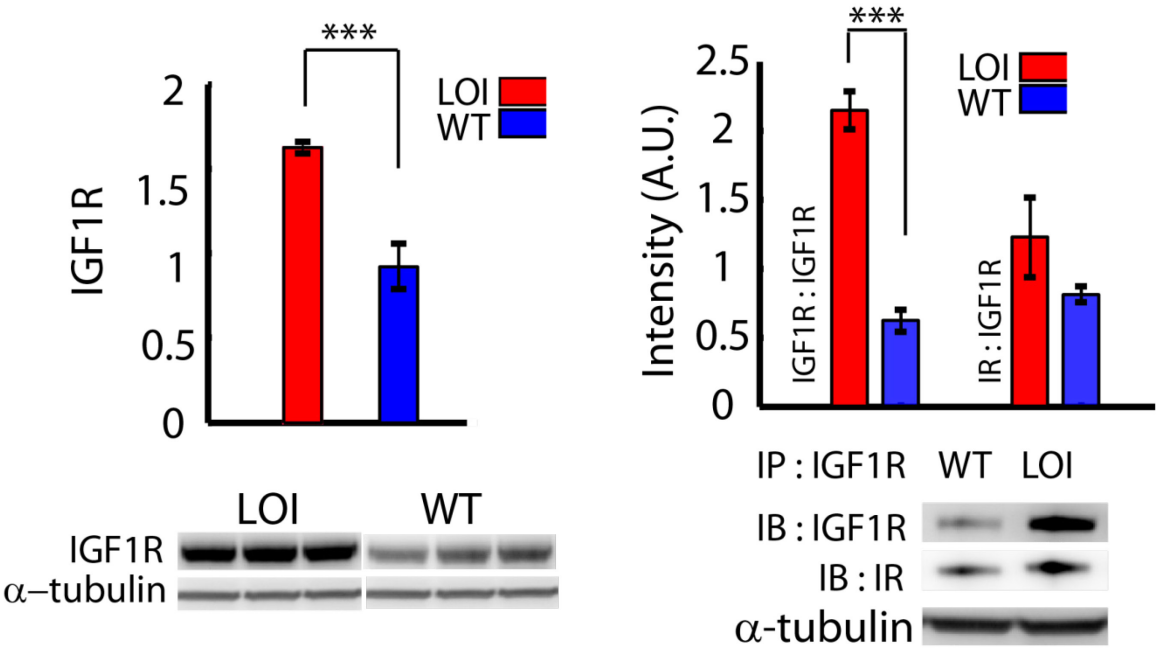

Figure S 1 : Receptor expression

Exponentially growing LOI and WT cells were harvested and A) analysed by Western blots for A) total IGF-1R levels. B) Cell lysates were immunoprecipitated with IGF-1R antibodies and immunoblotted for IGF1R and IR levels respectively.

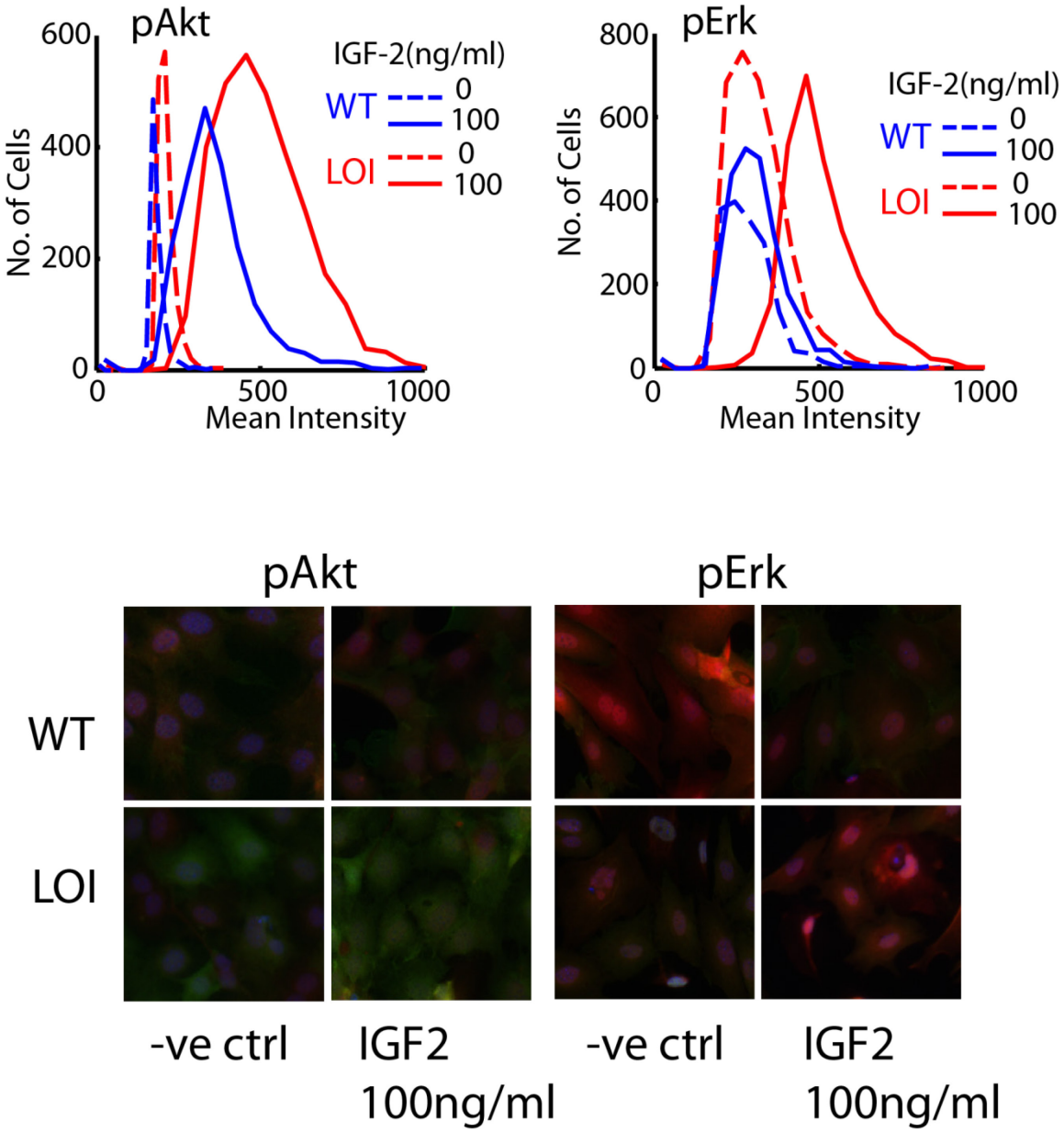

Figure S 2 : Fold increase in pErk and pAkt

Exponentially growing LOI and WT cells were serum starved overnight and stimulated with IGF-2 for 10 minutes and fixed on glass coverslips and analysed by immunofluorescence for fold increase in pAkt and pErk when compared to non-stimulated control.

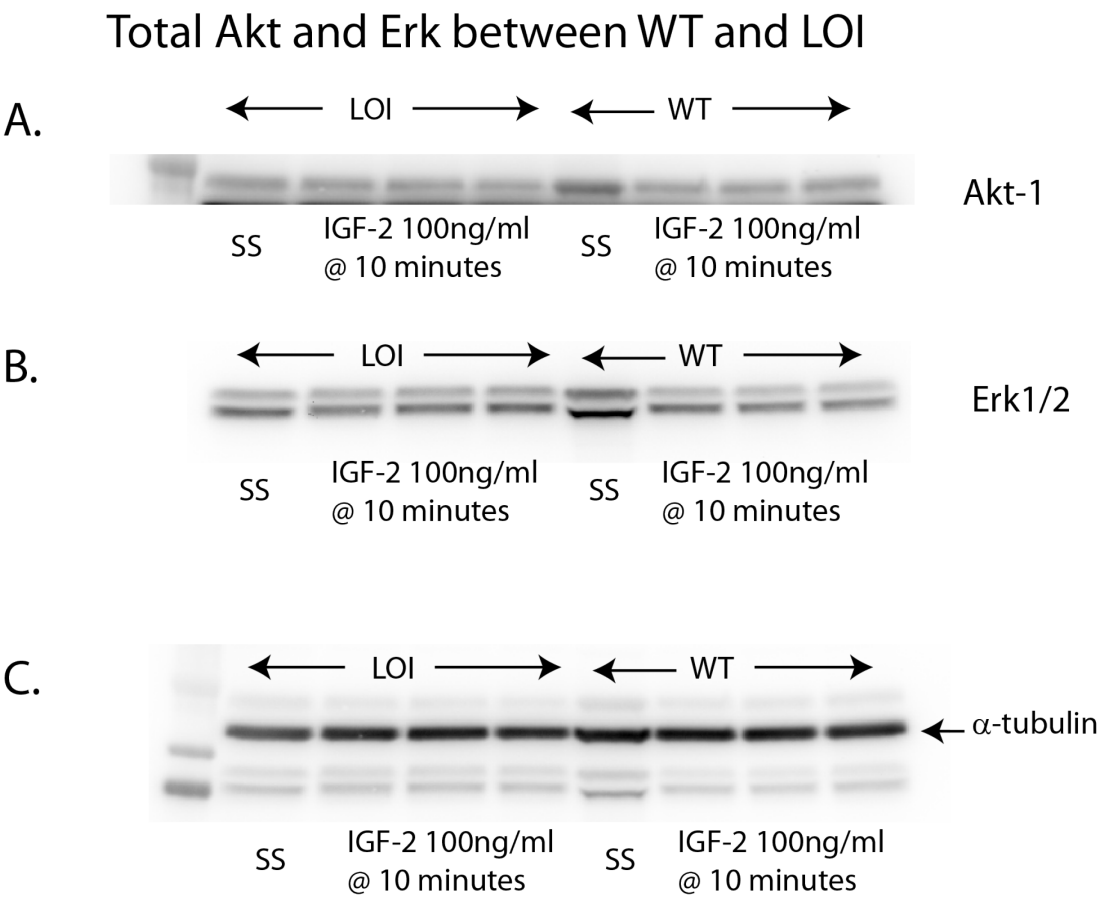

Figure S 3 : Total Akt and Erk

Exponentially growing LOI and WT cells were harvested and analysed by Western blots for A)total Akt and B)total Erk. The total Akt and Erk were seen to be the same in both LOI and WT cells.

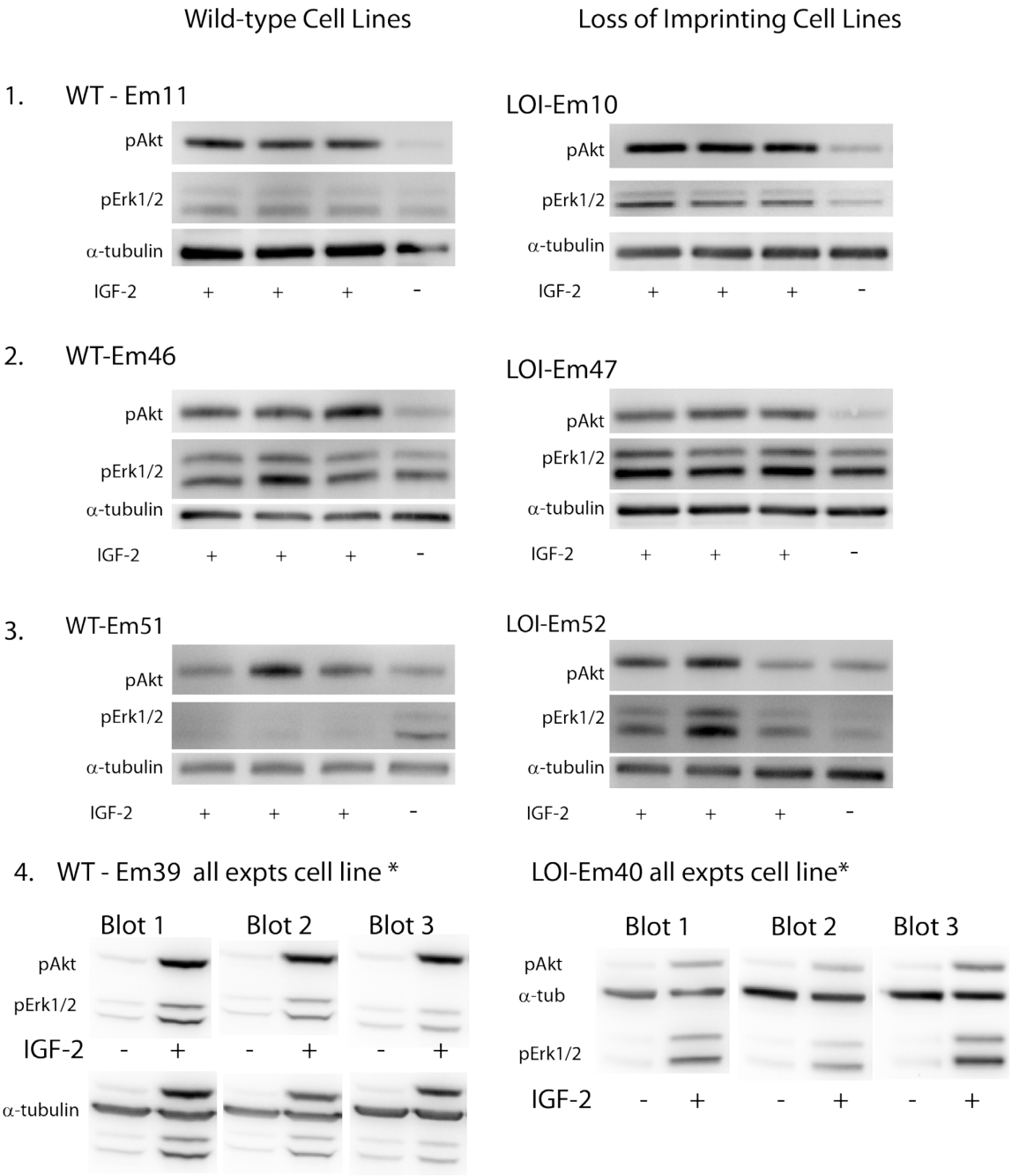

Figure S 4 : Multiple WT and LOI lines

4 different LOI cell lines and 4 different WT cell lines were extracted from E16 mouse embryos. These cell lines were passaged for 3 to 4 times. Exponentially growing cells (75 to 80% confluency) were serum starved overnight, stimulated with 100ng/ml IGF-2 for 10 minutes, harvested and analyzed by Western blots for pAkt and pErk expression.

Fold Akt and Erk change in WT and LOI (All 4 LOI and WT cell lines combined together)

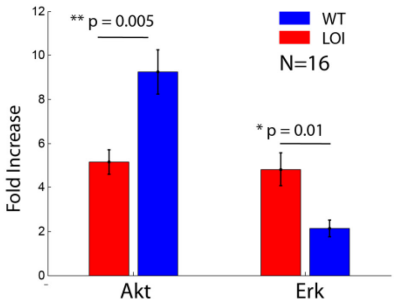

The fold change in induction of Akt and Erk in LOI and WT cells, across all cell lines used, in response to IGF-2 activation was plotted by combining all the fold induction data (N=16) for Akt and Erk for all the LOI and WT cell lines used (4 each). The mean of the data is plotted and the standard error of means is shown as the errorbars. As shown above, the fold increase in induction of Akt in WT cells is greater (statistically significant)

Figure S 5 : Multiple cell lines quantification

4 different LOI cell lines and 4 different WT cell lines were extracted from E16 mouse embryos. These cell lines were passaged for 3 to 4 times. Exponentially growing cells (75 to 80% confluency) were serum starved overnight, stimulated with 100ng/ml IGF-2 for 10 minutes, harvested and analyzed by Western blots for pAkt and pErk expression.

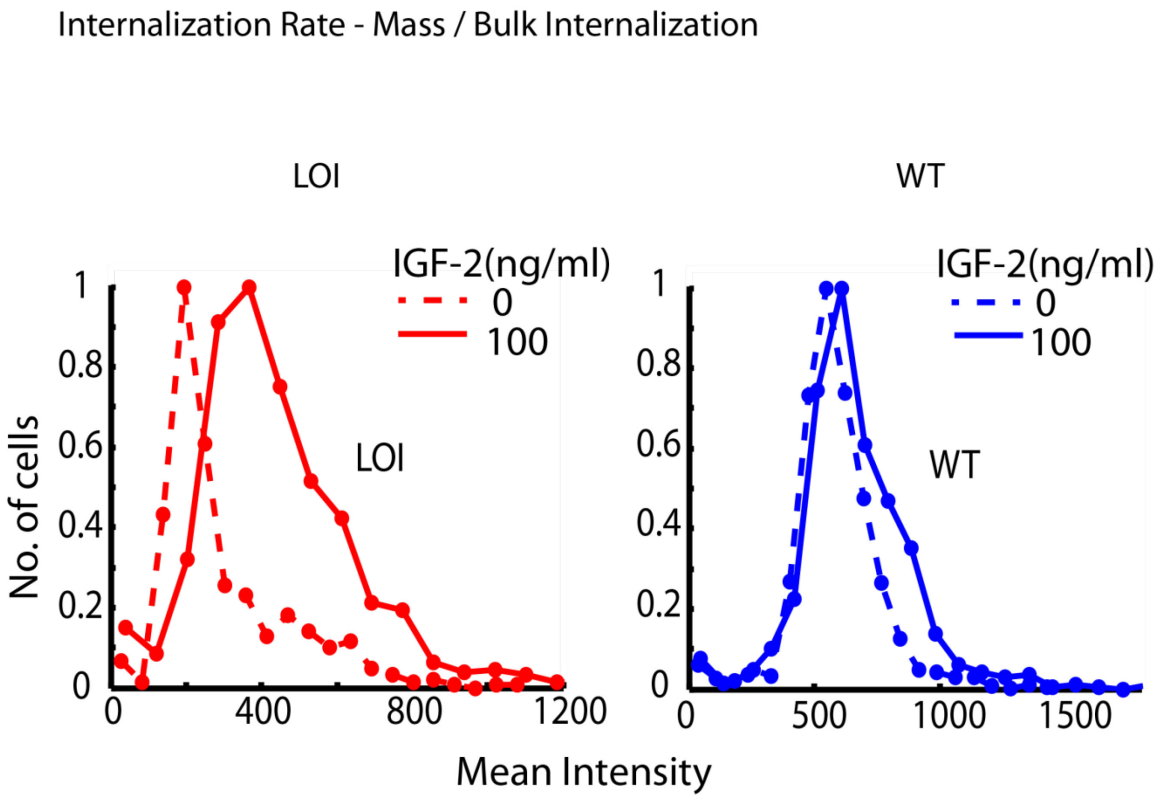

Figure S 6 : Bulk Internalization

WT and LOI cells were grown on cover slips to confluency. The cells were labelled for 15 min at 4degC with the dye FM-143 that labels the plasma membrane and then washed to remove excess dye. The cells were then treated with 100ng/ml IGF-2 to allow for internalization of the dye for the indicated timepoints. The cells are then fixed and the amount of internalized dye quantified using Immunofluorescence.

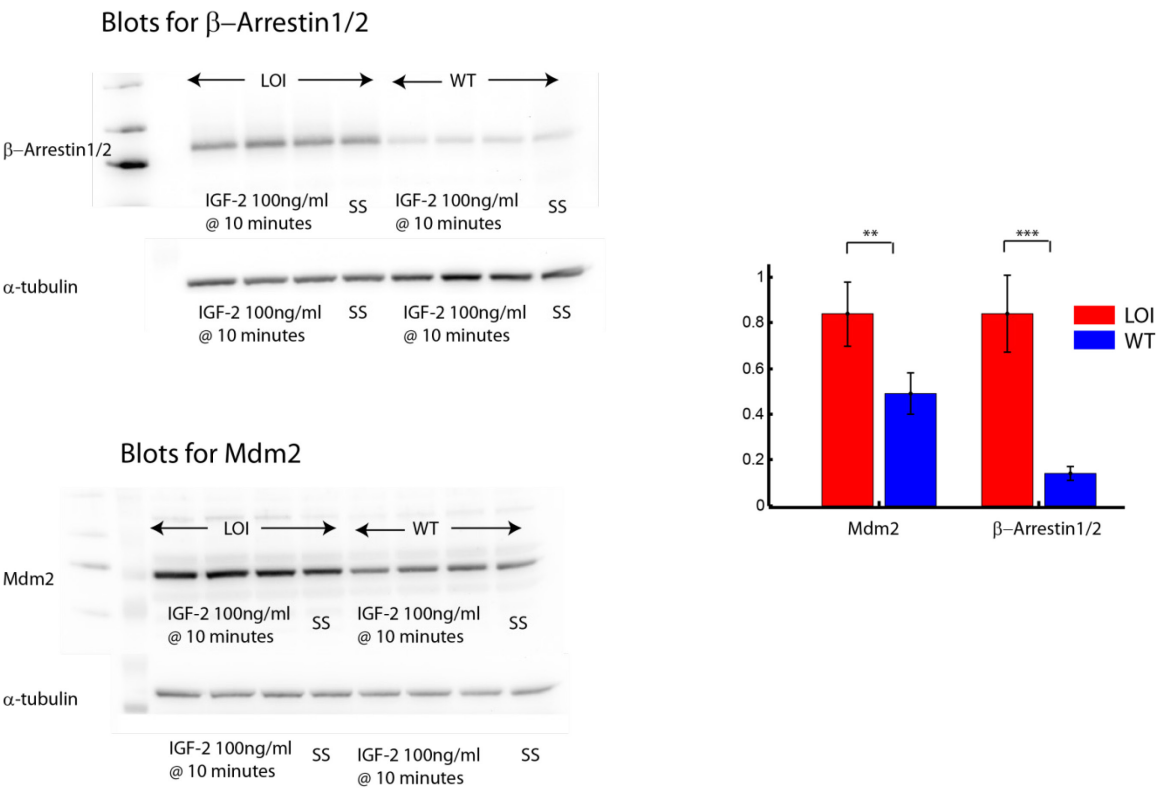

Figure S 7 : β-Arrestin and Mdm2

Exponentially growing WT and LOI cells were harvested and analyzed by Western blotting for the expression of beta-Arrestin1/2 and Mdm2

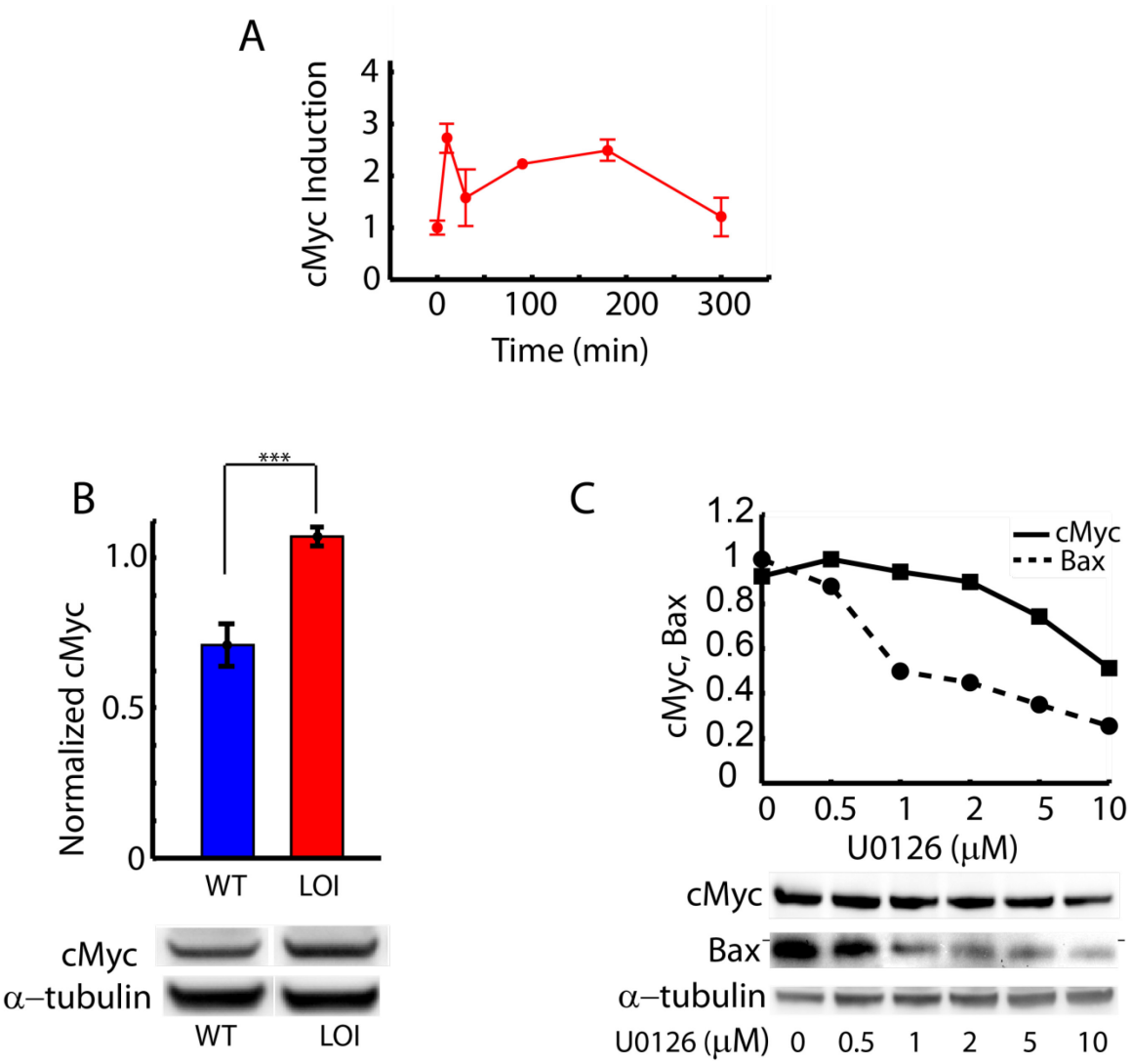

Figure S 8 : cMyc induction and expression

A) Exponentially growing LOI cells were serum starved overnight, stimulated with IGF-2 for the indicated time points, harvested and analyzed by qRT-PCR for cMyc expression. cMyc expression was normalized to β-Actin in each well and plotted as fold increase over the value at time=0. cMyc is a direct target of IGF1R signaling. *Akt-Erk signaling balance is reflected in cMyc levels* : B) Exponentially growing WT and LOI cells were serum starved overnight and stimulated with 10%FBS for 24 hours, they were then harvested in lysates and analyzed by Western blotting. cMyc levels in the LOI cells reflect the increased Erk signaling in LOI cells vis-a-vis the WT cells. *Pro-apoptotic Bax is a cMyc target :* C) LOI cells were serum starved overnight and then treated with varying concentrations of U0126 (Mek inhibitor) for 60 min followed by IGF-2 for 24 hours. The cells were harvested in lysates and analyzed via Western blotting. Bax signaling is regulated by levels of cMyc signaling.

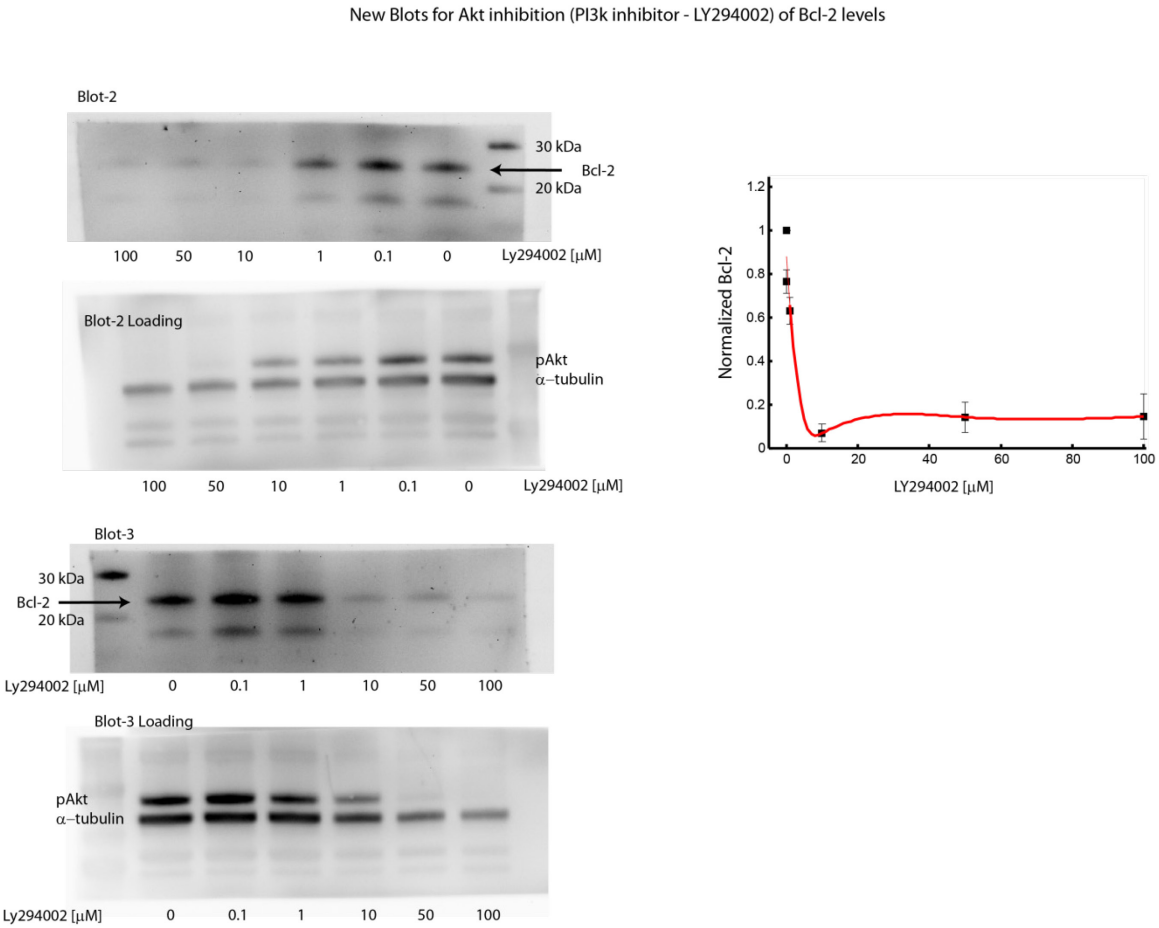

Figure S 9 : Bcl2 levels are affected by Akt signaling

Exponentially growing LOI cells were treated with various doses of the Pi3K inhibitor, LY294002 for 60 minutes, stimulated with IGF-2 for 24 hours, harvested and analyzed for Akt and Bcl-2 levels.

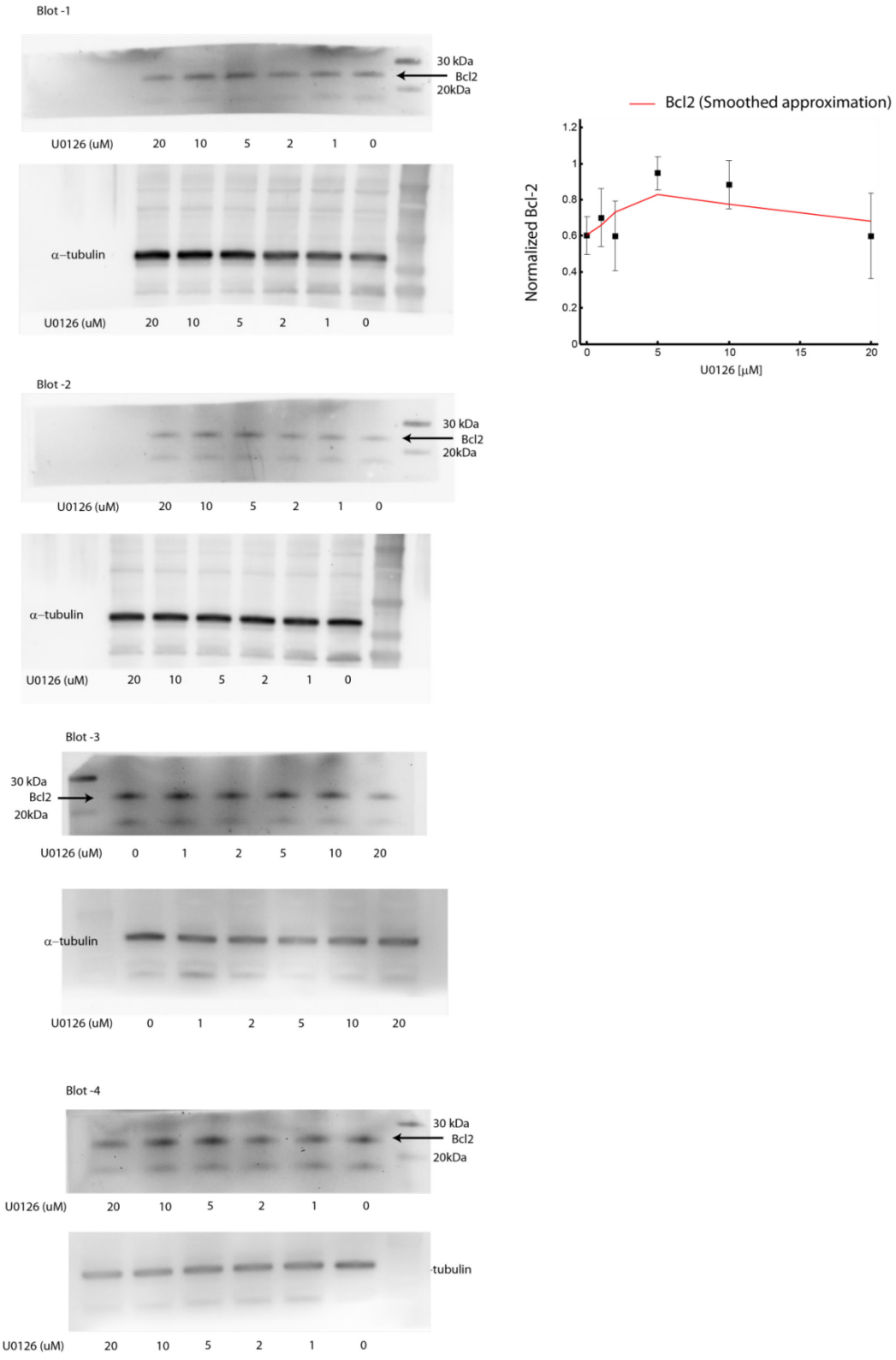

Figure S 10: Bcl2 levels are not affected by Erk signaling

Exponentially growing LOI cells were treated with various doses of the Erk inhibitor, U0126 for 60 minutes, stimulated with IGF-2 for 24 hours, harvested and analyzed for Bcl-2 levels.

Caspase activation quantification

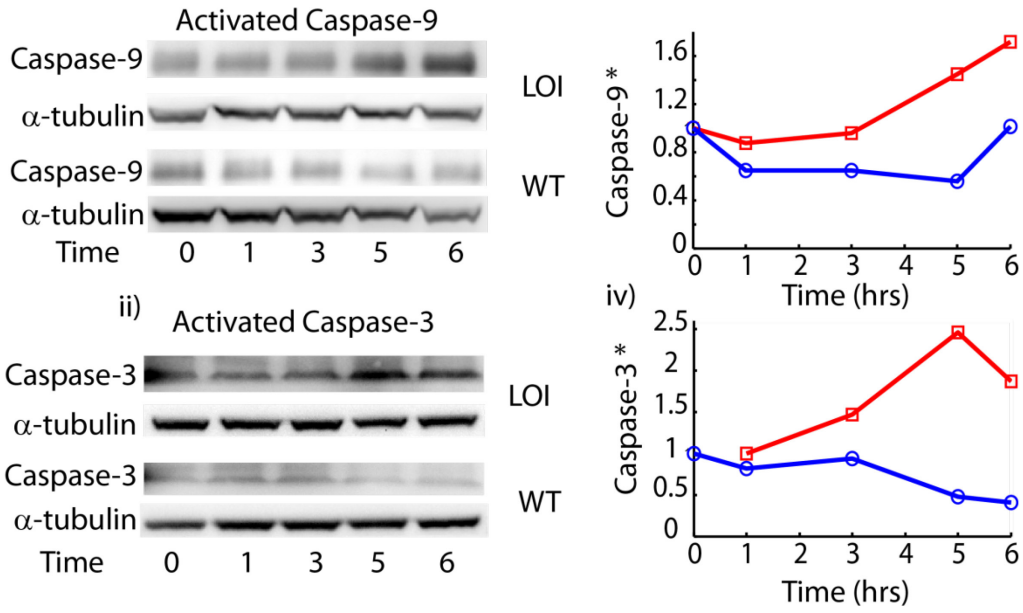

Figure S 11 : Activated Caspase-9 and -3

WT and LOI cells were serum starved and treated with 5µM NVPAEW541 for the indicated time points, harvested in lysates and analyzed by Western Blotting for activated Caspase-9 and Caspase-3. Both the early Caspase-9 and the effector Caspase-3 are seen to activated by t=5 hours in LOI cells while no activation is seen in WT cells.

Annexin -V staining for NVP treated LOI cells.

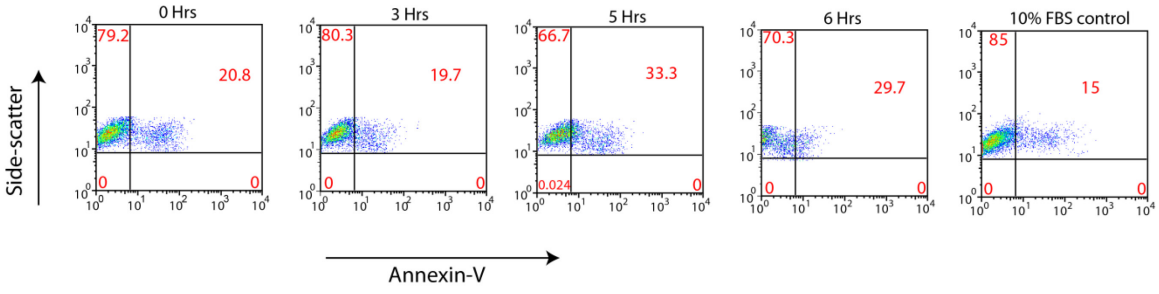

Figure S 12: Annexin V staining

Exponentially growing LOI cells were serum starved overnight and treated with 5µM NVPAEW541 for the indicated time points and stained for the early apoptosis marker Annexin V. By 5 hours after NVP treatment, LOI cells show Annexin V positive stain.

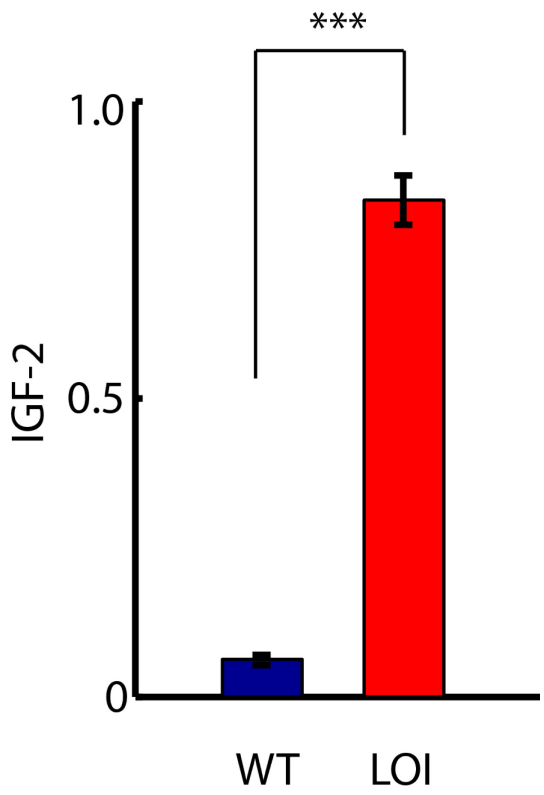

Figure S 13: IGF-2 expression

Exponentially growing LOI and WT cells were analyzed by qRT-PCR for IGF-2 mRNA expression. LOI cells show increased expression of IGF-2

References

Acconcia, F., Sigismund, S., and Polo, S. (2009). Ubiquitin in trafficking: the network at work. Experimental cell research *315*, 1610-1618.

Barnett, S.F., Defeo-Jones, D., Fu, S., Hancock, P.J., Haskell, K.M., Jones, R.E., Kahana, J.A., Kral, A.M., Leander, K., Lee, L.L.*, et al.* (2005). Identification and characterization of pleckstrin-homology-domain-dependent and isoenzyme-specific Akt inhibitors. The Biochemical journal *385*, 399-408.

Biedi, C., Panetta, D., Segat, D., Cordera, R., and Maggi, D. (2003). Specificity of insulin-like growth factor I and insulin on Shc phosphorylation and Grb2 recruitment in caveolae. Endocrinology *144*, 5497-5503.

Chen, J.Y., Lin, J.R., Cimprich, K.A., and Meyer, T. (2012). A two-dimensional ERK-AKT signaling code for an NGF-triggered cell-fate decision. Molecular cell *45*, 196-209.
Chow, J.C., Condorelli, G., and Smith, R.J. (1998). Insulin-like growth factor-I receptor internalization regulates signaling via the Shc/mitogen-activated protein kinase pathway, but not the insulin receptor substrate-1 pathway. The Journal of biological chemistry *273*, 4672-4680.
Clemmons, D.R. (2007). Modifying IGF1 activity: an approach to treat endocrine disorders, atherosclerosis and cancer. Nature reviews Drug discovery *6*, 821-833.
Clevers, H. (2013). The intestinal crypt, a prototype stem cell compartment. Cell *154*, 274-284.
D. R. Jones, C.D.P., B. E. Stuckman (1993). Lipschitzian Optimization Without the Lipschitz Constant. Journal of Optimization Theory and Applications *79*, 157-181
Danielsen, A., Larsen, E., and Gammeltoft, S. (1990). Chromaffin cells express two types of insulin-like growth factor receptors. Brain research *518*, 95-100.
Du, K., and Montminy, M. (1998). CREB is a regulatory target for the protein kinase Akt/PKB. The Journal of biological chemistry *273*, 32377-32379.
Forbes, B.E., Hartfield, P.J., McNeil, K.A., Surinya, K.H., Milner, S.J., Cosgrove, L.J., and Wallace, J.C. (2002). Characteristics of binding of insulin-like growth factor (IGF)-I and IGF-II analogues to the type 1 IGF receptor determined by BIAcore analysis. European journal of biochemistry / FEBS *269*, 961-968.
Genua, M., Pandini, G., Sisci, D., Castoria, G., Maggiolini, M., Vigneri, R., and Belfiore, A. (2009). Role of cyclic AMP response element-binding protein in insulin-like growth factor-i receptor up-regulation by sex steroids in prostate cancer cells. Cancer research *69*, 7270-7277.
Girnita, L., Girnita, A., and Larsson, O. (2003). Mdm2-dependent ubiquitination and degradation of the insulin-like growth factor 1 receptor. Proceedings of the National Academy of Sciences of the United States of America *100*, 8247-8252.
Goustin, A.S., Leof, E.B., Shipley, G.D., and Moses, H.L. (1986). Growth factors and cancer. Cancer research *46*, 1015-1029.
Greenman, C., Stephens, P., Smith, R., Dalgliesh, G.L., Hunter, C., Bignell, G., Davies, H., Teague, J., Butler, A., Stevens, C.*, et al.* (2007). Patterns of somatic mutation in human cancer genomes. Nature *446*, 153-158.
Hatakeyama, M., Kimura, S., Naka, T., Kawasaki, T., Yumoto, N., Ichikawa, M., Kim, J.H., Saito, K., Saeki, M., Shirouzu, M.*, et al.* (2003). A computational model on the modulation of mitogen-activated protein kinase (MAPK) and Akt pathways in heregulin-induced ErbB signalling. The Biochemical journal *373*, 451-463.
Haugh, J.M., and Meyer, T. (2002). Active EGF receptors have limited access to PtdIns(4,5)P(2) in endosomes: implications for phospholipase C and PI 3-kinase signaling. Journal of cell science *115*, 303-310.
Hayashi, K., Takahashi, M., Kimura, K., Nishida, W., Saga, H., and Sobue, K. (1999). Changes in the balance of phosphoinositide 3-kinase/protein kinase B (Akt) and the mitogen-activated protein kinases (ERK/p38MAPK) determine a phenotype of visceral and vascular smooth muscle cells. The Journal of cell biology *145*, 727-740.
Holbrook, M.R., O'Donnell, J.B., Jr., Slakey, L.L., and Gross, D.J. (1999). Epidermal growth factor receptor internalization rate is regulated by negative charges near the SH2 binding site Tyr992. Biochemistry *38*, 9348-9356.
Jullien, J., Guili, V., Reichardt, L.F., and Rudkin, B.B. (2002). Molecular kinetics of nerve growth factor receptor trafficking and activation. The Journal of biological chemistry *277*, 38700-38708.
Kaneda, A., Wang, C.J., Cheong, R., Timp, W., Onyango, P., Wen, B., Iacobuzio-Donahue, C.A., Ohlsson, R., Andraos, R., Pearson, M.A.*, et al.* (2007). Enhanced sensitivity to IGF-II signaling links

loss of imprinting of IGF2 to increased cell proliferation and tumor risk. Proceedings of the National Academy of Sciences of the United States of America *104*, 20926-20931.
Kennedy, S.G., Wagner, A.J., Conzen, S.D., Jordan, J., Bellacosa, A., Tsichlis, P.N., and Hay, N. (1997). The PI 3-kinase/Akt signaling pathway delivers an anti-apoptotic signal. Genes & development *11*, 701-713.
Kratchmarova, I., Blagoev, B., Haack-Sorensen, M., Kassem, M., and Mann, M. (2005). Mechanism of divergent growth factor effects in mesenchymal stem cell differentiation. Science *308*, 1472-1477.
Lemmon, M.A., and Schlessinger, J. (2010). Cell signaling by receptor tyrosine kinases. Cell *141*, 1117-1134.
Lindner, A.U., Concannon, C.G., Boukes, G.J., Cannon, M.D., Llambi, F., Ryan, D., Boland, K., Kehoe, J., McNamara, D.A., Murray, F*., et al.* (2013). Systems analysis of BCL2 protein family interactions establishes a model to predict responses to chemotherapy. Cancer research *73*, 519-528.
Liu, W., Akhand, A.A., Takeda, K., Kawamoto, Y., Itoigawa, M., Kato, M., Suzuki, H., Ishikawa, N., and Nakashima, I. (2003). Protein phosphatase 2A-linked and -unlinked caspase-dependent pathways for downregulation of Akt kinase triggered by 4-hydroxynonenal. Cell death and differentiation *10*, 772-781.
Lu, Y., Muller, M., Smith, D., Dutta, B., Komurov, K., Iadevaia, S., Ruths, D., Tseng, J.T., Yu, S., Yu, Q*., et al.* (2011). Kinome siRNA-phosphoproteomic screen identifies networks regulating AKT signaling. Oncogene *30*, 4567-4577.
Marnell, M.H., Stookey, M., and Draper, R.K. (1982). Monensin blocks the transport of diphtheria toxin to the cell cytoplasm. The Journal of cell biology *93*, 57-62.
McMahon, H.T., and Boucrot, E. (2011). Molecular mechanism and physiological functions of clathrin-mediated endocytosis. Nature reviews Molecular cell biology *12*, 517-533.
Nguyen, L.K., Kolch, W., and Kholodenko, B.N. (2013). When ubiquitination meets phosphorylation: a systems biology perspective of EGFR/MAPK signalling. Cell communication and signaling : CCS *11*, 52.
Normanno, N., De Luca, A., Bianco, C., Strizzi, L., Mancino, M., Maiello, M.R., Carotenuto, A., De Feo, G., Caponigro, F., and Salomon, D.S. (2006). Epidermal growth factor receptor (EGFR) signaling in cancer. Gene *366*, 2-16.
Oda, K., Matsuoka, Y., Funahashi, A., and Kitano, H. (2005). A comprehensive pathway map of epidermal growth factor receptor signaling. Molecular systems biology *1*, 2005 0010.
Oltvai, Z.N., Milliman, C.L., and Korsmeyer, S.J. (1993). Bcl-2 heterodimerizes in vivo with a conserved homolog, Bax, that accelerates programmed cell death. Cell *74*, 609-619.
Ostman, A., Hellberg, C., and Bohmer, F.D. (2006). Protein-tyrosine phosphatases and cancer. Nature reviews Cancer *6*, 307-320.
Park, C.S., Schneider, I.C., and Haugh, J.M. (2003). Kinetic analysis of platelet-derived growth factor receptor/phosphoinositide 3-kinase/Akt signaling in fibroblasts. The Journal of biological chemistry *278*, 37064-37072.
Perlman, H., Zhang, X., Chen, M.W., Walsh, K., and Buttyan, R. (1999). An elevated bax/bcl-2 ratio corresponds with the onset of prostate epithelial cell apoptosis. Cell death and differentiation *6*, 48-54.
Raychaudhuri, S., and Das, S.C. (2013). Low probability activation of Bax/Bak can induce selective killing of cancer cells by generating heterogeneity in apoptosis. Journal of healthcare engineering *4*, 47-66.

Ren, B., Deng, Y., Mukhopadhyay, A., Lanahan, A.A., Zhuang, Z.W., Moodie, K.L., Mulligan-Kehoe, M.J., Byzova, T.V., Peterson, R.T., and Simons, M. (2010). ERK1/2-Akt1 crosstalk regulates arteriogenesis in mice and zebrafish. The Journal of clinical investigation *120*, 1217-1228.

Schayek, H., Haugk, K., Sun, S., True, L.D., Plymate, S.R., and Werner, H. (2009). Tumor suppressor BRCA1 is expressed in prostate cancer and controls insulin-like growth factor I receptor (IGF-IR) gene transcription in an androgen receptor-dependent manner. Clinical cancer research : an official journal of the American Association for Cancer Research *15*, 1558-1565.

Scheid, M.P., Schubert, K.M., and Duronio, V. (1999). Regulation of bad phosphorylation and association with Bcl-x(L) by the MAPK/Erk kinase. The Journal of biological chemistry *274*, 31108-31113.

Schutze, S., Machleidt, T., Adam, D., Schwandner, R., Wiegmann, K., Kruse, M.L., Heinrich, M., Wickel, M., and Kronke, M. (1999). Inhibition of receptor internalization by monodansylcadaverine selectively blocks p55 tumor necrosis factor receptor death domain signaling. The Journal of biological chemistry *274*, 10203-10212.

Sehat, B., Andersson, S., Vasilcanu, R., Girnita, L., and Larsson, O. (2007). Role of ubiquitination in IGF-1 receptor signaling and degradation. PloS one *2*, e340.

Sharma, S.V., Gajowniczek, P., Way, I.P., Lee, D.Y., Jiang, J., Yuza, Y., Classon, M., Haber, D.A., and Settleman, J. (2006). A common signaling cascade may underlie "addiction" to the Src, BCR-ABL, and EGF receptor oncogenes. Cancer cell *10*, 425-435.

Sharma, S.V., and Settleman, J. (2007). Oncogene addiction: setting the stage for molecularly targeted cancer therapy. Genes & development *21*, 3214-3231.

Siddle, K. (2011). Signalling by insulin and IGF receptors: supporting acts and new players. Journal of molecular endocrinology *47*, R1-10.

Sorkin, A., and von Zastrow, M. (2009). Endocytosis and signalling: intertwining molecular networks. Nature reviews Molecular cell biology *10*, 609-622.

Surinya, K.H., Forbes, B.E., Occhiodoro, F., Booker, G.W., Francis, G.L., Siddle, K., Wallace, J.C., and Cosgrove, L.J. (2008). An investigation of the ligand binding properties and negative cooperativity of soluble insulin-like growth factor receptors. The Journal of biological chemistry *283*, 5355-5363.

Tallquist, M., and Kazlauskas, A. (2004). PDGF signaling in cells and mice. Cytokine & growth factor reviews *15*, 205-213.

Tan, W.H., Popel, A.S., and Mac Gabhann, F. (2013). Computational Model of Gab1/2-Dependent VEGFR2 Pathway to Akt Activation. PloS one *8*, e67438.

Thompson, C.B. (2009). Metabolic enzymes as oncogenes or tumor suppressors. The New England journal of medicine *360*, 813-815.

Ulaner, G.A., Vu, T.H., Li, T., Hu, J.F., Yao, X.M., Yang, Y., Gorlick, R., Meyers, P., Healey, J., Ladanyi, M*., et al.* (2003). Loss of imprinting of IGF2 and H19 in osteosarcoma is accompanied by reciprocal methylation changes of a CTCF-binding site. Human molecular genetics *12*, 535-549.

Vasilcanu, R., Vasilcanu, D., Sehat, B., Yin, S., Girnita, A., Axelson, M., and Girnita, L. (2008). Insulin-like growth factor type-I receptor-dependent phosphorylation of extracellular signal-regulated kinase 1/2 but not Akt (protein kinase B) can be induced by picropodophyllin. Molecular pharmacology *73*, 930-939.

Vieira, A.V., Lamaze, C., and Schmid, S.L. (1996). Control of EGF receptor signaling by clathrin-mediated endocytosis. Science *274*, 2086-2089.

Weinstein, I.B. (2002). Cancer. Addiction to oncogenes--the Achilles heal of cancer. Science *297*, 63-64.

Weinstein, I.B., and Joe, A. (2008). Oncogene addiction. Cancer research *68*, 3077-3080; discussion 3080.

Werner, H. (2012). Tumor suppressors govern insulin-like growth factor signaling pathways: implications in metabolism and cancer. Oncogene *31*, 2703-2714.
Werner, H., Karnieli, E., Rauscher, F.J., and LeRoith, D. (1996). Wild-type and mutant p53 differentially regulate transcription of the insulin-like growth factor I receptor gene. Proceedings of the National Academy of Sciences of the United States of America *93*, 8318-8323.
Wiley, H.S., Shvartsman, S.Y., and Lauffenburger, D.A. (2003). Computational modeling of the EGF-receptor system: a paradigm for systems biology. Trends in cell biology *13*, 43-50.
Worster, D.T., Schmelzle, T., Solimini, N.L., Lightcap, E.S., Millard, B., Mills, G.B., Brugge, J.S., and Albeck, J.G. (2012). Akt and ERK control the proliferative response of mammary epithelial cells to the growth factors IGF-1 and EGF through the cell cycle inhibitor p57Kip2. Science signaling *5*, ra19.
Wu, G.-Y., Deisseroth, K., and Tsien, R.W. (2001). Activity-dependent CREB phosphorylation: Convergence of a fast, sensitive calmodulin kinase pathway and a slow, less sensitive mitogen-activated protein kinase pathway. Proceedings of the National Academy of Sciences *98*, 2808-2813.

Acconcia, F., Sigismund, S., and Polo, S. (2009). Ubiquitin in trafficking: the network at work. Experimental cell research *315*, 1610-1618.
Bach, S.P., Renehan, A.G., and Potten, C.S. (2000). Stem cells: the intestinal stem cell as a paradigm. Carcinogenesis *21*, 469-476.
Barker, N., van Es, J.H., Kuipers, J., Kujala, P., van den Born, M., Cozijnsen, M., Haegebarth, A., Korving, J., Begthel, H., Peters, P.J.*, et al.* (2007). Identification of stem cells in small intestine and colon by marker gene Lgr5. Nature *449*, 1003-1007.
Barnett, S.F., Defeo-Jones, D., Fu, S., Hancock, P.J., Haskell, K.M., Jones, R.E., Kahana, J.A., Kral, A.M., Leander, K., Lee, L.L.*, et al.* (2005). Identification and characterization of pleckstrin-homology-domain-dependent and isoenzyme-specific Akt inhibitors. The Biochemical journal *385*, 399-408.
Baserga, R. (2005). The insulin-like growth factor-I receptor as a target for cancer therapy. Expert opinion on therapeutic targets *9*, 753-768.
Baserga, R., Resnicoff, M., D'Ambrosio, C., and Valentinis, B. (1997). The role of the IGF-I receptor in apoptosis. Vitamins and hormones *53*, 65-98.
Biedi, C., Panetta, D., Segat, D., Cordera, R., and Maggi, D. (2003). Specificity of insulin-like growth factor I and insulin on Shc phosphorylation and Grb2 recruitment in caveolae. Endocrinology *144*, 5497-5503.
Bjerknes, M., and Cheng, H. (2002). Multipotential stem cells in adult mouse gastric epithelium. Am J Physiol Gastrointest Liver Physiol *283*, G767-777.
Boman, B.M., Fields, J.Z., Cavanaugh, K.L., Guetter, A., and Runquist, O.A. (2008). How dysregulated colonic crypt dynamics cause stem cell overpopulation and initiate colon cancer. Cancer Res *68*, 3304-3313.
Boman, B.M., Wicha, M.S., Fields, J.Z., and Runquist, O.A. (2007). Symmetric division of cancer stem cells--a key mechanism in tumor growth that should be targeted in future therapeutic approaches. Clin Pharmacol Ther *81*, 893-898.

Borisov, N., Aksamitiene, E., Kiyatkin, A., Legewie, S., Berkhout, J., Maiwald, T., Kaimachnikov, N.P., Timmer, J., Hoek, J.B., and Kholodenko, B.N. (2009). Systems-level interactions between insulin-EGF networks amplify mitogenic signaling. Molecular systems biology *5*, 256.
Burke, P., Schooler, K., and Wiley, H.S. (2001). Regulation of epidermal growth factor receptor signaling by endocytosis and intracellular trafficking. Molecular biology of the cell *12*, 1897-1910.
Buske, P., Galle, J., Barker, N., Aust, G., Clevers, H., and Loeffler, M. (2011). A comprehensive model of the spatio-temporal stem cell and tissue organisation in the intestinal crypt. PLoS Comput Biol *7*, e1001045.
Chen, J.Y., Lin, J.R., Cimprich, K.A., and Meyer, T. (2012). A two-dimensional ERK-AKT signaling code for an NGF-triggered cell-fate decision. Molecular cell *45*, 196-209.
Chow, J.C., Condorelli, G., and Smith, R.J. (1998). Insulin-like growth factor-I receptor internalization regulates signaling via the Shc/mitogen-activated protein kinase pathway, but not the insulin receptor substrate-1 pathway. The Journal of biological chemistry *273*, 4672-4680.
Clemmons, D.R. (2007). Modifying IGF1 activity: an approach to treat endocrine disorders, atherosclerosis and cancer. Nature reviews Drug discovery *6*, 821-833.
Cox, D. (1970). Renewal Theory (London: Methuen & Co.).
D. R. Jones, C.D.P., B. E. Stuckman (1993). Lipschitzian Optimization Without the Lipschitz Constant. Journal of Optimization Theory and Applications *79*, 157-181
Danielsen, A., Larsen, E., and Gammeltoft, S. (1990). Chromaffin cells express two types of insulin-like growth factor receptors. Brain research *518*, 95-100.
Du, K., and Montminy, M. (1998). CREB is a regulatory target for the protein kinase Akt/PKB. The Journal of biological chemistry *273*, 32377-32379.
Feinberg, A.P. (2013). The epigenetic basis of common human disease. Transactions of the American Clinical and Climatological Association *124*, 84-93.
Forbes, B.E., Hartfield, P.J., McNeil, K.A., Surinya, K.H., Milner, S.J., Cosgrove, L.J., and Wallace, J.C. (2002). Characteristics of binding of insulin-like growth factor (IGF)-I and IGF-II analogues to the type 1 IGF receptor determined by BIAcore analysis. European journal of biochemistry / FEBS *269*, 961-968.
Frank, S.A. (2007). Dynamics of Cancer: Incidence, Inheritance, and Evolution, 2010/09/08 edn (Princeton University Press).
Genua, M., Pandini, G., Sisci, D., Castoria, G., Maggiolini, M., Vigneri, R., and Belfiore, A. (2009). Role of cyclic AMP response element-binding protein in insulin-like growth factor-i receptor up-regulation by sex steroids in prostate cancer cells. Cancer research *69*, 7270-7277.
Gerike, T.G., Paulus, U., Potten, C.S., and Loeffler, M. (1998). A dynamic model of proliferation and differentiation in the intestinal crypt based on a hypothetical intraepithelial growth factor. Cell Prolif *31*, 93-110.
Ghazizadeh, S., and Taichman, L.B. (2001). Multiple classes of stem cells in cutaneous epithelium: a lineage analysis of adult mouse skin. EMBO J *20*, 1215-1222.
Girnita, L., Girnita, A., and Larsson, O. (2003). Mdm2-dependent ubiquitination and degradation of the insulin-like growth factor 1 receptor. Proceedings of the National Academy of Sciences of the United States of America *100*, 8247-8252.
Girnita, L., Shenoy, S.K., Sehat, B., Vasilcanu, R., Vasilcanu, D., Girnita, A., Lefkowitz, R.J., and Larsson, O. (2007). Beta-arrestin and Mdm2 mediate IGF-1 receptor-stimulated ERK activation and cell cycle progression. The Journal of biological chemistry *282*, 11329-11338.
Goustin, A.S., Leof, E.B., Shipley, G.D., and Moses, H.L. (1986). Growth factors and cancer. Cancer research *46*, 1015-1029.

Greenman, C., Stephens, P., Smith, R., Dalgliesh, G.L., Hunter, C., Bignell, G., Davies, H., Teague, J., Butler, A., Stevens, C.*, et al.* (2007). Patterns of somatic mutation in human cancer genomes. Nature *446*, 153-158.
Hatakeyama, M., Kimura, S., Naka, T., Kawasaki, T., Yumoto, N., Ichikawa, M., Kim, J.H., Saito, K., Saeki, M., Shirouzu, M.*, et al.* (2003). A computational model on the modulation of mitogen-activated protein kinase (MAPK) and Akt pathways in heregulin-induced ErbB signalling. The Biochemical journal *373*, 451-463.
Haugh, J.M., and Meyer, T. (2002). Active EGF receptors have limited access to PtdIns(4,5)P(2) in endosomes: implications for phospholipase C and PI 3-kinase signaling. Journal of cell science *115*, 303-310.
Hayashi, K., Takahashi, M., Kimura, K., Nishida, W., Saga, H., and Sobue, K. (1999). Changes in the balance of phosphoinositide 3-kinase/protein kinase B (Akt) and the mitogen-activated protein kinases (ERK/p38MAPK) determine a phenotype of visceral and vascular smooth muscle cells. The Journal of cell biology *145*, 727-740.
Holbrook, M.R., O'Donnell, J.B., Jr., Slakey, L.L., and Gross, D.J. (1999). Epidermal growth factor receptor internalization rate is regulated by negative charges near the SH2 binding site Tyr992. Biochemistry *38*, 9348-9356.
Hu, J.F., Nguyen, P.H., Pham, N.V., Vu, T.H., and Hoffman, A.R. (1997). Modulation of Igf2 genomic imprinting in mice induced by 5-azacytidine, an inhibitor of DNA methylation. Molecular endocrinology *11*, 1891-1898.
Itzkovitz, S., Blat, I.C., Jacks, T., Clevers, H., and van Oudenaarden, A. (2012). Optimality in the development of intestinal crypts. Cell *148*, 608-619.
Jin, K., Mao, X.O., Zhu, Y., and Greenberg, D.A. (2002). MEK and ERK protect hypoxic cortical neurons via phosphorylation of Bad. Journal of neurochemistry *80*, 119-125.
Johnston, M.D., Edwards, C.M., Bodmer, W.F., Maini, P.K., and Chapman, S.J. (2007). Mathematical modeling of cell population dynamics in the colonic crypt and in colorectal cancer. Proc Natl Acad Sci U S A *104*, 4008-4013.
Juin, P., Hunt, A., Littlewood, T., Griffiths, B., Swigart, L.B., Korsmeyer, S., and Evan, G. (2002). c-Myc functionally cooperates with Bax to induce apoptosis. Molecular and cellular biology *22*, 6158-6169.
Jullien, J., Guili, V., Reichardt, L.F., and Rudkin, B.B. (2002). Molecular kinetics of nerve growth factor receptor trafficking and activation. The Journal of biological chemistry *277*, 38700-38708.
Kaneda, A., Wang, C.J., Cheong, R., Timp, W., Onyango, P., Wen, B., Iacobuzio-Donahue, C.A., Ohlsson, R., Andraos, R., Pearson, M.A.*, et al.* (2007). Enhanced sensitivity to IGF-II signaling links loss of imprinting of IGF2 to increased cell proliferation and tumor risk. Proceedings of the National Academy of Sciences of the United States of America *104*, 20926-20931.
Kennedy, S.G., Wagner, A.J., Conzen, S.D., Jordan, J., Bellacosa, A., Tsichlis, P.N., and Hay, N. (1997). The PI 3-kinase/Akt signaling pathway delivers an anti-apoptotic signal. Genes & development *11*, 701-713.
Kratchmarova, I., Blagoev, B., Haack-Sorensen, M., Kassem, M., and Mann, M. (2005). Mechanism of divergent growth factor effects in mesenchymal stem cell differentiation. Science *308*, 1472-1477.
Lemmon, M.A., and Schlessinger, J. (2010). Cell signaling by receptor tyrosine kinases. Cell *141*, 1117-1134.
Lindner, A.U., Concannon, C.G., Boukes, G.J., Cannon, M.D., Llambi, F., Ryan, D., Boland, K., Kehoe, J., McNamara, D.A., Murray, F.*, et al.* (2013). Systems analysis of BCL2 protein family interactions establishes a model to predict responses to chemotherapy. Cancer research *73*, 519-528.

Liu, W., Akhand, A.A., Takeda, K., Kawamoto, Y., Itoigawa, M., Kato, M., Suzuki, H., Ishikawa, N., and Nakashima, I. (2003). Protein phosphatase 2A-linked and -unlinked caspase-dependent pathways for downregulation of Akt kinase triggered by 4-hydroxynonenal. Cell death and differentiation *10*, 772-781.
Lu, Y., Muller, M., Smith, D., Dutta, B., Komurov, K., Iadevaia, S., Ruths, D., Tseng, J.T., Yu, S., Yu, Q*., et al.* (2011). Kinome siRNA-phosphoproteomic screen identifies networks regulating AKT signaling. Oncogene *30*, 4567-4577.
Marnell, M.H., Stookey, M., and Draper, R.K. (1982). Monensin blocks the transport of diphtheria toxin to the cell cytoplasm. The Journal of cell biology *93*, 57-62.
McMahon, H.T., and Boucrot, E. (2011). Molecular mechanism and physiological functions of clathrin-mediated endocytosis. Nature reviews Molecular cell biology *12*, 517-533.
Morrison, S.J., and Kimble, J. (2006). Asymmetric and symmetric stem-cell divisions in development and cancer. Nature *441*, 1068-1074.
Nguyen, L.K., Kolch, W., and Kholodenko, B.N. (2013). When ubiquitination meets phosphorylation: a systems biology perspective of EGFR/MAPK signalling. Cell communication and signaling : CCS *11*, 52.
Nolan, C.M., Kyle, J.W., Watanabe, H., and Sly, W.S. (1990). Binding of insulin-like growth factor II (IGF-II) by human cation-independent mannose 6-phosphate receptor/IGF-II receptor expressed in receptor-deficient mouse L cells. Cell regulation *1*, 197-213.
Normanno, N., De Luca, A., Bianco, C., Strizzi, L., Mancino, M., Maiello, M.R., Carotenuto, A., De Feo, G., Caponigro, F., and Salomon, D.S. (2006). Epidermal growth factor receptor (EGFR) signaling in cancer. Gene *366*, 2-16.
Oda, K., Matsuoka, Y., Funahashi, A., and Kitano, H. (2005). A comprehensive pathway map of epidermal growth factor receptor signaling. Molecular systems biology *1*, 2005 0010.
Oltvai, Z.N., Milliman, C.L., and Korsmeyer, S.J. (1993). Bcl-2 heterodimerizes in vivo with a conserved homolog, Bax, that accelerates programmed cell death. Cell *74*, 609-619.
Ostman, A., Hellberg, C., and Bohmer, F.D. (2006). Protein-tyrosine phosphatases and cancer. Nature reviews Cancer *6*, 307-320.
Park, C.S., Schneider, I.C., and Haugh, J.M. (2003). Kinetic analysis of platelet-derived growth factor receptor/phosphoinositide 3-kinase/Akt signaling in fibroblasts. The Journal of biological chemistry *278*, 37064-37072.
Perlman, H., Zhang, X., Chen, M.W., Walsh, K., and Buttyan, R. (1999). An elevated bax/bcl-2 ratio corresponds with the onset of prostate epithelial cell apoptosis. Cell death and differentiation *6*, 48-54.
Peruzzi, F., Prisco, M., Dews, M., Salomoni, P., Grassilli, E., Romano, G., Calabretta, B., and Baserga, R. (1999). Multiple signaling pathways of the insulin-like growth factor 1 receptor in protection from apoptosis. Molecular and cellular biology *19*, 7203-7215.
Pollak, M. (2012). The insulin and insulin-like growth factor receptor family in neoplasia: an update. Nature reviews Cancer *12*, 159-169.
Potten, C.S., and Booth, C. (2002). Keratinocyte stem cells: a commentary. J Invest Dermatol *119*, 888-899.
Ramanan, V., Agrawal, N.J., Liu, J., Engles, S., Toy, R., and Radhakrishnan, R. (2011). Systems biology and physical biology of clathrin-mediated endocytosis. Integrative biology : quantitative biosciences from nano to macro *3*, 803-815.
Raychaudhuri, S., and Das, S.C. (2013). Low probability activation of Bax/Bak can induce selective killing of cancer cells by generating heterogeneity in apoptosis. Journal of healthcare engineering *4*, 47-66.

Ren, B., Deng, Y., Mukhopadhyay, A., Lanahan, A.A., Zhuang, Z.W., Moodie, K.L., Mulligan-Kehoe, M.J., Byzova, T.V., Peterson, R.T., and Simons, M. (2010). ERK1/2-Akt1 crosstalk regulates arteriogenesis in mice and zebrafish. The Journal of clinical investigation *120*, 1217-1228.
Schayek, H., Haugk, K., Sun, S., True, L.D., Plymate, S.R., and Werner, H. (2009). Tumor suppressor BRCA1 is expressed in prostate cancer and controls insulin-like growth factor I receptor (IGF-IR) gene transcription in an androgen receptor-dependent manner. Clinical cancer research : an official journal of the American Association for Cancer Research *15*, 1558-1565.
Scheid, M.P., Schubert, K.M., and Duronio, V. (1999). Regulation of bad phosphorylation and association with Bcl-x(L) by the MAPK/Erk kinase. The Journal of biological chemistry *274*, 31108-31113.
Schutze, S., Machleidt, T., Adam, D., Schwandner, R., Wiegmann, K., Kruse, M.L., Heinrich, M., Wickel, M., and Kronke, M. (1999). Inhibition of receptor internalization by monodansylcadaverine selectively blocks p55 tumor necrosis factor receptor death domain signaling. The Journal of biological chemistry *274*, 10203-10212.
Sciacca, L., Mineo, R., Pandini, G., Murabito, A., Vigneri, R., and Belfiore, A. (2002). In IGF-I receptor-deficient leiomyosarcoma cells autocrine IGF-II induces cell invasion and protection from apoptosis via the insulin receptor isoform A. Oncogene *21*, 8240-8250.
Sears, R., Nuckolls, F., Haura, E., Taya, Y., Tamai, K., and Nevins, J.R. (2000). Multiple Ras-dependent phosphorylation pathways regulate Myc protein stability. Genes & development *14*, 2501-2514.
Sehat, B., Andersson, S., Girnita, L., and Larsson, O. (2008). Identification of c-Cbl as a new ligase for insulin-like growth factor-I receptor with distinct roles from Mdm2 in receptor ubiquitination and endocytosis. Cancer research *68*, 5669-5677.
Sehat, B., Andersson, S., Vasilcanu, R., Girnita, L., and Larsson, O. (2007). Role of ubiquitination in IGF-1 receptor signaling and degradation. PloS one *2*, e340.
Sharma, S.V., Gajowniczek, P., Way, I.P., Lee, D.Y., Jiang, J., Yuza, Y., Classon, M., Haber, D.A., and Settleman, J. (2006). A common signaling cascade may underlie "addiction" to the Src, BCR-ABL, and EGF receptor oncogenes. Cancer cell *10*, 425-435.
Sharma, S.V., and Settleman, J. (2007). Oncogene addiction: setting the stage for molecularly targeted cancer therapy. Genes & development *21*, 3214-3231.
Siddle, K. (2011). Signalling by insulin and IGF receptors: supporting acts and new players. Journal of molecular endocrinology *47*, R1-10.
Simons, B.D., and Clevers, H. (2011). Strategies for homeostatic stem cell self-renewal in adult tissues. Cell *145*, 851-862.
Sorkin, A., and Goh, L.K. (2009). Endocytosis and intracellular trafficking of ErbBs. Experimental cell research *315*, 683-696.
Sorkin, A., and von Zastrow, M. (2009). Endocytosis and signalling: intertwining molecular networks. Nature reviews Molecular cell biology *10*, 609-622.
Surinya, K.H., Forbes, B.E., Occhiodoro, F., Booker, G.W., Francis, G.L., Siddle, K., Wallace, J.C., and Cosgrove, L.J. (2008). An investigation of the ligand binding properties and negative cooperativity of soluble insulin-like growth factor receptors. The Journal of biological chemistry *283*, 5355-5363.
Tallquist, M., and Kazlauskas, A. (2004). PDGF signaling in cells and mice. Cytokine & growth factor reviews *15*, 205-213.
Tan, W.H., Popel, A.S., and Mac Gabhann, F. (2013). Computational Model of Gab1/2-Dependent VEGFR2 Pathway to Akt Activation. PloS one *8*, e67438.
Thompson, C.B. (2009). Metabolic enzymes as oncogenes or tumor suppressors. The New England journal of medicine *360*, 813-815.

Ulaner, G.A., Vu, T.H., Li, T., Hu, J.F., Yao, X.M., Yang, Y., Gorlick, R., Meyers, P., Healey, J., Ladanyi, M.*, et al.* (2003a). Loss of imprinting of IGF2 and H19 in osteosarcoma is accompanied by reciprocal methylation changes of a CTCF-binding site. Human molecular genetics *12*, 535-549.
Ulaner, G.A., Yang, Y., Hu, J.F., Li, T., Vu, T.H., and Hoffman, A.R. (2003b). CTCF binding at the insulin-like growth factor-II (IGF2)/H19 imprinting control region is insufficient to regulate IGF2/H19 expression in human tissues. Endocrinology *144*, 4420-4426.
Ullrich, A., Gray, A., Tam, A.W., Yang-Feng, T., Tsubokawa, M., Collins, C., Henzel, W., Le Bon, T., Kathuria, S., Chen, E.*, et al.* (1986). Insulin-like growth factor I receptor primary structure: comparison with insulin receptor suggests structural determinants that define functional specificity. The EMBO journal *5*, 2503-2512.
Vasilcanu, R., Vasilcanu, D., Sehat, B., Yin, S., Girnita, A., Axelson, M., and Girnita, L. (2008). Insulin-like growth factor type-I receptor-dependent phosphorylation of extracellular signal-regulated kinase 1/2 but not Akt (protein kinase B) can be induced by picropodophyllin. Molecular pharmacology *73*, 930-939.
Vecchione, A., Marchese, A., Henry, P., Rotin, D., and Morrione, A. (2003). The Grb10/Nedd4 complex regulates ligand-induced ubiquitination and stability of the insulin-like growth factor I receptor. Molecular and cellular biology *23*, 3363-3372.
Vieira, A.V., Lamaze, C., and Schmid, S.L. (1996). Control of EGF receptor signaling by clathrin-mediated endocytosis. Science *274*, 2086-2089.
Wang, Z., and Zhang, J. (2011). Impact of gene expression noise on organismal fitness and the efficacy of natural selection. Proc Natl Acad Sci U S A *108*, E67-76.
Ward, C.W., and Garrett, T.P. (2004). Structural relationships between the insulin receptor and epidermal growth factor receptor families and other proteins. Current opinion in drug discovery & development *7*, 630-638.
Watt, F.M., and Hogan, B.L. (2000). Out of Eden: stem cells and their niches. Science *287*, 1427-1430.
Weinstein, I.B. (2002). Cancer. Addiction to oncogenes--the Achilles heal of cancer. Science *297*, 63-64.
Weinstein, I.B., and Joe, A. (2008). Oncogene addiction. Cancer research *68*, 3077-3080; discussion 3080.
Werner, H. (2012). Tumor suppressors govern insulin-like growth factor signaling pathways: implications in metabolism and cancer. Oncogene *31*, 2703-2714.
Werner, H., Karnieli, E., Rauscher, F.J., and LeRoith, D. (1996). Wild-type and mutant p53 differentially regulate transcription of the insulin-like growth factor I receptor gene. Proceedings of the National Academy of Sciences of the United States of America *93*, 8318-8323.
Wiley, H.S., Shvartsman, S.Y., and Lauffenburger, D.A. (2003). Computational modeling of the EGF-receptor system: a paradigm for systems biology. Trends in cell biology *13*, 43-50.
Worster, D.T., Schmelzle, T., Solimini, N.L., Lightcap, E.S., Millard, B., Mills, G.B., Brugge, J.S., and Albeck, J.G. (2012). Akt and ERK control the proliferative response of mammary epithelial cells to the growth factors IGF-1 and EGF through the cell cycle inhibitor p57Kip2. Science signaling *5*, ra19.
Wu, G.-Y., Deisseroth, K., and Tsien, R.W. (2001). Activity-dependent CREB phosphorylation: Convergence of a fast, sensitive calmodulin kinase pathway and a slow, less sensitive mitogen-activated protein kinase pathway. Proceedings of the National Academy of Sciences *98*, 2808-2813.

Yang, Y., Hu, J.F., Ulaner, G.A., Li, T., Yao, X., Vu, T.H., and Hoffman, A.R. (2003). Epigenetic regulation of Igf2/H19 imprinting at CTCF insulator binding sites. Journal of cellular biochemistry *90*, 1038-1055.

CURRICULUM VITAE FOR Ph.D. CANDIDATES

The Johns Hopkins University School of Medicine

Kiran Gireesan Vanaja 1/17/2014

Educational History :

Ph. D.(Expected)	2014	Biomedical Engineering Advisor:Dr. Andre Levchenko	Johns Hopkins University
M.S.	2004	Electrical Engineering	The Indian Institute of Science, Bangalore, India
B.E.	2000	Electrical Engineering	The University of Mysore, Mysore, India.

Professional Experience :

- Teaching Assistant for the BME course Molecules and Cells course taught at the Johns Hopkins University – 2008-2007, 2006-2005.
- Lab rotation with Dr. Linzhao Cheng, Institute of Cell Engg. 2006.
- Lab rotation with Dr. Chandrasegaran, Bloomberg School of Public Health, 2005.

Current Publications:

- "Stem cell differentiation as a renewal-reward process: predictions and validation in the colonic crypt", Kiran Vanaja, Andrew Feinberg and Andre Levchenko, Chapter in Advances in Systems Biology, 2012.
- On the IGF-2 Loss of Imprinting, cellular signaling rebalancing and the physiological manifestations of the network rebalancing, Kiran Vanaja, Winston Timp, Andrew Feinberg and Andre Levchenko (Manuscript in preparation)

Previous Publications :

- "On-line Signature Verification System Using Probabilistic Feature Modelling", Kiran G.V., Kunte R.S.R., Samuel S, International Symposium on Signal Processing and its Applications 2001, Vol 1, pp 355-358
- "A One Parameter Controlled Gamma-Chirp Filterbank for Auditory Models", Kiran G.V., Srinivas T.V., Workshop on Spoken Language Processing (WSLP) 2003, pp 41-48.
- "A Novel Method of Analysing and Comparing Responses of Hearing Aid Algorithms Using Auditory Time-Frequency Representations", Kiran G.V., Sreenivas T.V., Proceedings of the 8th European Conference on Speech Communications and Technology – Eurospeech 2003, pp 61-64.
- "Neural Spike Rate Spectrum as a Noise Robust, Speaker Invariant Feature for Automatic Speech Recognition", Kiran G.V., Krishna A.G., Sreenivas T.V., Proceedings of the 8th International Conference on Spoken Language Processing - ICSLP 2004, pp 929-932.
- "A Hearing Aid Algorithm Using Spectral Contrast and Auditory Models", Kiran G.V., Sreenivas T.V., International Hearing Aid Conference –IHCON 2004 (Accepted but couldn't present participate and present poster)